THE DORMANCY-LIKE RESPONSE OF *PLASMODIUM FALCIPARUM* TO AMINO ACID STARVATION

by

Kyle Jarrod McLean

A dissertation submitted to Johns Hopkins University in conformity with the requirements for the degree of Doctor of Philosophy

Baltimore, Maryland

June, 2016

Abstract

The frontline antimalarial Artemisinin is decreasing in efficacy across the Greater Mekong Subregion. The study of parasites from this region has led several authors to propose that *Plasmodium falciparum* may be able to enter state of dormancy—programmed cell cycle arrest—as a means of drug resistance. An independent line of reasearch recently described a similar dormancy-like state *in vitro* when *P. falciparum* parasites are starved of the essential amino acid isoleucine, raising the possibility that a shared genetic pathway may underlie survival of both starvation and drug treatment. Here, we revisit and expand upon the dormancy-like response of *P. falciparum* to isoleucine starvation. We have found that the parasite does not exit the cell cycle upon starvation, but instead enters a state of slow growth. This change in growth rate occurs only if isoleucine is removed prior to the onset of S-phase. After DNA replication has begun, the parasite traverses the cell cycle at its normal pace, and only enters slow growth in the next generation; a response reminiscent of the nutrient-dependent G_1 cell cycle checkpoints described in other organisms. We have also implicated the *P. falciparum* ortholog of the RNA Polymerase III repressor Maf1 in maintaining viability of parasites undergoing starvation-induced slow growth. Parasites defective in Maf1 expression fail to shut-down tRNA expression and display decreased growth and survival under a number of growth-limiting treatments. Lastly, we have assayed the ability of an Artemisinin-resistant field isolate to survive long term isoleucine star-

vation and found that resistant parasites display increased recovery from isoleucine deprivation. Combined, these results suggest that while the parasite may not exit the cell cycle as in the dormancy responses of other organisms, *P. falciparum* possesses growth regulatory pathways that can affect the parasite's ability to survive growth-retarding treatments, including both amino acid starvation and Artemisinin.

Advisor

Marcelo Jacobs-Lorena, PhD

Readers

Gary Ketner, PhD

Michael Matunis, PhD

Sean Prigge, PhD

Theresa Shapiro, MD, PhD

Preface

Hofstadter's Law: It always takes longer than you expect, even when you take into account Hofstadter's Law.

—Douglas Hofstadter

Gödel, Escher, Bach: An Eternal Golden Braid

1979

With one more victory like this, we shall be utterly ruined.

—Pyrrhus of Epirus

The Battle of Asculum

279 B.C.

Table of Contents

List of Figures

Chapter 1

Introduction

Recrudescence, Relapse, and Dormancy

It has long been known that clinical malaria can recur in patients months after the individual has left an endemic region. Shute was the first to classify these "long-latency-infections" into two groups: *Recrudescence* and *Relapse* (Shute, 1946). *Recrudescence* is generally attributed to insufficient chemotherapy or the emergence of drug-resistant parasites. Symptomatic malaria disappears after the initial treatment due to the suppression of parasite numbers, but returns as the few surviving parasites re-establish themselves.

Relapse was used to describe the long latency periods regularly observed between episodes in patients suffering from *benign tertian* malaria—what we know today to be *Plasmodium vivax* infection. The observation that relapse never occurred when infection was intiated from blood transfusion (Shute, 1946), and that *Plasmodium* sporozoites could survive for long periods in the mosquito salivary glands led to the hypothesis that *Plasmodium vivax* was able to enter a state of dormancy after being inoculated by the mosquito into the human host. The later discovery of what appeared to be latent parasite stages in the livers of chimpanzees experimentally infected with *Plasmodium vivax* (Krotoski et al., 1982) solidified the formulation the *hypnozoite* hypothesis (Krotoski, 1985): *Plasmodium vivax* (as well as the human *P. ovale* and the simian *P. cynomolgi*, *P. fieldi*, and *P. simiovale*) is capable of entering a programmed state of developmental arrest within hepatocytes prior to blood stage infection. *Relapse* occurs when this dormant *hypnozoite* stage reactivates months or years after initial infection and commences the intraerythrocytic cycle.

No developmentally arrested parasites have ever been observed in liver cells after infection with *Plasmodium falciparum*. And yet, while less common than with *Plasmodium vivax*, there is an extensive literature on the recurrance of *P. falciparum* malaria

after long periods of latency in cases where *de novo* mosquito transmission can be decisively ruled out (Ashley and White, 2014). In the most extreme case, a patient contracted *P. falciparum* after a blood transfusion from a donor that had not traveled to an endemic region for over thirteen years (Besson et al., 1976). Often, recurrent patency follows a traumatic event, such as surgery, a severe wound, famine, or war (Shanks, 2015), suggesting reemergence of the parasite is triggered by changes in host physiology, much they way *P.vivax* relapse is believed to be triggered for reactivation (Shanks and White, 2013). Formally, these events are considered to be cases of *Recrudescence*. It is presumed the afflicted individuals were continuously infected but simply asymptomatic during the prolonged latency periods. The parasite is thought to be maintained at low levels through the actions of the host's immune system, and only increases to a density capable of causing clinical disease when the immune system wanes for any number of reasons. However, recent observations may suggest an alternate explanation.

Studies of the decreased efficacy of artemisinin-based anti-antimalarials in the field has found persistent ring stage parasites in the blood hours after parasites would normally be expected to be cleared (Dondorp et al., 2009). Supporting *in vitro* studies have also observed peculiar developmentally arrested parasites after artemisinin treatment, leading several authors to suggest *P. falciparum* may enter a state of dormancy as a mechanism of drug resistance (Teuscher et al., 2010)(Witkowski et al., 2010)(Codd et al., 2011)(Cheng et al., 2012). In an intriguing parallel line of research, a study found that starvation of the essential amino acid isoleucine can trigger a dormancy-like state in blood stage *P. falciparum* (Babbitt et al., 2012). If these studies hold true, then the distinction between *Recrudescence* and *Relapse* in cases of *falciparum* malaria may need to be re-evaluated.

The work reported in this thesis is aimed at investigating and evaluating the na-

ture of these dormancy-like states of *P. falciparum* in *in vitro* culture. *Chapter 2* is a study of the response of the parasite to isoleucine starvation as it relates to cell cycle progression and the observed dormancy-like survival mechanism of artemisinin-resistant field isolates. *Chapter 3* is an analysis of a mutant parasite line incapable of surviving prolonged amino acid starvation and a discussion of the conserved eukaryote genetic pathways that regulate growth arrest and recovery. *Chapter 4* is a slight departure, and details a study of the genetic basis of sexual differentiation in the parasite, and its relation to cell cycle progression and growth.

As of the end of 2015, ninety-five countries across the globe still experience ongoing malaria transmission, leading to more than two hundred million cases and over four hundred thousand deaths each year (World Health Organization, 2015). Despite great successes in the last fifteen years in decreasing incidence (18% decrease) and death (48% decrease)(World Health Organization, 2015), *Plasmodium falciparum* remains a substantial public health burden. Further insights into the nature of the parasite life cycle and transmission dynamics, including the possibility of programmed blood stage dormancy as a mechanism of drug resistance and relapse, promise to benefit future efforts to control and eliminate the parasite.

Chapter 2

The dormancy-like response to isoleucine starvation induces growth-retardation related to artemisinin-resistance

Abstract

It has been reported that the malaria parasite *Plasmodium falciparum* enters a dormancy-like state upon starvation of the essential amino acid isoleucine by first slowing its cell cycle and then arresting prior to S-phase. We have reexamined this response and found that the parasite does not exit the cell cycle prior to DNA replication, but instead, continuously grows at a dramatically reduced pace. Moreover, slow growth occurs only if isoleucine is removed prior to the onset of schizogeny. After S-phase has commenced, the parasite is insensitive to isoleucine depletion and transits through the cell cycle at the normal pace, reminiscent of the nutrient-dependent G_1 cell cycle checkpoints described in other organisms. Similar to isoleucine-starvation, artemisinin derivatives have also been reported to induce growth retardation in ring-stage parasites, and resistant parasites carrying variants of the K13 gene have been reported to survive drug-treatment due to an increased capacity to resume growth after drug concentrations have declined. We show that one such artemisinin-resistant K13 mutant parasite line displays increased survival upon prolonged isoleucine-induced growth retardation, suggesting a connection between the underlying molecular pathways governing artemisinin-resistance and the dormancy-like response to isoleucine starvation.

Introduction

Dormancy is a strategy used by many organisms to overcome unfavorable environmental conditions. While the term is often used loosely, in its strictest sense in unicellular organisms, dormancy typically refers to an exit from the mitotic cell cycle and differentiation into a distinct cellular state (*i.e.*: G_0), that exhibits low metabolic activity. The *Plasmodium* life cycle includes several stages of programed dormancy such as the mature gametocyte, the salivary gland sporozoite, and the poorly understood hepatic hypnozoites of certain *Plasmodium* species. These are specialized differentiated cells with low metabolic activity, capable of waiting long periods before activating and re-entering the cell cycle.

In recent years, the frontline antimalarial drug artemisinin has been exhibiting decreased efficacy in clearing *Plasmodium falciparum* from the blood stream in regions of South East Asia. While there has yet to be widespread clinical failure, parasite isolates that display delayed clearance, detectable in the blood as ring stages hours after artemisinin therapy, are referred to as artemisinin resistant (Dondorp et al., 2009).

The fact that this resistance phenotype manifests as the persistence of a defined morphological stage (ring), and the fact that artemisinin is most effective when parasites are actively metabolizing hemoglobin in the trophozoite stage and later (Klonis et al., 2013), has led several authors to propose a dormancy model of artemisinin resistance (Kyle DE, Webster HK, 1996)(Hoshen et al., 2000)(Teuscher et al., 2010)(Witkowski et al., 2010)(Codd et al., 2011) (Cheng et al., 2012). In this model, non-hemoglobin digesting ring stage parasites exit the cell cycle upon artemisinin treatment and assume an arrested state of low metabolic activity for a prolonged period until drug concentrations have decayed (Figure 2.1A). It is not clear how artemisinin would trigger such a response, as the drug itself is unlikely to

be a natural trigger for the dormancy pathway. Instead, it is more likely that there is a pre-existing dormancy response in the intraerythrocytic cycle and resistant isolates have acquired mutations that allow the co-option of this pathway when under drug pressure.

In many organisms, differentiation into a dormant state is triggered by unfavorable nutrient conditions. In human cells in culture, removal of serum growth factors causes G_1 cells to exit the cell cycle and enter a state of quiescence (Pardee, 1974). Similarly, in haploid stages of the yeast *Saccharomyces cerevisiae*, starvation of nitrogen or carbohydrates during the G_1 phase causes an arrest of the mitotic cycle and entry into a dormant state that can be maintained for a prolonged period with little loss of viability (Lillie and Pringle, 1980). In a recent landmark study, Babbitt *et al.* reported that *Plasmodium falciparum* enters an analogous dormancy-like state when starved of the essential amino acid isoleucine (Babbitt et al., 2012).

During the intraerythrocytic life cycle, *Plasmodium falciparum* acquires most of its amino acid supply through the digestion of hemoglobin. However, as human hemoglobin does not contain isoleucine and the parasite cannot synthesize it *de novo*, it must obtain isoleucine from the extracellular environment (human serum or culture medium *in vitro*). In human blood, isoleucine concentrations can drop well below the levels needed to support *P. falciparum* growth in culture (Baertl et al., 1974)(Liu et al., 2006), which would be lethal for the parasite without an adaptive mechanism. When starved of isoleucine, Babbit *et al.* reported that the parasite dramatically slows its cell cycle, eventually arresting prior to DNA synthesis (Figure 2.1B). The parasite can remain in this state of low metabolic activity for upwards of several days, and then resume growth with little loss of viability upon isoleucine resupplementation. In contrast, glucose starvation leads to rapid parasite death within a few hours (Babbitt et al., 2012).

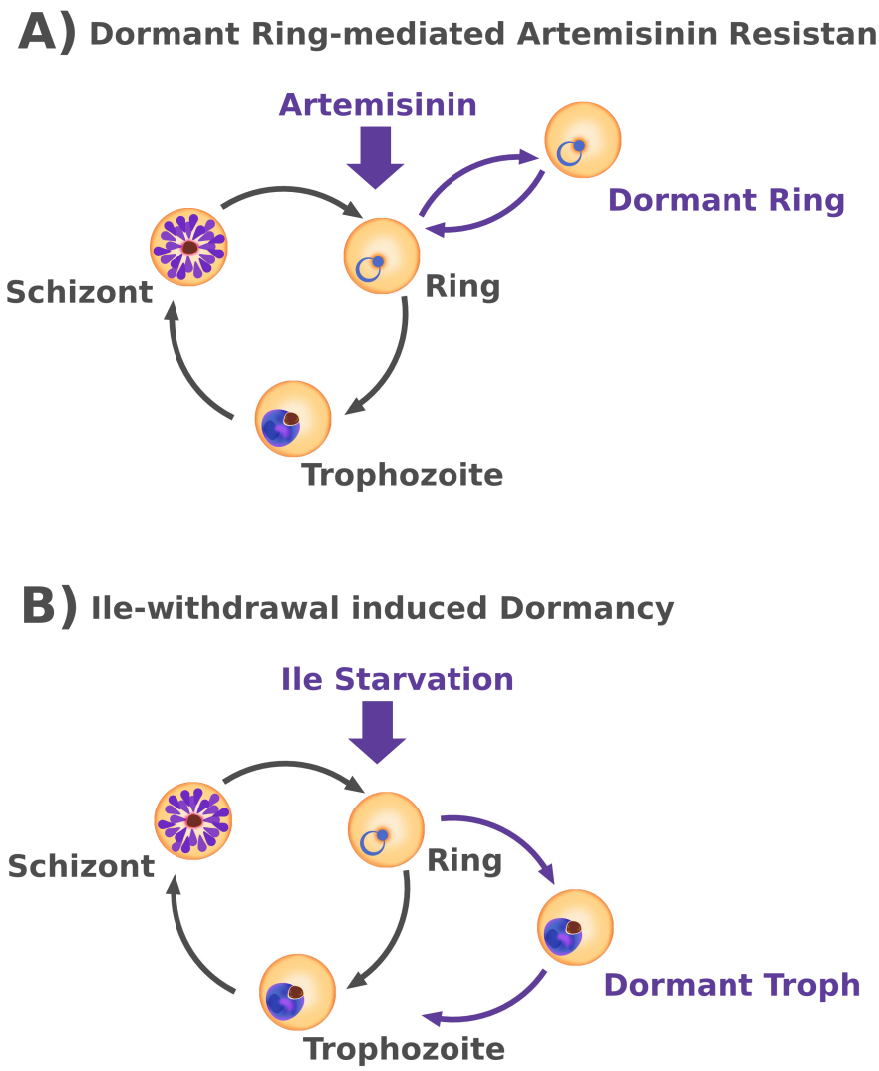

Figure 2.1: ***Plasmodium falciparum* survives artemisinin and isoleucine starvation by entering a state of programmed dormancy. A)** Upon artemisinin treatment, ring stage parasites exit the cell cycle and enter a programmed state of dormancy to avoid drug-induced cellular damage, and resume growth once drug levels have subsided. While initial observations appeared to support this model, recent studies of artemisinin-resistant field isolates suggest an alternate model. **B)** Upon withdrawal of extracellular isoleucine *in vitro*, *Plasmodium falciparum* initially slows growth, then exits the cell cycle and arrests at the trophozoite stage prior to DNA replication. Isoleucine-arrested parasites can remain viable for several days and resume growth again upon isoleucine resupplementation.

The similarities between the observed response of resistant parasites to artemisinin derivatives *in vivo* and isoleucine-starved parasites *in vitro* suggested further investigation for potential overlap of the underlying molecular pathways. Here, we revisit and expand upon the isoleucine-induced dormancy-like state. Our results suggest that the pathways necessary for growth modulation and recovery upon artemisinin treatment may be the same or overlap with those required for maintaining viability during the dormancy-like state induced by isoleucine starvation.

Results

Plasmodium falciparum completes the cell cycle in the dormancy-like state in the absence of extracellular isoleucine

Babbitt *et al.* reported that when young rings are deprived of extracellular isoleucine the parasites enter a phsysiological state reminiscent of hibernation or aestivation in higher animals: a reversible state of low-metabolic activity and high resource conservation (Babbitt et al., 2012). When resupplemented with isoleucine, parasites immediately resumed normal growth, displaying only modest losses in viability after 72h of starvation. Over the course of isoleucine starvation, the parasite's progression through the cell cycle was drastically retarded, advancing at 40% of the pace of control cultures until seemingly arresting as hemozoin-containing, pre-S-phase trophozoites. We repeated the Babbit *et al* methodology to verify that the phenotype held for the NF54 clone of *P. falciparum* used in our laboratory.

As observed by Babbit *et al.*, young rings (~6 hpi) washed thoroughly with PBS and transferred to culture medium lacking isoleucine remained at the starting para-

sitemia after 72 h, whereas control parasites (standard RPMI 1640 with 382 μM Ile) completed a cell cycle and re-invaded red blood cells over the same time period (Figure 2.2). When the starved parasites were resupplemented with complete medium for 72h, they displayed growth similar to the control cultures that had never been starved (Figure 2.2). Thus, the isoleucine response described by Babbit *et al.* is robust and reproducible in this parasite clone.

Over the course of our experiments, we noticed the appearance of parasites with greater than 1C DNA content in cultures deprived of isoleucine for over 48h, suggesting that, despite growth retardation, some parasites were able to commence DNA synthesis in the absence of isoleucine. This observation was not noted by Babbit *et al.*, however, most of their study focused on earlier time points. To investigate this in more detail, we initiated isoleucine-starved and isoleucine-normal cultures from late-stage, percoll-isolated schizonts and tracked their development over the ensuing six days.

Control parasites developed as expected, with schizonts appearing in Giemsa-stained smears roughly every 45 h, followed by an increase in parasitemia with each generation (Figure 2.3, Figure 2.5A). DNA content analysis by flow cytometry was used to track the proportion of 1C DNA content parasites at each time point, and displayed a 45 h periodicity for 1C peaks (Figure 2.4).

Isoleucine-starved parasites also progressed through the cell cycle, albeit at a much reduced pace (Figure 2.3). Using a correlative transcriptome analysis, Babbitt *et al.* calculated that isoleucine-deprived young rings traversed the cell cycle at a pace 40% of that of controls over 48 h of analysis (Babbitt et al., 2012). However, they concluded that the parasites did not progress further into S-phase of the cell cycle. In our experiments, schizonts first became detectable at around 90 h of incubation, and

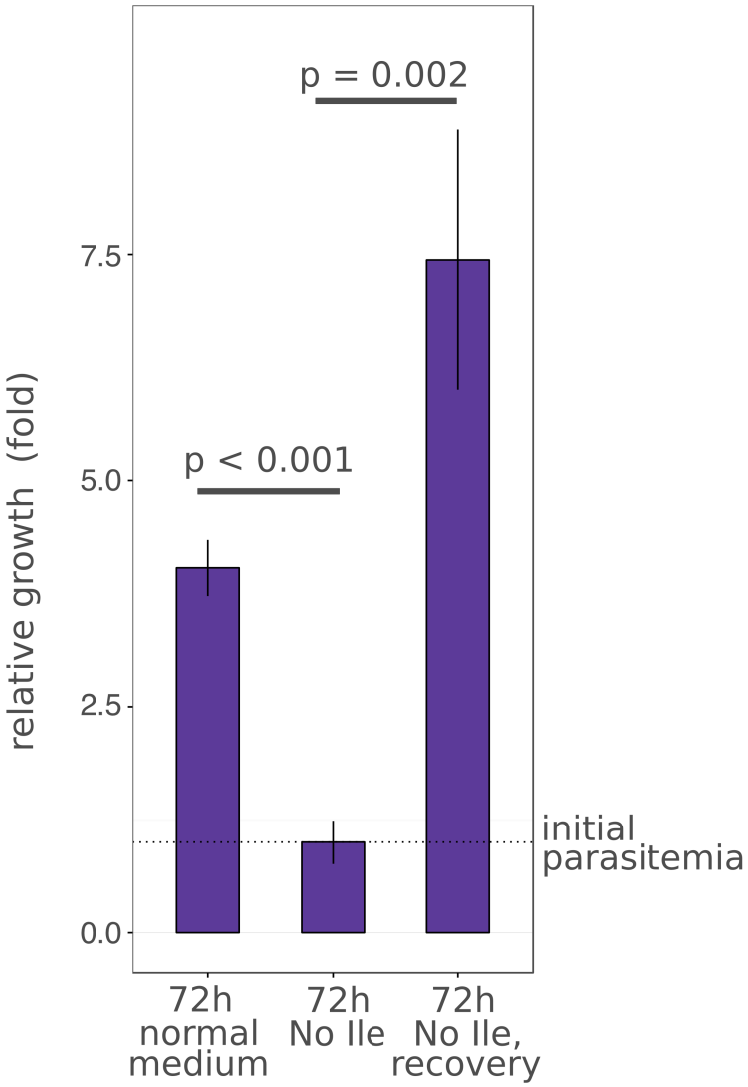

Figure 2.2: ***Plasmodium falciparum*** **enters a dormancy-like state upon prolonged isoleucine starvation from which it can recover.** Synchronous young ring NF54 parasites were cultured in normal culture medium, or culture medium lacking isoleucine (No Ile) for 72 h. ”Recovery” denotes parasites transferred back to normal medium for 72 h of regrowth.

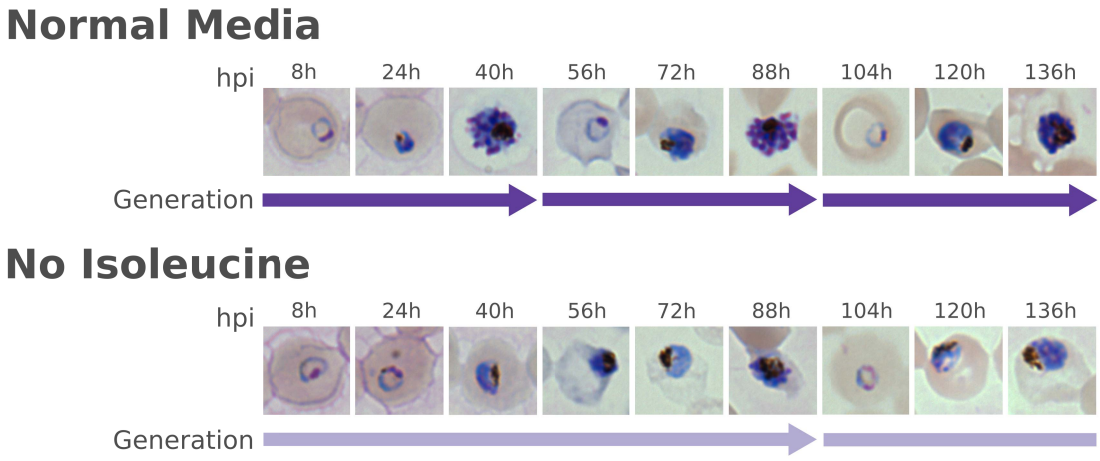

Figure 2.3: ***Plasmodium falciparum* traverses the full cell cycle at a retarded rate of growth in the absence of isoleucine.** Synchronous cultures NF54 parasites were initiated with percoll-isolated late schizonts in either normal medium, or medium lacking isoleucine. Progression of each culture was tracked every eight hours for 136h. Images are representative of the major forms observed at each time point. ”Generation” represents the time required to transition from ring through the cell cycle to ring again.

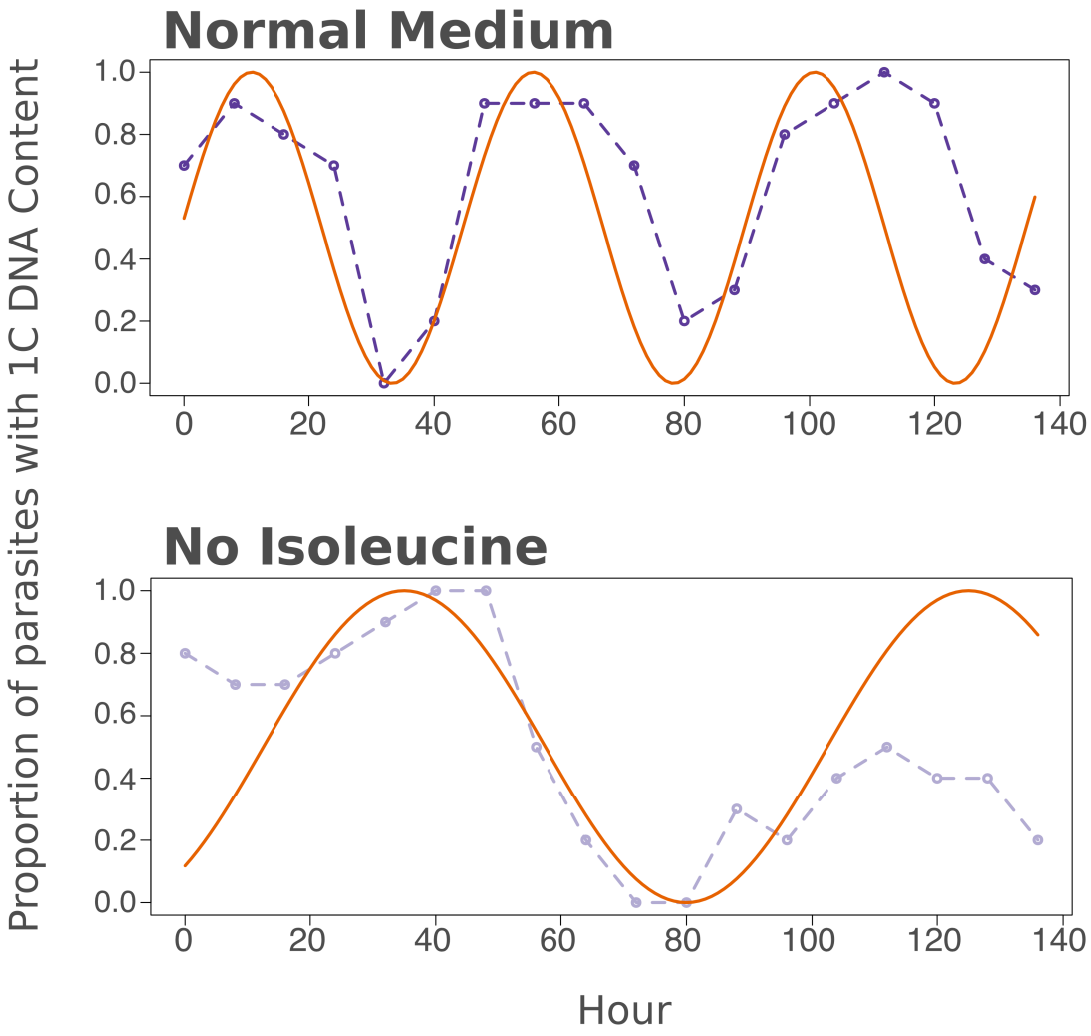

Figure 2.4: **Isoleucine-starved parasites traverse the cell cycle at approximately half their normal rate.** Synchronous cultures NF54 parasites were initiate with percoll-isolated late schizonts in either normal medium, or medium lacking isoleucine. Flow cytometry was used to track the DNA content of the cultures for 136 h. Plots represent the proportion of parasites with a 1C DNA content. Isoleucine-starved parasites proceed through the cell cycle approximately twice as slowly as those in normal medium.

the first rings of the second generation were observed at 100 h of incubation. DNA content tracking of 1C parasites also revealed an extended periodicity of roughly 90h, corresponding to at least a 50% reduction in the pace of the cell cycle (Figure 2.4). It appears the isoleucine-starved parasites do not arrest pre-S-phase to asssume a dormant state, but instead continuously progress through the cell cycle at a retarded pace.

It should be noted that the isoleucine-withdrawal-induced growth retardation is not without its costs. While control parasites increased in parasitemia with each generation, the isoleucine-starved parasites decreased in numbers at a modest, but steady rate over the course of a six-day incubation (Figure 2.5A). This suggests that, despite completing the cell cycle and re-invading at roughly four-day intervals, the overall viabilty of the slow growing parasites decreased as starvation progressed. This is in agreement with Babbitt *et al.*'s observation of diminished recovery upon isoleucine resupplemenation as a function of increased starvation. The cause of this loss of viability is not clear, however, the mean DNA-content of parasites at schizont-enriched time points was substantially lower for isoleucine-starved parasites compared to controls (Figure 2.5B). This suggests that either isoleucine starvation produced schizonts with a lower average merozoite count, decreasing the growth potential of each cell, or that a majority of cells experienced catastrophic failure early in schizogeny and produced no viable progeny.

The dormancy-like slow growth response is cell cycle stage-dependent

Mammalian cells respond to serum starvation by exiting the cell cycle and entering a quiescent state (Pardee, 1974). However, this quiescence-response program is only induced if serum is removed prior to a specific point in the cell cycle known as the

Restriction Point. Once this *Restriciton Point* is crossed, the cells become refractory to the serum starvation, and continue on with the mitotic cell cycle to produce daughter cells. The daughter cells once again become sensitive to the serum starvation until they too cross *Restriction Point* and become refractory. A similar phenomenon occurs in the haploid stages of the yeast *Saccharomyces cerevisiae* with a time threshold referred to as *Start*. Yeast cells starved of nitrogen or glucose, or treated with mating factor prior to *Start* will differentiate into stress tolerant stationary phase cells or commit to the mating pathway (Hartwell et al., 1974)(Hartwell, 1974). Once *Start* is crossed, yeast cells commit to cell division and are refractory to the starvation or mating factor stimulus. We investigated whether the dormancy-like slow growth response to isoleucine starvation in *P. falciparum* exhibited a similar cell cycle stage-dependent refractoriness to nutrient removal.

A culture of highly synchronous young rings was initiated in normal culture medium. At three hour intervals, an aliquot of the culture was removed, washed repeatedly to remove any traces of isoleucine, and resuspended in medium lacking isoleucine. After 30 h or 60 h of incubation (for time points >24 h or <24 h respectively), the parasitemia of the cultures was quantified by flow cytometry to determine the relative growth of each sample over the analysis period.

As expected from earlier experiments, young rings remained at roughly the starting parasitemia over the course of the incubation. However, as the post-invasion age of the culture increased, a notable increase in the final parasitemia became evident (Figure 2.6). A logistic regression performed on the data confirmed that the likelihood of completing the cell cycle increased as the age of the culture at the time of isoleucine removal increased. Based on the logistic model fit to the data, at approximately 30 h post-invasion, 50% of parasites transferred from normal culture medium to isoleucine-lacking medium enter the growth-retarded 'hibernatory' state described

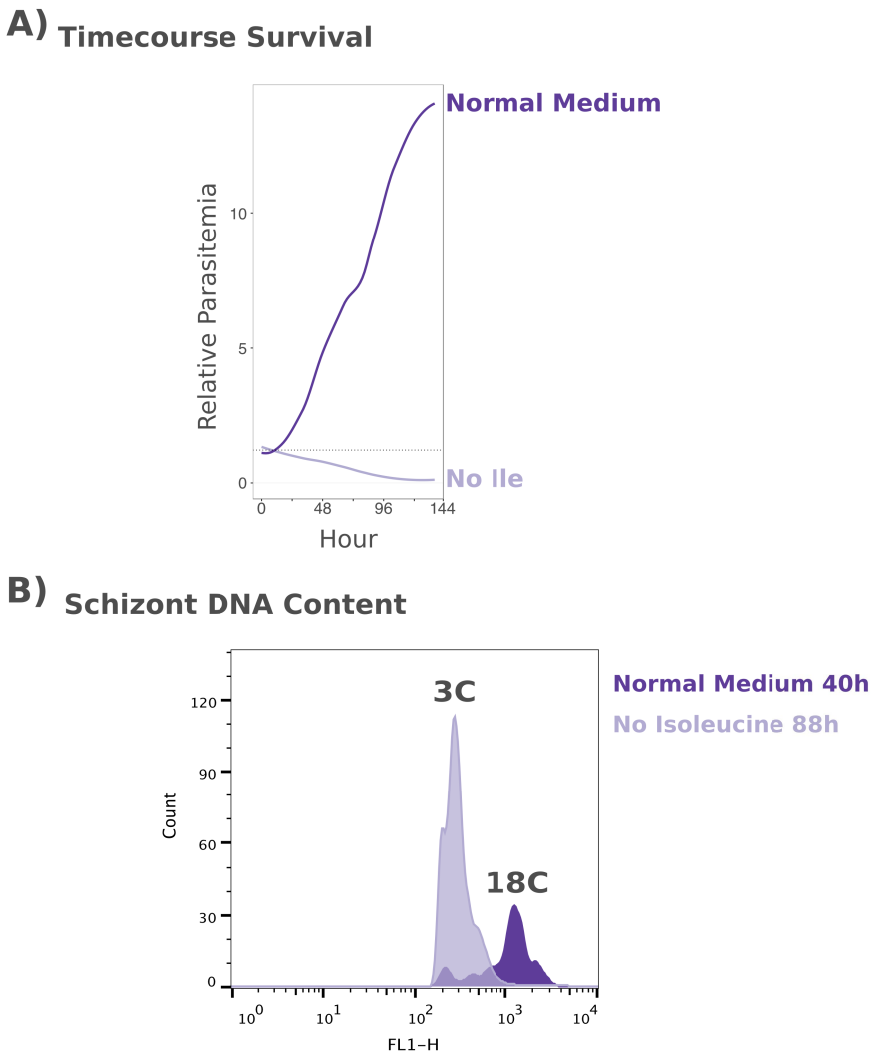

Figure 2.5: **Parasite viability decreases with increasing time of isoleucine withdrawal. A)** Parasitemia of cultures over the course of a 136 h incubation. **B)** SYBR GREEN I staining and flow cytometry was used to determine the average DNA content at the first schizont-enriched time point for each treatment. ”C” refers to the number of genome complements per cell.

by Babbitt *et al*, while the remaining 50% continue through the cell cycle to completion at the normal pace and enter the slow-growth response in the subsequent cycle. Beyond 30 h, an increasing number of parasites complete the cell cycle uninhibited by the absence of isoleucine.

The *Restriction Point* in mammalian cells and *Start* in yeast represent a "point of no return" in commitment to the cell cycle, typically referred to as a cell cycle checkpoint. These checkpoints arise due the irreversible positive-feedback loops regulated by the underlying molecular interactions of cyclins, cyclin-depdendent kinases (CDKs), and their downstream targets. Checkpoints that regulate the exit from the mitotic cycle and into a state of quiescence or differentiation typically occur prior to commencement of S-Phase, and for this reason, are generally referred to as a *G_1 Checkpoints*. The time-dependent binary response of *P. falciparum* to isoleucine withdrawal fits well within the classical definition of a cell cycle checkpoint. However, without evidence for the involvement of cyclins or cyclin-dependent kinases, we consider this assignment to be tentative. The data suggest that some molecular changes occur at around the 30 h into the cell cycle to render the parasite refractory to isoleucine withdrawal.

The isoleucine refractory point coincides with the onset of DNA synthesis

Inferring cellular events in the *Plasmodium* cell cycle based on time estimates alone can be misleading, as the methods used for synchronization are imperfect, and the *in vitro* length of the intraerythrocytic cycle has been reported to range anywhere from 38 h to 50 h for different parasite isolates and clones (Babbitt et al., 2012)(Reilly et al., 2007). To get a more definitive understanding of what this underlying event may be, we attempted to link this response to well-established physiological milestones of the *Plasmodium* cell cycle.

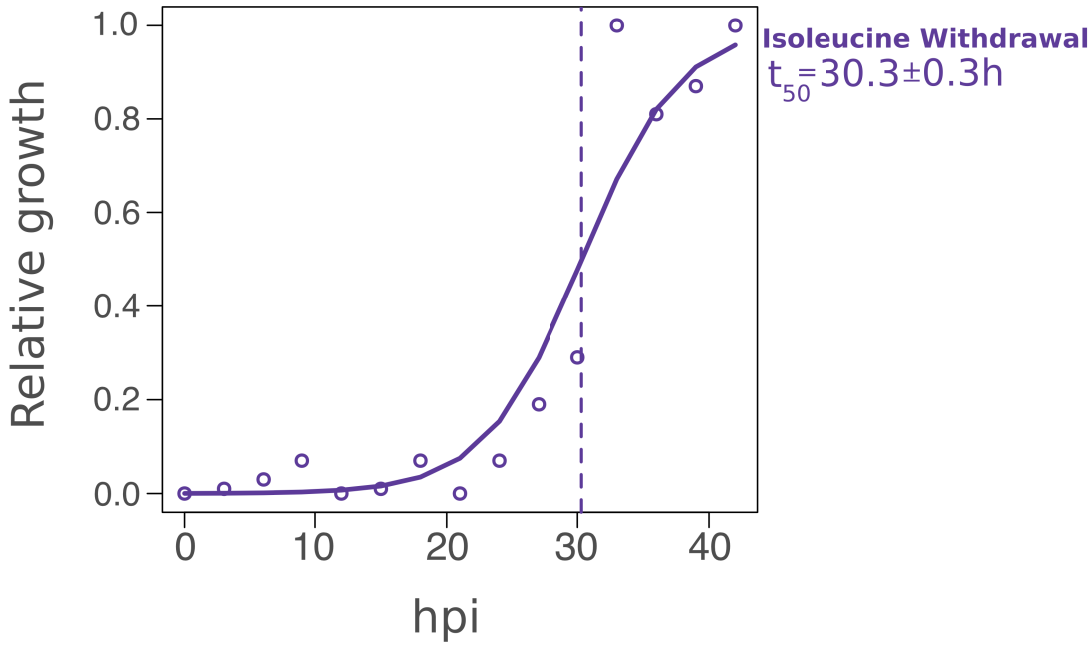

Figure 2.6: **Entry into the dormancy-like growth-retarded state is dependent on the point in the cell cycle at which isoleucine is removed.** Synchronous rings were transferred from normal medium to isoleucine-depleted medium every 3 h over a 45 h cycle. The relative growth was quantified by flow cytometry after 30 h (for > 24 hpi) or 60h (for < 24 hpi) in isoleucine lacking medium. A logistic regression of relative growth on hours post invasion (hpi) shows the likelihood of completing the cell cycle increases with hpi ($p < 2.00x10^{-16}$). t_{50} = the time at which 50% of parasites exhibit growth.

The transition of the parasite from the ring stage to the trophozoite stage is marked by a dramatic change in the permeability of the host erythrocyte to a range of solutes. This *New Permeability Pathway* (NPP) is due to the activation of a parasite-derived or modified pump in the host plasma membrane (Desai, 2012). Isoleucine is one of the biologically relevant solutes affected by the NPP. While erythrocytes display a basal permeability to isoleucine via the host L-system, activation of the NPP increases isoleucine uptake by 5-fold (Martin and Kirk, 2007). *In vitro*, NPP activation renders parasites permeable to sorbitol, which leads to rapid lysis of infected erythrocytes with an active NPP (trophozoites and schizonts), but leaves impermeable cells (rings stages) unharmed. This property provided the basis for the preferred method for ring-stage synchronization (Lambros and Vanderberg, 1979). The ring-to-trophozoite transition and by extension activation of the NPP, should occur well before the 30 h mark of a 45 h parasite cell cycle. However, given the role of the NPP in isoleucine uptake and the feasibilty with which NPP activation can be assayed, we re-determined the timing of the isoleucine refractory point in relation to NPP activation.

As before, synchronous young rings in normal medium were transferred to medium lacking isoleucine at three-hour intervals across the 45 h life cycle. At each time point, duplicate aliquots of culture were treated with 5% w/v sorbitol and re-suspended in normal culture medium for a 72h recovery period. The relative growth of the two treatments is plotted in Figure 2.7A. As with isoleucine withdrawal, a logistic regression fit to the sorbitol treated cultures shows a marked time-dependent response. Sorbitol treated samples dispaly decreased growth with increasing parasite age post-invasion, as would be expected from parasites becoming susceptible to sorbitol lysis as they reach the point of NPP activation. Notably, the logistic model fit to the data maps the 50% relative survival point for sorbitol treament (23.3+/-0.4 h) well in advance of the isoleucine refractory point (in this case, 32.2+/-0.5h).

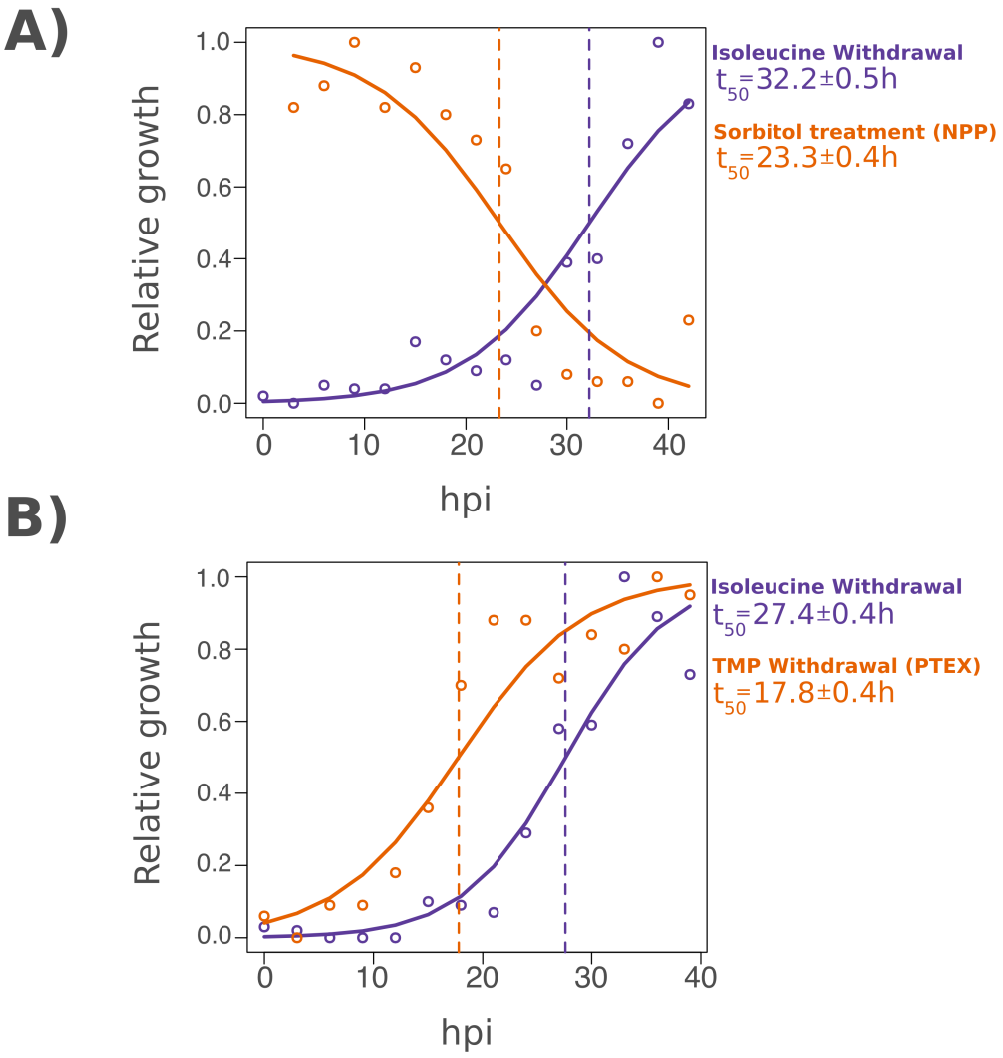

Figure 2.7: **The isoleucine refractory point occurs after establishment of the New Permeability Pathway (NPP) and the *Plasmodium* Translocon of Exported Proteins (PTEX). A** Synchronous early rings were transferred from normal medium to isoleucine lacking medium, or treated with 5% w/v sorbitol then transferred to normal culture medium, every 3 h over a 45 h cycle. Logistic regressions of relative growth on hour post invasion (hpi) shows the likelihood of completing the cell cycle increases with hpi for isoleucine withdrawal ($p < 2.00x10^{-16}$) but decreases for sorbitol treatment ($p < 2.00x10^{-16}$). The logistic models fit to the data predict the t_{50} point for sorbitol treatment to be well in advance of the isoleucine refractory point. **B)** As above, but cells were washed to remove trimethoprim (TMP) to inhibit the PTEX translocon, and transferred to normal medium in the place of sorbitol treatment. Logistic regression models show hpi dependent increase in relative growth for both treatments (Isoleucine withdrawal $p < 2.00x10^{-16}$, TMP withdrawal $p < 2.00x10^{-16}$), though the t_{50} for TMP withdrawal is earlier than the isoleucine refractory point. t_{50} = the time at which 50% of parasites exhibit growth.

Another molecular milestone in the *Plasmodium* cell cycle is the establishment of the *Plasmodium* Translocon of Exported Proteins (PTEX) complex for export of specific parasite proteins across the parasitophorous vacuolar membrane into the host erythrocyte. Protein export is generally thought to occur in the early trophozoite. Beck *et al.* (Beck et al., 2014), produced a transgenic parasite line in which an essential component of the PTEX complex, Hsp101, was modified such that its activity could be regulated by the chemical ligand trimethoprim (TMP). Removal of TMP from the culture medium leads to inhibition of Hsp101 function, blocking protein export by the PTEX complex. When TMP was removed from the culture at the ring stage, parasites arrested growth as morphological rings, but could resume growth without a loss in viability if the culture was resupplemented with TMP within 48 h. However, if TMP was removed from the culture during the mid-trophozoite phase, the parasites completed the cell cycle unperturbed and reinvaded new cells whereupon they arrested at the late ring stage (Beck et al., 2014). This suggests that establishment of the PTEX complex is another checkpoint-like event in the *Plasmodium* cell cycle. Beck *et al.* generously provided us with the 13F10 Hsp101-DD 3D7 clone used in their study so we could test whether the PTEX-dependent checkpoint-like event overlaps with isoleucine refractory point.

Again, synchronous young rings were sampled at three-hour intervals across the cell cycle and transferred either to medium lacking isoleucine (but supplemented with TMP), or normal medium lacking TMP. The relative growth of each sample is plotted in Figure 2.7B. Logistic regression models fit to both treatments show a time-dependent binary response. However, once again, the 50% growth point for PTEX-dependent growth-arrest (17.8+/-0.4 h) is well ahead of the isoleucine-dependent growth-retardation point (here 27.4+/-0.4 h). The 3D7 Hsp101-DD clone used for this assay displays a shorter cell cycle time than our normal NF54 clone, which likely contributes to the slightly earlier timing the isoleucine response point. While it is dif-

ficult to project the PTEX-arrest point onto the sorbitol-NPP point calculated above in our NF54 clone, Beck *et al.* demonstrated that PTEX-arrested parasites were resistant to sorbitol treatment, placing activation of the NPP after PTEX establishment.

The 30-hour time point predicting the response of parasites to isoleucine deprivation lies after two of the molecular events traditionally associated with trophozoite stage of the cell cycle. We next tested where it mapped relative to the transition into S-phase and schizogeny. Synchronous young rings were once again transferred from normal medium into isoleucine-depleted medium at three-hour intervals. At each time point, aliquots were fixed, permeabilized, and stained with SYBR GREEN I for DNA content analysis by flow cytometry (Figure 2.8). A logistic regression model fit to the proportion of parasites with >1C DNA content overlaps with the proportion of parasites continuing normal growth, with 50% of the parasites transitioning from 1C DNA content to >1C content (29.9+/-0.5h) at a point indistinguishable from the point at which 50% of the parasites become refractory to isoleucine starvation (29.4+/-0.4h). In fact, when a regression model was fit with both age post-invasion and proportion of >1C parasites as factors, the DNA content alone predicts the response of the parasites to isoleucine. From the same data, we also tested where the transition from <2C to >2C DNA content occurred relative to the isoleucine-dependent point. While temporally close, the transition to from <2C to >2C (31.7+/-0.5h) occurs after cells have become refractory to the removal of isoleucine (Figure 2.9).

When deprived of extracellular isoleucine, *Plasmodium falciparum* enters a reversible slow growth program of low metabolic activity in which it progresses through the cell cycle at approximately half its normal pace (Figure 2.10). The parasite can complete the cell cycle and invade erythrocytes anew in the complete absence of isoleucine in the medium. However, if isoleucine is removed after DNA

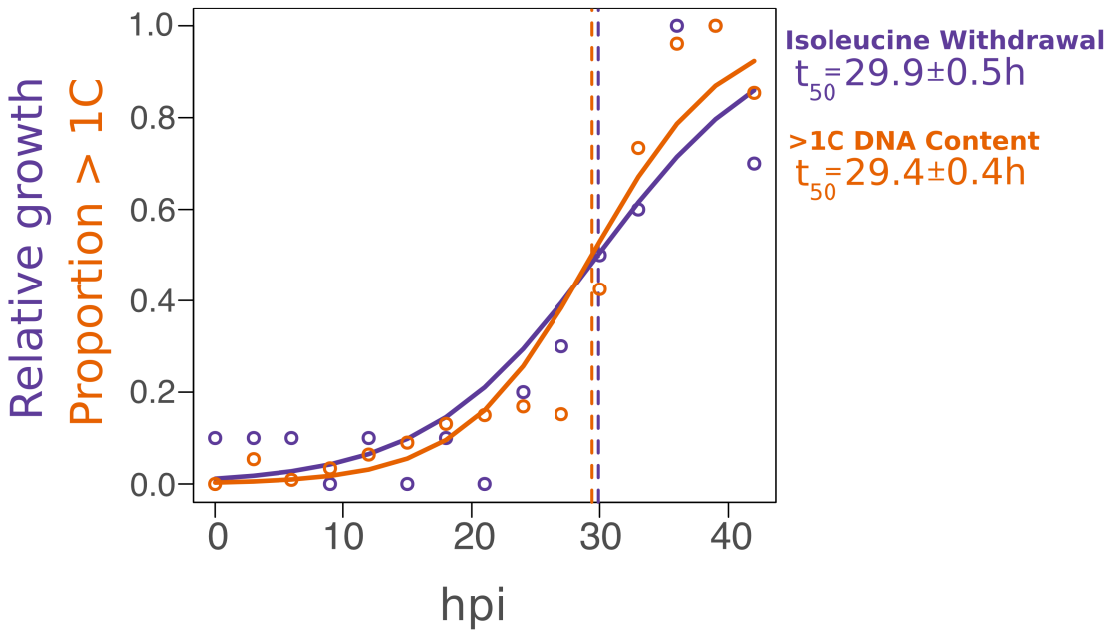

Figure 2.8: **The isoleucine refractory point coincides with the transition into S-phase.** Synchronous ring-stage parasites were transferred from normal medium to isoleucine-depleted medium every 3 h over a 45 h cycle. The relative growth was quantified by flow cytometry after 30 h (for > 24 hpi) or 60 h (for < 24 hpi) in isoleucine-depleted medium. Parallel samples were fixed and permeabilzed to quantify the proportion of parasites with >1C DNA content at each time point by flow cytometry. Logistic models fit to the data show both parasitemia in isoleucine lacking medium ($p < 2.00\text{x}10^{-16}$), and the proportion of parasites with >1C DNA content ($p < 2.00\text{x}10^{-16}$) increase with time. Note that t_{50} values overlap. When both hour post invasion (hpi) and >1C DNA content are treated as factors in a model of growth in the absence of isoleucine, DNA content alone predicts relative growth ($p < 5.38\text{x}10^{-12}$). t_{50} = the time at which 50% of parasites exhibit growth or >1C DNA content.

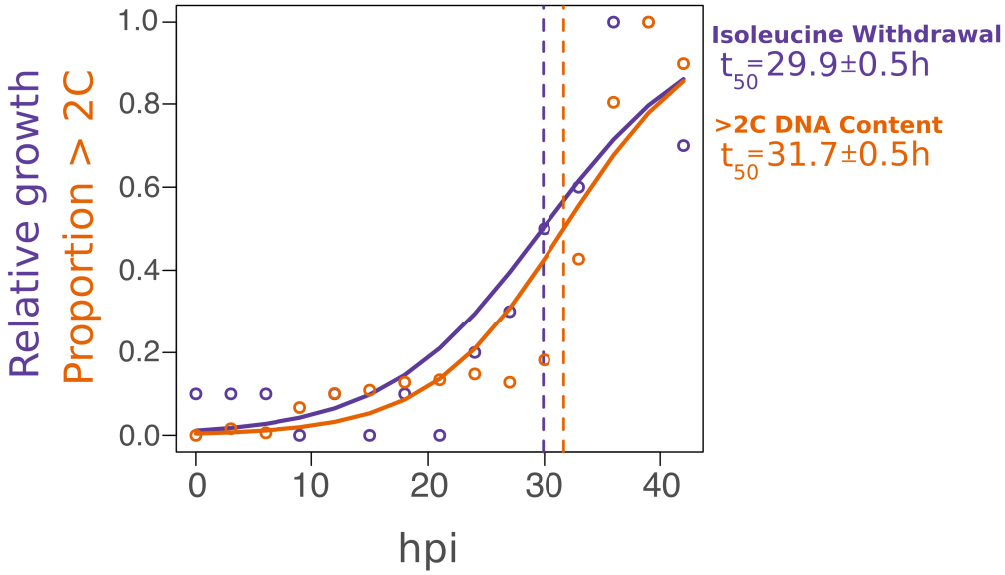

Figure 2.9: **The transition from <2C to >2C occurs after the isoleucine refractory point.** Synchronous ring-stage parasites were transferred from normal medium to isoleucine-depleted medium every 3 h over a 45 h cycle. The relative growth was quantified by flow cytometry after 30 h (for > 24 hpi) or 60 h (for < 24 hpi) in isoleucine lacking medium. Parallel samples were fixed and permeabilzed to quantify the proportion of parasites with <2C or >2C DNA content at each time point by flow cytometry. Logistic models fit to the data show both parasitemia in isoleucine lacking medium ($p < 2.00x10^{-16}$), and the proportion of parasites with >2C DNA content ($p < 2.00x10^{-16}$) increase with time. The t_{50} point for the transition to >2C DNA content occurs after the isoleucine refractory point. t_{50} = the time at which 50% of parasites exhibit growth or >1C DNA content.

replication has commenced, the parasite does not enter the slow program and instead continues its mitotic cycle at the normal pace. This behavior is reminiscent of classic G_1 checkpoint events such as the *Restriction Point* in mammalian cells and the *Start Checkpoint* in *S. cerevisiae*. It remains to be shown whether this stage-dependent response can be directly attributed to events involving cyclins and CDKs of the cell cycle, as it is in other system. The mechanism by which the parasite detects isoleucine withdrawal to modulate its growth rate in G_1 also remains unknown, however, recent evidence the artemisinin-resistance literature offers some potential clues.

*Pf*PI3K inhibition induces growth retardation similar to isoleucine starvation

Our understanding of the molecular basis for delayed-clearance of certain field isolates upon artemisinin treatment has advanced greatly in recent years. The ring-stage of any *Plasmodium* isolates (artemisinin "resistant" or sensitive) is much less sensitive to artemisinin than later stages of the parasite (Klonis et al., 2013). This is because the heme released from hemoglobin digestion in trophozoite and schizont stages activates the drug's epoxide ring, leading to oxidative damage (Klonis et al., 2011).

In rings, a brief six-hour treatment with a sub-lethal dose of artemisinin induces a slowing of the cell cycle reminiscent of that induced by isoleucine deprivation (Klonis et al., 2011). When high, clinically-relevant doses of dihydroartemisinin (DHA) are used *in vitro*, only artemisinin-resistant field isolates are able to recover after growth-retardation (Dogovski et al., 2015). This DHA-induced slow growth likely accounts for the delayed ring clearance phenotype observed *in vivo*. Thus, resistance to artemisinin is not due to an exit from the mitotic cycle into a dormant state, as originally proposed (Figure 2.1). Rather, resistance can be attributed to the ability

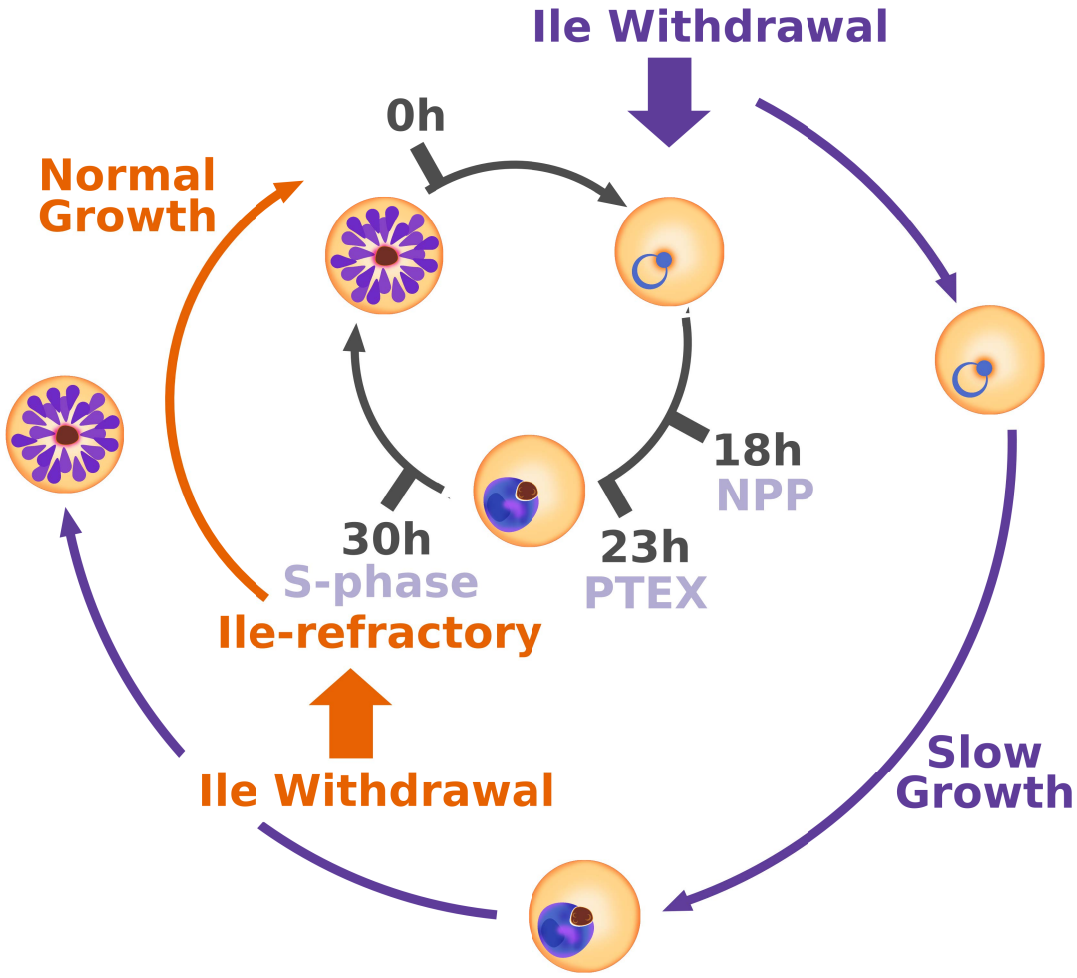

Figure 2.10: ***Plasmodium falciparum* enters a cell cycle stage-dependent slow growth program upon isoleucine starvation.** If isoleucine is removed in the early stages of the cell cycle, *P. falciparum* enters a state of slow growth in which it can complete schizogeny and reinvade new erythrocytes. If isoleucine is removed after approximately 30 h post-invasion, the parasite continues schizogeny at the normal pace without retarding growth. This refractory point coincides with the onset of S-phase and is well after establishment of the New Permeability Pathway (NPP) and PTEX translocon.

of parasites to recover and resume growth after a transient slowing of the cell cycle, much like we have observed during isoleucine starvation. The mechanistic basis of this ability to recover from artemisinin-induced growth retardation is still being elucidated. However, recent observations have identified additional similarities to the isoleucine slow growth response.

Genomic analyses of delayed clearance isolates identified mutations in the kelch-propeller domain of the previously uncharacterized K13 gene (PF3D7_1343700) (Ariey et al., 2014). When these mutant K13 alleles of artemisinin-resistant field isolates were reverted back to the 3D7 "wild type" allele, the parasites were rendered susceptible to DHA treatment (Straimer et al., 2015). Similarly, the introduction of the different mutant K13 alleles into artemisinin sensitive lab strains rendered parasites resistant to clincially-relevant DHA concentrations (Ghorbal et al., 2014)(Straimer et al., 2015). These results have led to the conclusion that mutations in K13 are likely responsible for the observed *in vivo* delayed clearance phenotype.

A single study has put forth evidence for the molecular basis underlying K13-mediated artemisinin resistance. Mbengue *et al.* reported that, in the absence of hemoglobin digestion, artemisinin derivatives specifically inhibit the *Plasmodium* Class III Phosphositide 3-kinase (PI3K) (PF3D7_0515300) (Mbengue et al., 2015). The K13 protein product normally targets PI3K for destruction by the ubiquitin-proteasome pathway, however, K13-mutations decrease the interaction needed for ubiquitination, leading to higher protein levels of *Pf*PI3K. As a result, parasite lines with higher PI3K levels exhibit increased resistance to artemisinin derivatives (Mbengue et al., 2015).

Class III PI3Ks are known for catalyzing the assembly protein complexes at intracellular membrane surfaces. They are essential components of the endocytosis

and autophagy machinery, two processes used for the acquisition and reclamation of amino acids (Backer, 2008). In mammalian cells, several studies have also implicated the Class III PI3K Vps34 in sensing and signaling of intracellular amino acid levels as part of the mTOR pathway (Gulati et al., 2008)(Munson et al., 2015)(Yoon et al., 2011)(Nobukuni et al., 2005)(Byfield et al., 2005)(Yan et al., 2009); a pathway known to regulate progression through the cell cycle in response to nutrient levels.

The *Plasmodium falciparum* PI3K has been previously implicated in the endocytosis and trafficking of hemoglobin from the host cell into the parasite digestive vacuole. Chemical inhibition of *Pf* PI3K causes accumulation of hemoglobin-containing vesicles in the parasite cytoplasm (Vaid et al., 2010). Artemisinin has also been reported to block hemoglobin import (Hoppe et al., 2004) (Klonis et al., 2011). Vaid *et al.* concluded that PI3K inhibitors induces growth-retardation upon blocking hemoglobin uptake, although they did not directly measure advancement through the cell cycle (Vaid et al., 2010). Nonetheless, this potentially explains the mechanism of growth retardation observed upon artemisinin treatment.

We revisited this effect by treating young ring NF54 parasites (artemisinin-sensitive) to a high, six-hour dose of the PI3K inhibitor LY294002 using a method adapted from the standard Ring-stage Survival Assay (RSA) used to evaluate artemisinin resistance (Witkowski et al., 2013). By monitoring the DNA content of the culture at 32 h and 72 h after treatment, it was evident that PI3K-inhibited cells were growth-retarded much like parasites deprived of extracellular isoleucine (Figure 2.11). PI3K-inhibited or isoleucine-starved parasites displayed a predominantly 1C DNA content at 32 h when controls had progressed into schizogeny. By 72 h post-treatment, controls had completed the cell cycle and were predominantly at the 1C stage of the second generation, while treated parasites were lagging in S-phase of the first generation.

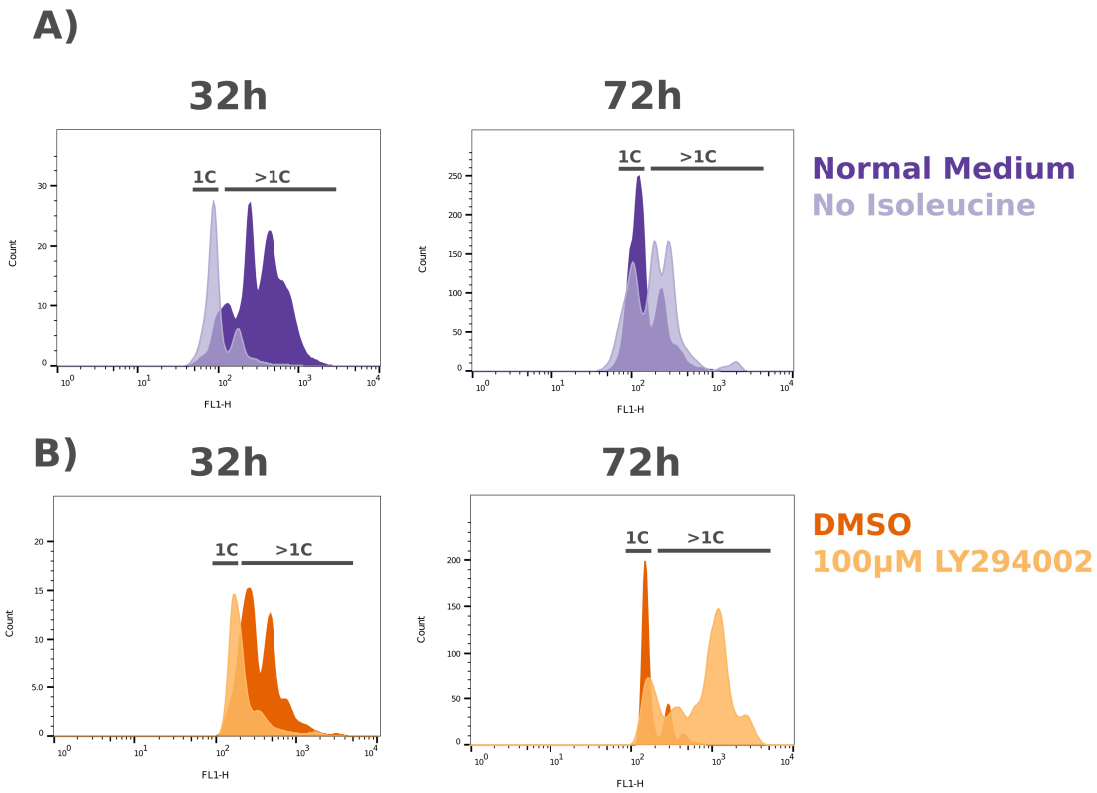

Figure 2.11: **PI3K inhibtion slows the cell cycle in a manner reminiscent to isoleucine starvation induced slow growth.** Rings at 0-3h post-invasion were **A)** washed and transferred to isoleucine lacking medium or returned to normal medium as a control, or **B)** treated with a six-hour pulse of the PI3K inhibitor LY294002 (100 μM) or DMSO. DNA content was quantified by flow cytometry at 32 h and 72 h post-treatment.

The artemisinin-resistant K13 allele confers an increased growth rate

Direct *Pf* PI3K inhibition retards the *Plasmodium* cell cycle. It is not clear whether this is due to inhibition of amino acid acquisition or another mechanism. Artemisinin-resistant K13 mutants have been reported to have increased intracellular *Pf* PI3K levels and increased *Pf* PI3K activity (Mbengue et al., 2015). Given that *Pf* PI3K inhibition can slow growth, we investigated whether elevated *Pf* PI3K activity can enhance growth. Straimer *et al.* produced lines of several artemisinin-resistant field clones that are syngenic to originals save for reversion of the single amino acid mutation in the K13 gene back to the artemisinin-sensitive allele (Straimer et al., 2015). We evaluated the growth of one of these clones and its artemisinin-resistant counterpart (K13 allele R593T, isolated from Battambang, Cambodia) in normal culture medium over 18 days of growth. The artemisinin-resistant isolate displayed a significant increase in growth rate relative to its revertant counterpart (Figure 2.12A).

Plasmodium falciparum growth *in vitro* is unaffected by variation in the concentration of isoleucine above 20 μM (standard RPMI 1640 concentraion is 382 μM) (Liu et al., 2006). Below 20 μM, the parasite exhibits a concentration dependent decrease in growth before entering the dormancy-like slow growth state (Liu et al., 2006) (Babbitt et al., 2012). We found 8 μM isoleucine to be the lowest concentration capable of supporting longterm, albeit slow growing, culture. We assayed the growth rate of the artemisinin-resistant field isolate alongside the revertant counterpart over 18 days in 8 μM isoleucine. The low isoleucine treatment increased the doubling time of both isolates, however, the growth rate of artemisinin-resistant isolate remained notably higher than the revertant (Figure 2.12B). When the growth rate of the two parasite genotypes in both forms of media was analyzed in a multifactor regression, no genotype by media interaction was detected (ie: the difference in growth rate between two parasite genotypes is not increased or decreased by low isoleucine).

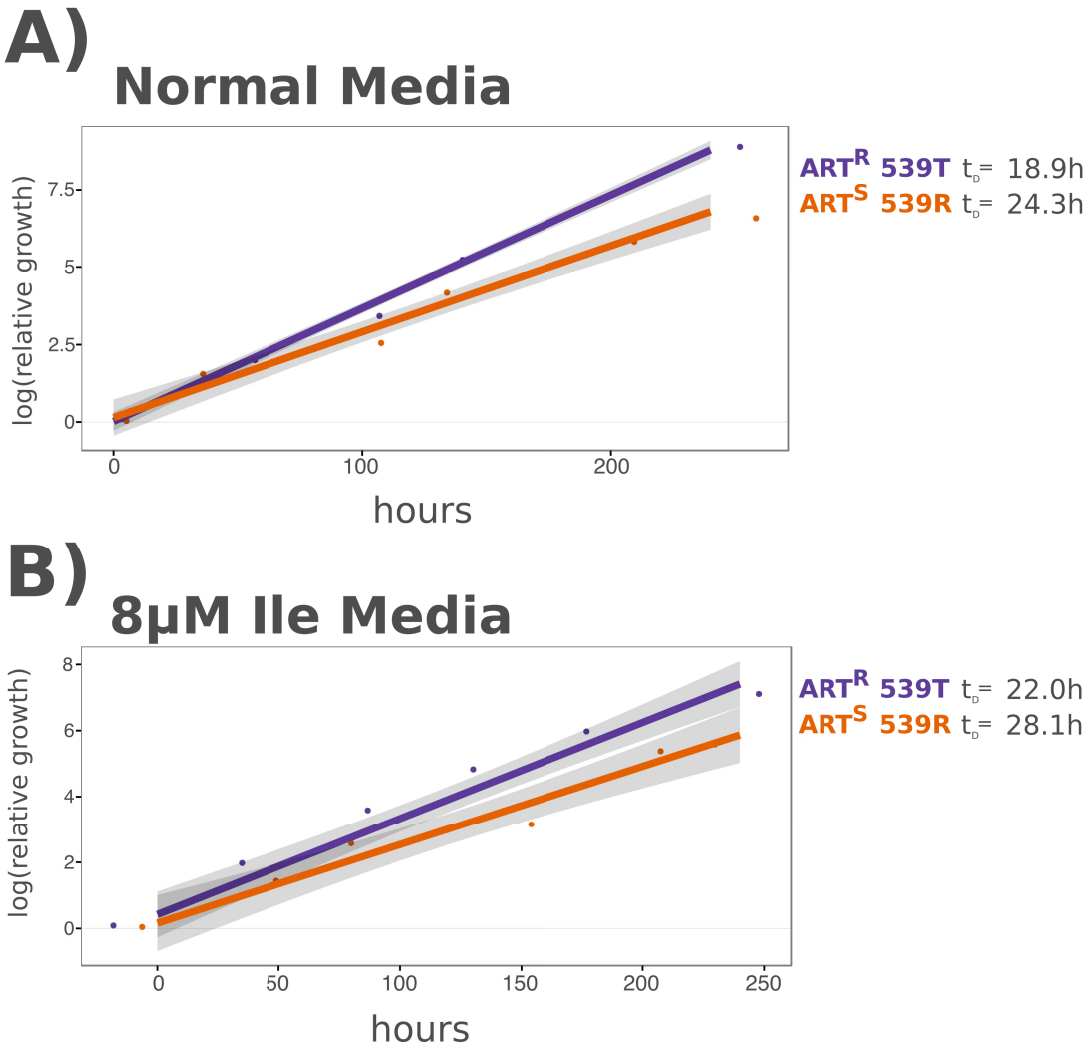

Figure 2.12: **An artemisinin-resistant isolate has higher growth rates relative to a sensitive revertant line, both in normal and in low isoleucine medium.** Growth rates of an artemisinin-resistant isolate with a 539T K13 allele and its syngenic 539R artemisinin-sensitive revertant counterpart were determined by linear regression after monitoring growth in **A)** normal medium and **B)** low (8 μM) isoleucine over 18 days. While both resistance status (p = 0.0013) and media type (p = 0.0124) affected growth rate, no genotype by medium interaction was detected (p = 0.8709). Doubling time, t_D, was calculated from regression coefficients. Shading indicates the 95% confidence interval of the model.

Together, these data show that the single amino acid change in the K13 gene that confers artemisinin-resistance also confers an increased rate of growth. It is not clear whether this growth is due to faster progression through the cell cycle, production of increased merozoite numbers, or a combination of several factors. The fact that *Pf* PI3K inhibition retards cell cycle progression (Figure 2.11), and that artemisinin-resistant K13 mutants have higher *Pf* PI3K levels (Mbengue et al., 2015), suggests that the incraesed growth rate may be due to faster progression through the cell cycle as a result of increased *Pf* PI3K activity.

Artemisinin-resistance confers increased recovery upon isoleucine starvation and extends the G_1 phase of the cell cycle

We next evaluated the response of the artemisinin-resistant K13 mutant and its revertant to prolonged incubation in the complete absence of extracellular isoleucine. As done earlier with NF54 parasites (Figure 2.2), young rings of the artemisinin-resistant isolate and the revertant parasites were washed repeatedly then transferred to isoleucine-lacking culture medium to induce dormancy-like slow growth. After 72 h of starvation, isoleucine was added back to the medium and the parasites were cultured for an additional 72 h of recovery. The artemisinin-resistant mutant displayed robust recovery from starvation (Figure 2.13A), as expected from our earlier experiments with our NF54 clone (Figure 2.2), and the initial report using a 3D7 line (Babbitt et al., 2012). Surprisingly, the revertant line was not able to recover from the growth retardation induced by prolonged isoleucine starvation, displaying a final parasitemia of only 60% of its starting parasitemia after recovery. The genetic background of this parasite isolate must differ from NF54 and 3D7 in a manner that renders it vulnerable to prolonged amino acid starvation. However, the change of a single amino acid in the K13 gene reverses this effect, allowing the parasite to re-

cover from isoleucine induced growth retardation. The fact that this same mutation also allows the parasite to recover from the growth retarding effects of artemisinin derivatives, further suggests a common underlying mechanism of growth regulation.

In a transcriptomic study of (non-syngenic) artemisinin-resistant and sensitive field isolates, Mok *et al.* observed that artemisinin-resistant isolates appeared to have an extended G_1 phase of the cell cycle relative to sensitive isolates when grown in normal culture medium *in vitro* (Mok et al., 2015). This finding seems to be at odds with our observation that the artemisinin-resistant line displays an increased rate of growth. However, when we measured the DNA content of the K13 mutant and the revertant line after 72 h of isoleucine starvation, the artemisinin-sensitive revertant displayed a much higher proportion of cells with greater than 1C DNA content (Figure 2.13B and C). This suggests that the artemisinin-resistant mutant is taking longer to reach S-phase during isoleucine-starvation induced slow growth. This could be explained either by to the resistant mutant having a slower overall growth rate, which is contradicted by our observations in both normal and low isoleucine media (Figure 2.12), or by an extended G_1 phase, as suggested by Mok *et al.* (Mok et al., 2015). Artemisinin is least effective during ring stages of G_1 prior to the onset of hemoglobin digestion (Klonis et al., 2013). An extension of G_1 could potentially contribute to the resistance phenotype by increasing the amount of time the parasite remains in its least vulnerable state. It is not clear how or if this extension of G_1 contributes to increased recovery from prolonged isoleucine starvation.

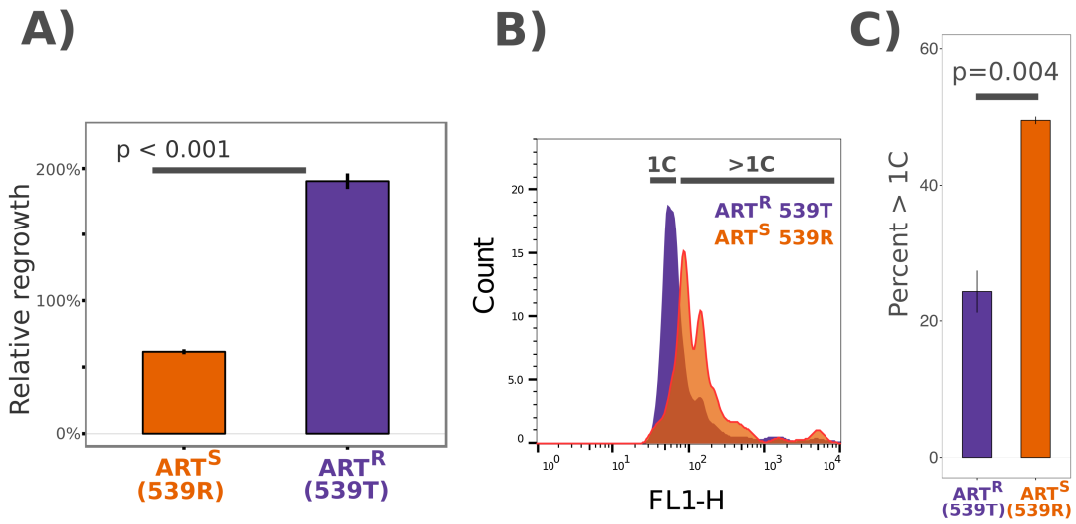

Figure 2.13: **An artemisinin-resistant isolate exhibits increased survival and an extended G_1-phase upon prolonged isoleucine starvation. A)** Young ring intiated cultures of the artemisinin-resistant isolate (539T) and its syngenic artemisinin-sensitive counterpart (539R) were washed and transferred to isleucine-depleted medium for 72 h, then supplemented with normal culture medium for 72 h of regrowth. **B)** A representative histogram of SYBR GREEN I stained DNA content of the artemisinin-resistant (539T) and sensitive (539R) cultures after 72 h of isoleucine starvation as measured by flow cytometry. **C)** A summary plot of the proportion of parasites with greater than 1C DNA content after 72 h of isoleucine starvation. P-values represent t-test of three biological replicates.

Discussion

In *S. cerevisiae*, transition into quiescence upon nutrient limitation has longed served as a model for cellular dormancy. When one of a number of nutrients is exhausted, yeast appears to reversibly arrest transit through the cell cycle prior to DNA replication, and enter a state of low metabolic activity in which the cells can remain viable for an extended period of time ("G_0"). Transcriptomic profiling of yeast batch cultures as they enter stationary phase quiescence demonstrated a progressive slowing of growth as nutrients were exhausted and the eventual induction of a stress response trancriptional program as dormancy was established (Saldanha et al., 2004). With the exception of a stress response trancriptional program, many of these characteristics of yeast quiescence fit those observed by Babbit *et al.* in their initial description of the *P. falciparum* response to isoleucine starvation namely, initial transcriptomic slowing of the cell cycle, apparent arrest prior to DNA synthesis, decreased metabolic activity, and maintenance of viability over extended starvation. However, more recent studies of the yeast quiescence response using modern genomic tools and gene knockout collections have complicated, instead of clarified, the understanding of this response. Studies have shown that the stress adaptations and metabolic changes once thought to be unique to the G_0 state can be induced in other phases of the cell cycle (Laporte et al., 2011). Furthermore, experiments controlling yeast growth by nutrient limitation in chemostat culture demonstrated that the higher the growth rate was limitation, the longer cells spent in G_1 of the cell cycle, and the more the transcriptomic profiles resembled those of quiescent cells in stationary phase attained in batch cultures (Brauer et al., 2008). Combined, these data suggest that dormancy or quiescence in yeast may not be due to a unified differentiation program, but instead, an extreme slowing of the cell cycle with a coincident induction of metabolic and transcriptional stress responses. Our study of the *P. falciparum* response to isoleucine

starvation suggest a similar conclusion.

We repeated the isoleucine starvation protocol described by Babbitt *et al.* using an NF54 clone of *Plasmodium falciparum*. Over the short term, the parasites appeared to slow progression through the cell cycle and remain in G_1, as Babbitt *et al.* had described. However, when tracked for extended periods, it became clear that the parasite continued through the cell cycle, completing schizogeny and reinvading, at a slow pace. Despite some death over the course of starvation, upon addition of isoleucine the slow growing parasites readily recovered and resumed normal growth. *P. falciparum* does not appear to enter a programmed state of dormancy during the asexual cycle upon amino acid starvation. Nonetheless, the ability to attenuate and resume growth is likely advantageous *in vivo*, where the parasite can experience transient periods of low isoleucine in malnourished human hosts (Baertl et al., 1974).

It is not clear how the parasite is able to continue the cell cycle without a source of extracellular isoleucine. Some isoleucine may be reclaimed from existing cellular proteins through autophagy or proteasomal degradation, but it seems unlikely that this would be sufficient to support completion of the cell cycle. A more likely source would be the small amount of other erythrocyte proteins imported and degraded along with hemoglobin. If this were the case, it may explain why the artemisinin-sensitive revertant line was unable to survive prolonged amino acid starvation. Chloroquine resistance genes are at or near fixation throughout the regions in which artemisinin resistance has emerged (Muhamad et al., 2011). The chloroquine resistance mutations in the *Pf*CRT gene cause digestion defects in the parasite's digestive vacuole, and parasites carrying the mutations have been shown to be much more reliant on extracellular amino acids (in addition to isoleucine) for normal growth (Lewis et al., 2014). Thus, the artemisinin-sensitive revertant line may suffer from greater isoleucine starvation than chloroquine sensitive parasites (such as

the NF54 clone used throughout this study) do to its vacuolar digestion defect. This question could be addressed by testing syngenic parasite lines that only differ in their chloroquine resistance alleles (Sidhu et al., 2002).

Babbitt *et al.* concluded from their observations of dormancy-like state that the regulation of cell cycle progression in *P. falciparum* is a passive process, determined mainly through limiting reaction rates, with isoleucine starvation decreasing translational processivity, and thereby arresting growth (Babbitt et al., 2012). Similar conclusions were drawn from similar observations in yeast, until the genetic factors responsible for nutrient-dependent growth rate modulation, namely the TORC1 pathway, were discovered (Loewith and Hall, 2011). Several pieces of evidence contradict interpretation of passive growth regulation. We found that the K13 revertant clone is less capable of surviving prolonged isoleucine starvation than its syngenic artemisinin-resistant counterpart. If growth retardation were due to translational stalling in the absence of isoleucine-charged tRNA, it would be expected to effect all parasite genotypes equally. Furthermore, several *Plasmodium falciparum*-specific inhibitors of tRNA-synthetases and translation initiation factors have been described (Herman et al., 2015)(Hoepfner et al., 2012)(Baragaña et al., 2015). All are potently lethal, and none produces a dormancy-like state like that observed from isoleucine starvation. Perhaps the most intriguing evidence to suggest that growth rate regulation in the parasite is an active process, however, is our observation that cells become refractory to isoleucine removal once DNA synthesis commences. This suggests, like in other organisms, the parasite is able to sense and respond to its environment in G_1, but ignores this sensing mechanism once the mitotic cycle initiated.

Yeast deprived of nitrogen, phosphate, glucose, or any of several other nutrients during early G_1 phase will slow growth and enter the quiescence program described above. If the nutrient is removed after a specific point late in G_1, however, the cell

proceeds with S-phase and mitosis, then enters the quiescent state in the subsequent generation (Hartwell, 1974). A similar process occurs in yeast for differentiation into budding cells when stimulated with mating factor (Hartwell et al., 1974), and an analogous phenomenon exist in mammalian cells starved of growth factors or amino acids (Pardee, 1974)(Saqcena et al., 2013). The point at which these cells "decide" to arrest growth or continue with mitosis is known as a G_1 checkpoint. We observed that *P. falciparum* will enter dormancy-like slow growth when deprived of isoleucine in G_1, but continues on with DNA-replication and schizogeny if isoleucine is removed after S-phase has commenced (at approximately ~30 hpi). This phenomenon follows the same behvior as the G_1 checkpoints in yeast and mammalian cells. In those systems, the G_1 checkpoint is determined through the interaction of cyclins and cyclin-dependent kinases (CDKs) which activate a positive feedback loop of S-phase transcription factors to irreversibly drive the cell cycle forward. The isoleucine refractory point we have observed in *Plasmodium falciparum* may follow a similar mechanism, however, we have no means of verifying it at present. The *P. falciparum* genome encodes three or four putative cyclins and five kinases of the CDK family, all of which display periodic expression profiles across the intra-erythrocytic cycle. Two CDKs (PF3D7_1014400, PF3D7_1014400), and a single cyclin (PF3D7_1463700), display changes from high expression in G_1 to low expression in schizogeny with an inflection point at roughly 30 h post invasion (Bozdech et al., 2003), making them potential candidates as regulators of the G_1/S transition. It would be interesting to investigate if manipulating the expression or stabiltity of these candidate proteins affects the timing of the isoleucine refractory point and entrance into S-phase.

Once the isoleucine refractory point is passed, the parasite is able to complete schizogeny, generating upwards of twenty or more merozoites, without a source of isoleucine. In their study, Babbitt *et al.* demonstrated that parasites maintained in low isoleucine media were no less capable of surviving isoleucine starvation than those

maintained in high isoleucine media, and that parasites instantly responded to the removal or readdition of isoleucine by phosphorylating IF2α (Babbitt et al., 2012). Together, these data suggest that it is unlikely that the parasite maintains an accessible intracellular pool of isoleucine. However, yeast starved of nitrogen (required for amino acid synthesis) after the G_1 checkpoint are similarly capable of undergoing S-phase and mitosis without an amino acid supply (Hartwell, 1974). The parasite, as well as yeast, may simply recycle existing proteins or produce the minimum proteome necessary in advance of the G_1-S checkpoint to sustain completion of the cell cycle.

In yeast, G_1 is the phase of the cell cycle at which cellular size (*i.e.* volume and mass) is determined. Yeast cells in which the G_1 phase has been artificially lengthened can attain much larger sizes than controls by the time they reach the G_1 checkpoint (Popolo et al., 1982). Extension of the G_1 ring and trophozoite stages of *P. falciparum* have a similar effect in establishing the size and nutrient content of the parasite at the onset of S-phase. It is well established that certain parasite isolates produce greater numbers of merozoites than others (Reilly et al., 2007). Perhaps an elongated G_1 phase allows increased nutrient acquisition for merozoite production during schizogeny. This would explain the apparent discrepancy we observed between the growth rate and G_1 length of the K13 mutant isolate and its revertant. Perhaps the mutant is able to produce more merozoites per cycle due to its prolonged G_1 phase, thereby increasing its effective growth rate.

Early studies of both artemisinin resistance and isoleucine-starvation led authors to put forth similar theories of dormancy-like strategies employed by the parasite to survive these seemingly different forms of stress. Our present observations, along with more recent studies by others of artemisinin survival in field isolates, suggest a different model. However, there is reason to suspect recovery from both treatments involves overlapping molecular mechanisms. Figure 2.14 summarizes the similarities

between recent findings in the artemisinin-resistance literature and observations generated in this study. Central to both responses is the observation that the treatments induce a retardation of parasite growth, and do not activate a programed differentiation into a dormant state. Surviving parasites are able to endure growth retardation and resume normal growth. Artemisinin-susceptible parasites cannot. The same single amino acid change in the K13 gene that renders parasites capable of recovery from artemisinin treatment also confers increased recovery from prolonged isoleucine starvation.

It is not yet understood how artemisinin and its derivatives induce growth retardation. However, artemisinin has been reported to be a direct inhibitor of *Pf*PI3K (Mbengue et al., 2015), and we have demonstrated that a PI3K inhibitor unrelated to artemisinin is capable of inducing growth retardation similar to that observed upon isoleucine starvation. Likewise, artemisinin-resistant parasites carrying K13 mutations have been reported to have higher intracellular levels and activity of *Pf*PI3K (Mbengue et al., 2015), and we have found that one such mutant displays an increased growth rate in normal or low isoleucine media, further implicating *Pf*PI3K activity and regulating parasite growth. The mechanism by which *Pf*PI3K would regulate growth is unknown. In mammalian cells, the human ortholog (*Hs*Vps34) has been implicated in detection of amino acids upstream of mTOR in the TORC1 pathway, the central nutrient and growth signalling pathway in eukaryotes (Gulati et al., 2008)(Munson et al., 2015)(Yoon et al., 2011)(Nobukuni et al., 2005)(Byfield et al., 2005)(Yan et al., 2009). As discussed in the ensuing chapter, the TORC1 pathway has been largely lost in *Apicomplexa*, though we report evidence that at least one other residual component of TORC1 is needed for *P. falciparum* to recover from prolonged isoleucine starvation. *Pf*PI3K may regulate parasite growth by activating a reduced, but residual growth-signalling pathway.

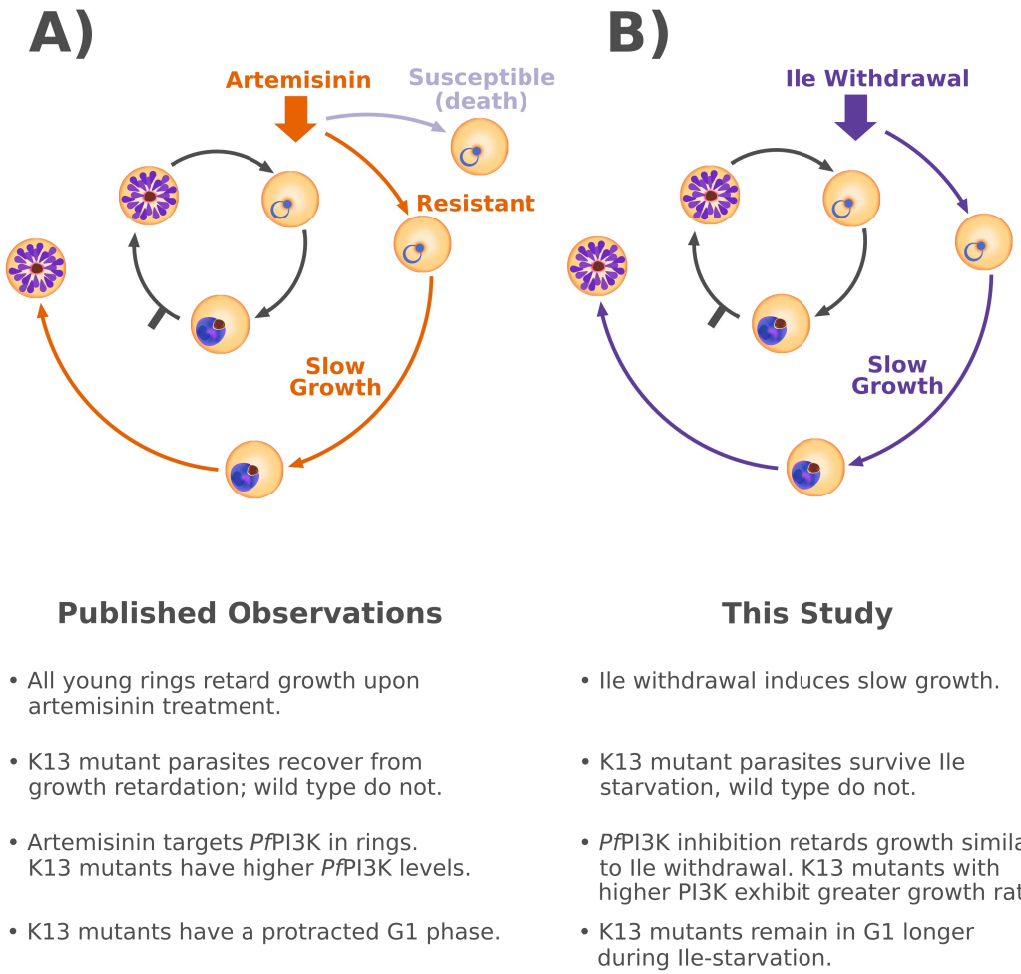

Figure 2.14: **Similarities between survival of artemisinin treatment and isoleucine starvation suggest common underlying mechanisms.** The initial models of artemisinin resistance and isoleucine starvation proposed programmed states of dormancy (see Figure 2.1). Recent data by others and from this study suggest otherwise. Nonetheless, similarities between the methods of survival of the two forms of stress suggest they may require similar underlying pathways for survival. **A)** All young rings treated with artemisinin undergo growth retardation. Only parasites with mutations in the kelch-propeller domain of the K13 gene are able to resume growth and recover. The *Pf*PI3K protein has been reported to be the molecular target of artemisinin in ring stage parasites, and resistant parasites exhibit higher intracellular levels of PI3K, though no published study to date has connected *Pf*PI3K to growth inhibition and recovery. Resistant K13 mutants have been suggested to have an elongated G_1-phase of the cell cycle. **B)** Isoleucine withdrawal from young rings induces slow growth, not arrest. Parasites with artemisinin-resistant K13 alleles exhibit greater recovery from prolonged isoleucine starvation than sensitive parasites. Inhibition of *Pf*PI3K with non-artemisinin inhibitors induces growth retardation similar to isoleucine starvation. K13 mutants with elevated *Pf*PI3K display elevated growth under all conditions, suggesting *Pf*PI3K activity may be central to growth regulation and recovery in *P. falciparum*. K13 mutants display a protracted G_1-phase during isoleucine starvation, confirming previous observations in other isolates.

An alternative possibility is that *Pf* PI3K regulates growth by directly affecting the acquisition of amino acids. In other eukaryotes, Class III PI3K kinases play a central role in vesicular trafficking, including coordinating the trafficking of endocytotic and phagocytotic vesicles (Backer, 2008). *Plasmodium falciparum* imports hemoglobin from the host cell through an analogous mechanism, and *Pf* PI3K inhibition by Wortmanin or LY294002 has been shown to inhibit the import process (Vaid et al., 2010). Additionally, *Pf* PI3K inhibitors are more potent when applied to cultures in media containing isoleucine as the only extracellular amino acid, presumably because blocking hemoglobin import renders extracellular amino acids the only remaining source (Vaid et al., 2010). Two independent studies have reported that artemisinin also inhibits hemoglobin endocytosis in *Plasmodium falciparum* (Hoppe et al., 2004) (Klonis et al., 2011). Thus, artemisinin may block hemoglobin import through *Pf* PI3K inhibition, and effectively cause the same amino acid starvation-induced slow growth as extracellular isoleucine withdrawal.

There is further circumstantial evidence suggesting that artemisinin may inhibit hemoglobin import and amino acid acquisition in early stage parasites. As mentioned earlier, chloroquine resistance causes digestion defects and increases the reliance on extracellular amino acids. When an artemisinin-resistance allele was introduced into a 3D7 (chloroquine sensitive) genetic background, the transgenic line displayed higher levels of artemisinin resistance than when introduced into a Dd2 (chloroquine resistant) background (Ghorbal et al., 2014)(Straimer et al., 2015). If the K13 mutations conferring artemisinin resistance lead to increased hemoglobin import through *Pf* PI3K elevation, it may partially overcome the fitness load of the chloroquine sensitive allele. In support of this, we found that the artemisinin resistant lines display higher growth rates in both normal and low isoleucine media, suggesting the single amino acid change that confers artemisinin resistance also confers a fitness advantage *in vitro*. This possibility could have major implications for the spread of artemisinin

resistance.

Methods

Parasite Strains

The NF54 clone used for most experiments was produced by and obtained from the lab of David A. Fidock at Columbia University (Adjalley et al., 2011). The The Hsp101-DD conditional PTEX export 3D7 clone was produced by and obtained from the lab of Dan Goldberg at Washington University (Beck et al., 2014). The K13 R539T artemisinin resistant isolate (Cam3.I IPC 5202) was isolated from a patient Battambang province, Cambodia, in 2011. It was obtained from the Malaria Research and Reference Reagent Resource Center (MR4) for distribution by BEI Resources NIAID, NIH, product number MRA-1240, and originally contributed by Didier Ménard. The corresponding revertant line, Cam3.I_rev, was also obtained from the BEI resources NIAID, NIH, product number MRA-1252, and was contributed by David A. Fidock (Straimer et al., 2015).

Parasite Culture and Media

Parasites were cultured using standard methods (Jensen and Trager, 1977) in flasks gassed with a mixture of 90% N_2, 5% CO_2, 5% O_2 (Airgas, #Z03NI9022000033). Normal culture medium consisted of RPMI 1640 with L-glutamine and 25 mM HEPES (Corning, #10-041-CV), with 5.0g/L Albumax II Lipid-Rich BSA (ThermoFisher Scientific, #11021029), 3.7mM Hypoxanthine, and 50μg/mL gentamicin. The Isoleucine deficient medium consisted of 10.3g/L RPMI 1640 Ile-Dropout medium (US Biologicals, #R9014), supplemented with 2.0g/L NaHCO3, 6.0g/L HEPES, 5.0g/L Alubmax II, 3.7mM Hypoxanthine, and 50μg/mL gentamicin.

The 8μM Isoleucine medium was the same as the Isoleucine medium, except was supplmented with 8μM L-Isoleucine. Trimethoprim was obtained from Sigma Aldrich (#T7883), and used at a final concentration of 10μM. The PI3K inhibitor LY294002 was obtained from Cell Signaling Technology (#9901) and used at a final concentration of 100μM.

Flow Cytometry

For each sample to be analyzed, 1mL of parasite culture was pelleted and resuspended in 1mL of PBS containing 4%w/v paraformaldehyde. Samples were rocked at 4°C for 20-30h of fixation. Samples were then pelleted and resuspended in PBS containing 0.1% v/v Triton-X 100 and rocked at room temperature for 1h for permeabilization. This process was then repeated three additional times with PBS (without Triton-X 100) to remove as much hemoglobin as possible. Samples were then diluted approximately 100-fold into normal culture medium containing 1x SYBR Green I (ThermoFisher Scientific, #S7563) and analyzed on a FACSCalibur (BD Biosciences) flow cytometer. The resulting data was further analyzed using FLOWJO 10.0.7 analysis software.

Growth Curves

Asynchronous parasite cultures were maintained under the conditions described and sampled every 48h to quantify parasitemia by flow cytometry. Cultures were then diluted between 2 and 10-fold to maintain a parasitemia between 0.5-1.0% parasitemia and the dilution factor was recorded. The growth at each time point was measured as the parasitemia multiplied by the dilution factor of the previous dilution. The fi-

nal dataset was normalized such that the initial parasitemia for each line started at 1.0 to account for differences in the starting parasitemias of the different parasite lines. A multi-factor regression of ln(adjusted parasitemia) ~ hour + genotype + media + media*genotype was fit to determine the potential effects of genotype (*i.e.*: artemisinin-resistance), isoleucine level in media, and potential interactions between isoleucine level and genotype while treating time as a covariate. Doubling time (t_D) was calculated for each clone from single factor regressions against time alone, using $t_D = \log(2)/\beta_o$, where β_o is the coefficient from the single factor regression.

Statistical Analysis

All statiscal analyses were performed using R version 3.2.3 (2015-12-10)(R Core Team, 2015). T-tests, linear and logistic regressions, and some figures were generated using R base functions. The *drc* package (Ritz, C. and Streibig, J.C., 2005) was used for determining the 50% effect points of logistic models, and the *ggplot2* package (Wickham, Hadley, 2009) was used for the production of several figures.

Chapter 3

Plasmodium falciparum Maf1, a relic of the TOR pathway, confers survival upon amino acid starvation

Abstract

The TORC1 pathway is a highly conserved signaling pathway across eukaryotes that responds to nutrient and stress signals to regulate the cellular rate of growth as well as the transition into and maintenance of dormancy. The majority of the pathway's components, including the central TOR kinase, have been lost in the Apicomplexan lineage. *Plasmodium falciparum* has retained a few peripheral components, including a putative ortholog of the TOR-regulated RNA Polymerase III repressor Maf1. Here, we confirm *Pf*Maf1 can functionally complement its well-described yeast counterpart, and investigate its role in regulating RNA Pol III expression under conditions of nutrient starvation and other stresses. Using a transposon-insertion mutant with an altered Maf1 expression profile, we demonstrate that proper Maf1 expression is necessary for survival of the dormancy-like state induced by prolonged amino acid starvation, and needed for full recovery from other stresses that slow or stall the parasite cell cycle. The Maf1 mutant is defective in the down-regulation of pre-tRNA synthesis under nutrient-limiting condtions, indicating Maf1's function as a stress-responsive regulator of structural RNA transcription is conserved in *P. falciparum*. Lastly, recent work has implicated other peripheral components of the TORC1 pathway in artemisinin resistance, and has demonstrated that parasites carrying artemisinin-resistant K13 alleles display an enhanced ability to recover from drug-induced growth retardation. We show that one such artemisinin-resistant line displays greater regulation of pre-tRNA expression, and higher levels of survival upon prolonged amino acid starvation, suggesting that the same residual TORC1-derived pathway may regulate growth recovery from both artemisinin-treatment and isoleucine starvation.

Introduction

Efficacy of the frontline antimalarial artemisinin is decreasing throughout Cambodia and other parts of Southeast Asia (Ashley et al., 2014). The drug resistance phenotype presents as a persistence, or delayed clearance, of ring-stage parasites in the peripheral blood at times post-treatment after susceptible parasites would have been cleared (Dondorp et al., 2009). Early theories derived from *in vitro* studies of susceptible parasites treated with drug proposed the so-called *Sleeping Beauty* hypothesis:ring-stage resistant parasites enter a state of dormancy, arresting the cell cycle and decreasing metabolic activity to limit damage, then resume growth after drug concentrations have decayed below effective levels (Kyle DE, Webster HK, 1996)(Hoshen et al., 2000)(Teuscher et al., 2010)(Witkowski et al., 2010)(Codd et al., 2011) (Cheng et al., 2012). However, more recent work using field isolates known to carry mutations conferring the delayed clearance phenotype has cast doubt on the model of a full cell cycle arrest and transition to dormancy. Instead, studies suggest that artemisinin and its derivatives induce a transient slowing of the cell cycle (Klonis et al., 2011), and that parasites carrying resistance-conferring mutations are able to survive this retardation and resume growth, while susceptible parasites are not (Dogovski et al., 2015). The mechanism by which the drug transiently slows the cell cycle or how the resistant alleles allow for recovery remain unclear.

The yeast *Saccharomyces cerevisiae* has long been a model for the induction and maintenance of dormancy. When nutrients are depleted in the stationary phase of growth, cells appear to cease cycling through the mitotic cycle and enter a state of low metabolic and translational activity. This state serves a protective function as yeast deprived of carbohydrates can remain viable and recover after more than one hundred days of starvation (Lillie and Pringle, 1980). However, the distinction between slow

growth and full cell cycle arrest has been brought into question (Daignan-Fornier and Sagot, 2011). As nutrients decline, the yeast cell cycle progressively slows (Brauer et al., 2008), leading some authors to suggest that stationary-phase dormancy may not be a distinct state of differentiation, but simply an "extreme manifestation of slow growth" (Daignan-Fornier and Sagot, 2011). As discussed below, the same pathway that governs the rate of progression through the cell cycle also regulates the transition into stationary phase and longterm survival in that state, suggesting that if dormancy and growth-retardation are not manifestations of the same process, their regulation, at a minimum, overlaps.

Asexual stages of the *Plasmodium falciparum* enter a state reminiscent of the yeast stationary phase upon nutrient limitation *in vitro*. When deprived of extracellular isoleucine, the only amino acid that cannot be obtained from the digestion of hemoglobin, the parasite dramatically slows its cell cycle and exhibits decreased translational and metabolic activity (Babbitt et al., 2012). The parasite can remain in this state for several days and resume normal growth upon isoleucine resupplementation with little loss in viability (Babbitt et al., 2012). Given the overlap between growth-regulation and long term nutrient starvation in yeast, there is reason to believe that there may be overlap in the pathways that govern the ability of *P. falciparum* to recover from long-term isoleucine starvation and the ability of artemisinin-resistant parasites to recover from drug-induced growth retardation.

A likely candidate to govern these responses is the TOR Complex 1 (TORC1) pathway, as it is known to integrate a range of positive and negative growth signals, most notably the presence of amino acids, to drive or inhibit cellular growth (Loewith and Hall, 2011). The TORC1 pathway is highly conserved throughout eukaryotes, and was likely a central signaling hub in the last eukaryote common ancestor (Serfontein et al., 2010)(van Dam et al., 2011). In mammalian cells in culture, in-

hibition of mTOR with the drug rapamycin induces G_1 arrest in certain cell types, but only slows cell cycle progression in others (Abraham and Wiederrecht, 1996). In yeast, complete chemical or genetic inhibition of TOR drives cells into dormancy or quiescence (Barbet et al., 1996), while partial inhibition slows cell cycle progression (Powers et al., 2006). Additionally, in yeast, TORC1 components were found to be the top hits in a genome wide screen for the ability to maintain viability in stationary phase during prolonged starvation (Powers et al., 2006).

However, the majority of the most familiar components of the TORC1 pathway, notably the TOR kinase itself, have been lost through genomic reduction in the evolution of the Apicomplexan lineage (Figure 3.1) (Serfontein et al., 2010) (van Dam et al., 2011). *P. falciparum* retains only a few peripheral orthologs. Intriguingly, two such components were recently associated with artemisinin resistance in parasites carrying K13-resistance alleles. Increased levels and activity of both *Pf*PI3K and *Pf*PKB (also known as *Pf*Akt) were demonstrated to confer increased survival to dihydroartemisinin (DHA) treatment *in vitro* (Mbengue et al., 2015), suggesting these remnants of a TORC1-like pathway may actively regulate the slow growth and recovery program required to survive artemisinin treatment.

*Pf*PI3K (PF3D7_0515300) is the *Plasmodium* ortholog of the Class III phosphoinositide 3-kinase PI3K. While several studies have implicated a direct role for mammalian PI3K (*Hs*Vps34) in amino acid sensing and TOR signaling (Nobukuni et al., 2005)(Byfield et al., 2005)(Gulati et al., 2008)(Yan et al., 2009)(Yoon et al., 2011), it is normally associated with functions in vesicular trafficking, phagocytosis, endocytosis, and coordination of autophagosome formation in autophagy (Backer, 2008); processes that can contribute to the intracellular amino acid supply through both anabolism and catabolism. In *P. falciparum*, *Pf*PI3K is involved in endocytosis of hemoglobin from the host cell, and chemical inhibition of *Pf*PI3K blocks

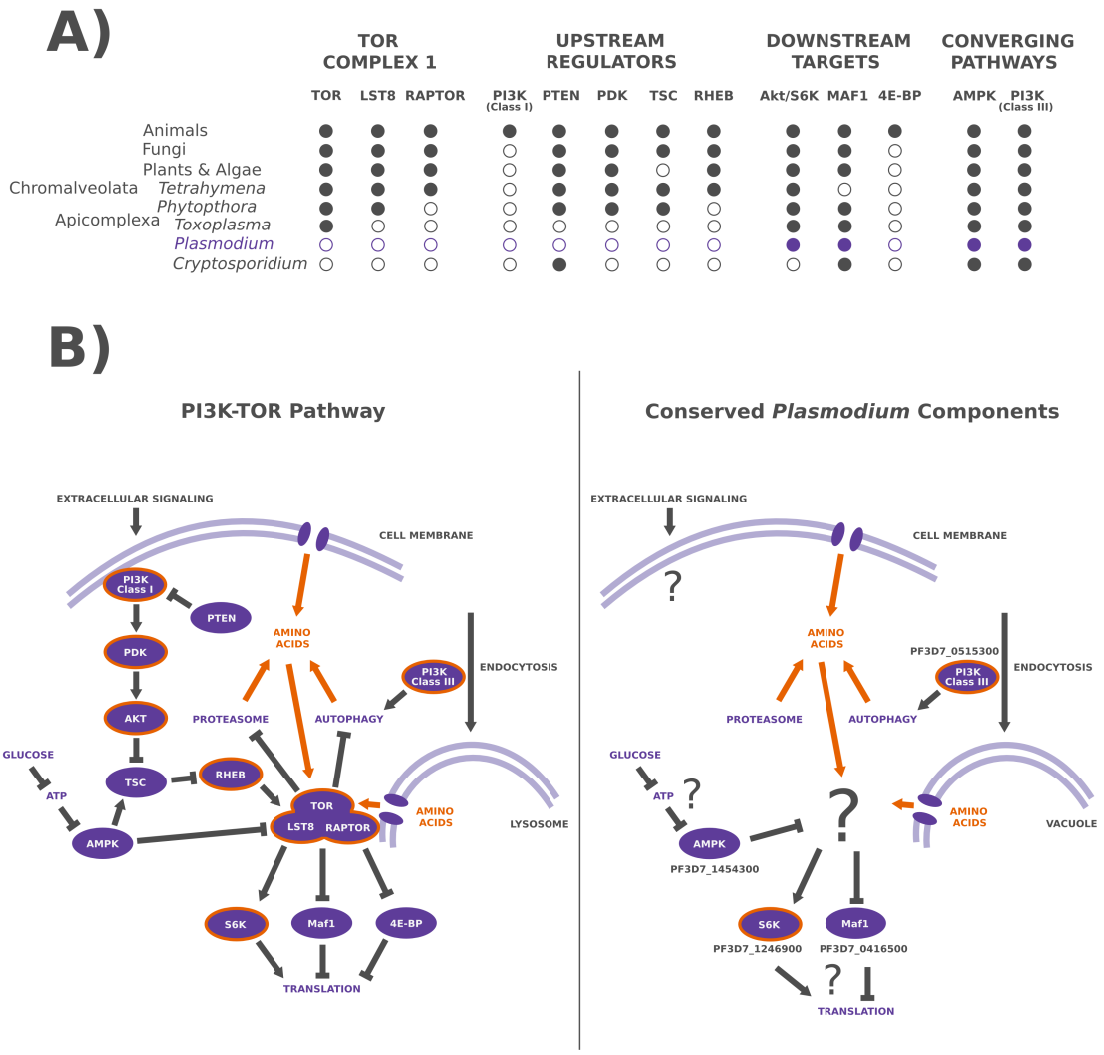

Figure 3.1: **Few components of the TORC1 pathway remain in the *P. falciparum* genome**. **A)** A simplified representation of the major *TOR Complex 1* (TORC1) components, regulators, targets, and converging pathways across several eukaryote lineages. Solid circles (●) indicate the presence of the gene coding for the component in representative members of the lineage, and hollow circles (○) indicate the absence of the corresponding component in the lineage. **B)** An illustration of the generalized animal PI3K-TORC1 signaling cascade used to regulate cellular growth in the presence of amino acids and other growth factors (left), and a projection of this pathway in *Plasmodium spp.* based on the conserved components (right). *Plasmodium spp.* lack a Class I PI3K enzyme and the other components (PTEN, PDK, a PH-domain containing Akt homolog) typically associated with this signaling cascade. *Plasmodium spp*, does encode a Class III PI3K enzyme (PF3D7_0515300) whose ortholog has been implicated in TORC1 signaling in human cells, as well as a PH-domain lacking PKB-family kinase (PF3D7_1246900) resembling human S6K. The genomes of *Plasmodium* parasites also encode an apparent ortholog of the TORC1-dependent RNA Polymerase III regulator Maf1 (PF3D7_0416500).

hemoglobin uptake and causes growth-retardation (Vaid et al., 2010)(*Chapter 2*). A recent study reported that PI3K is the mechanistic target of artemisinin in *Plasmodium* ring stages, and that increased intracellular levels of PI3K confer resistance to the drug (Mbengue et al., 2015). Conceivably, inhibtion of PI3K by artemisinin may slow growth by decreasing intracelluar amino acid levels via blockage of hemoglobin import, or may inhibit some unknown PI3K-mediated signaling.

The TORC1 complex exerts its growth-regulating effects by phosphorylating a range of downstream products. The kinase S6K is one such target, which in turn phosphorylates a cascade of downstream pro-growth substrates, such as the ribosomal protein S6, to increase cellular translational output (Tavares et al., 2015). Human S6K is part of a paralog family consisting of S6K, SGK, RSK, and PKB (also known as Akt), which expanded from a single origin in the last eukaryote common ancestor (van Dam et al., 2011). *P. falciparum* encodes a single homolog of this kinase family (PF3D7_1246900), which has previously been referred to as *Pf* PKB or *Pf* Akt (after the mammalian upstream TORC1 regulator) (Vaid and Sharma, 2006) (Mbengue et al., 2015), but the protein lacks the Pleckstrin Homology (PH) domain that distinguishes Akt form other family members, and the parasite does not encode the Class I PI3K and PDK1 enzymes that regulate human Akt activity. When *Plasmodium falciparum* cells are treated with artemisinin-derivatives, *Pf* PKB activity is inhibited (Mbengue et al., 2015), reminiscent of the of manner in which the mammalian or yeast orthologs, S6K and Sch9, are inhibited upon amino acid starvation or of treatments that inhibit or retard growth (Urban et al., 2007)(Tavares et al., 2015). Overexpression of *Pf* PKB in an artemisinin sensitive genetic background causes parasites to recover from DHA-treatment at levels comparable to artemisinin-resistant field isolates (Mbengue et al., 2015), suggesting increased *Pf* PKB activity may contribute to recovery from artemisinin induced growth-retardation.

A more recently appreciated downstream effector of the TORC1 pathway is the RNA Polymerase III regulator Maf1. Under nutrient replete conditions, TOR signaling keeps Maf1 phosphorylated and inactive. In human cells, Maf1 appears to be directly phosphorylated by the TOR kinase (Shor et al., 2010)(Kantidakis et al., 2010), but in yeast, phorphorylation is performed by the S6K family member Sch9 (Huber et al., 2009)(Lee et al., 2009). Upon starvation, inhibition of TORC1 leads to Maf1 dephosphorylation, allowing it to bind to the RNA Pol III holoenzyme, shutting down Pol III-dependent transcription of tRNAs, the 5S rRNA, and other structural RNAs (Pluta et al., 2001)(Vannini et al., 2010). Yeast null mutants of Maf1 die under nutrient limitation and other factors that inhibit TORC1 due to their inability to regulate Pol III transcription under stress (Upadhya et al., 2002)(Roberts et al., 2006)(Ciesla et al., 2007)(Huber et al., 2009). In yeast, Maf1 is one of the most important genes for maintaining viability during long term starvation in stationary phase (Powers et al., 2006)(Cai and Wei, 2015). A putative Maf1 ortholog appears to be conserved in the *Plasmodium* genus.

Here, we demonstrate that this gene is a functional ortholog of the yeast Maf1. A transposon-insertion line of *P. falciparum* with defective Maf1 expression is unable to regulate Pol III activity and maintain viability in the dormancy-like state induced by isoleucine starvation. This mutant displays additional growth and recovery defects for a range of growth-inhibiting forms of stress. Furthermore, an artemisin-resistant isolate displays increased Pol III regulation and survival upon amino acid starvation, potentially connecting *Pf*Maf1, *Pf*PKB, and *Pf*PI3K into a simplified, yet still functional, TORC1 pathway capable of regulating parasite growth in the presence of nutrient limitation and other growth-retarding forms of stress.

Results

PF3D7_0416500 is a functional ortholog of Maf1

The *Plasmodium falciparum* gene PF3D7_0416500 encodes a putative ortholog of Maf1. As with many *P. falciparum* proteins, the *P. falciparum* ortholog contains a large, asparagine-rich low-complexitiy region near the N-terminus accounting for 200/389 (51%) amino acids of the sequence. This region is not conserved in other *Plasmodium* species, and when this region is not considered, the *P. falciparum* sequence aligns well with the region of the human ortholog used in determining the crystal structure (PDB: 3NR5) (Vannini et al., 2010), and with the corresponding regions of the *S. cerevisiae* and *S. pombe* proteins (Figure 3.2).

In yeast, Maf1 knockout cells display severe growth defects and death when grown on a non-fermentable carbon source or when treated with the TOR pathway inhibitor rapamycin (Roberts et al., 2006). To test whether the *P. falciparum* gene is a true functional ortholog of Maf1, we attempted to complement this phenotype in yeast. Maf1 is regulated by phosphorylation in both yeast and human cells, however, the regions in which the phosphorylation occurs are the least conserved regions of the protein sequence. In yeast, phosphorylation has been described in two regions, the "mobile insertion" near the N-terminus (so-named for its sensitivity to limited proteolysis in recombinant proteins), and the "acidic tail" at the c-terminus (the c-terminus of all Maf1 orthologs, including *Pf*, have a high D and E content, but otherwise show little sequence identity) (Vannini et al., 2010). In order to account for these phospho-regulatory regions, we generated a chimeric Maf1 sequence consisting of the yeast N-terminus and mobile insertion, the *Pf* Maf1 central core, and the yeast acidic tail (Figure 3.3). While this chimera may appear to contain a small portion of *P.*

```
3NR5      MKLLENSSFEAINSQL-TVETGDAHIIGRIESYSCK-PL----SDKCSRKTLFYLIATLN
Sc        MKFIDELDIERVNQTL-NFETNDCKIVGSCDIFTTK-PI----NEPSSRKIFAYLIAILN
Sp        MKFLELADLDTVNNAL-SFDADDCRIRGKCELYTTK-PL----DQSSSRRTFMYIVATLN
Pf        MINLDIEILNDVNLILEKLDAHDRFIEAKIELFEDI-PEVINNNGKEKKSILTNIINILN
          *  ::   :: :*  * ..:: *  * .  : :    *     .   .:  :  ::  **

3NR5      ESFRPDYDFSTARSHEFSREPSLSWVVNAVNCSLFSAVREDFKDLKPQLWNAVDEEICLA
Sc        ASY-PDHDFSSVEPTDFVKTS-LKTFISKFENTLYSLGRQ----PEEWVWEVINSHMTLS
Sp        ASY-PDHDFSSLQPTDFYKEPSLSRVVDSVNSTLNNIGRGRL--SVNGIWEIIDRHINLS
Pf        YVF-PDYEFKYLNNSNYKYIKNINSVIDNINYNLFYIIENIYRGFNKKIWKILKELIDFK
            : **::*.  .  ::     :. .:. .: .*    .         :*: :.  : :

3NR5      ECDIYSYNPDLDSDPFGEDGSLWSFNYFFYNKRLKRIVFFSCRS--
Sc        DCVLFQYSPSNS-FLEDEPGYLWNLIGFLYNRKRKRVAYLYLICSR
Sp        DCSVYSYTPDSDSDPYGDDALIWGMSYFFFNKNMKRMLYLSLHG--
Pf        YCDVYTYLNDTDNDPYVDKESISSFNYFFFAKKNKRILFISCIT--
           * :: *  . .     :   :  :  *:: :. **: ::
```

Figure 3.2: **The sequence of the core region of Maf1 is conserved in *Plasmodium falciparum***. A Clustal Omega alignment of core Maf1 protein sequences from human (3NR5), *Saccharomyces cerevisiae* (Sc), *Schizosaccharomyces pombe* (Sp), and *Plasmodium falciparum* (Pf). Maf1 protein sequences contain two unstructured regions that display negligible sequence conservation between species. These regions were removed for the production of the *Homo sapiens* crystal structure (PDB: 3NR5). The corresponding regions of the other species were omitted for clarity. The sequences used for alignment were as follows: *H. sapiens* (NC_000008.11) 1-35, 83-210; *S. cerevisiae* (YDR005C) 1-35, 225-342; *S. pombe* (SPAC31G5.12c) 1-35, 78-197; *P. falciparum* (PF3D7_0416500) 1-36, 224-349.

falciparum sequence, the region used spans 67% of the human ortholog's core region used in producing the crystal sructure (Vannini et al., 2010).

When grown on medium containing 10 nM Rapamycin, wild type yeast cells were able to grow but Maf1-knockout cells were not (Figure 3.3). When either the full-length yeast protein or the yeast-*P. falciparum* chimera was expressed from an episomal plasmid, partial growth was restored, indicating that the core region of the *P. falciparum* ortholog is capable to functionally complementing the yeast knockout cells.

The PB-11 parasite clone carries a transposon insertion upstream of the Maf1 open reading frame

We attempted to disrupt the Maf1 ortholog PF3D7_0416500 with several different plasmids for single and double cross-over recombination, including multiple attempts using CRISPR-Cas9/guide-RNA. None of our efforts was successful, raising the possibility that this gene is essential for intraerythrocytic growth. We were not successful in integrating any C-terminal epitope tags or destabilization-domains either, and no 3' integration was ever detected by PCR in transfected parasites, suggesting an unmodified C-terminus may be necessary for proper function.

Surprisingly, we were also unable to express ectopic copies of Maf1 in wild type parasites, either using episomal plasmids or chromosomal-integration using the attB/attP system (Nkrumah et al., 2006). We attempted both N-terminal and C-terminal tags, as well as both strong (eEF1α) (Talman et al., 2010) and weak (mRPL2) (Balabaskaran Nina et al., 2011) promoters, but no stable transfectants could be obtained. Unrelated control plasmids routinely produced stable transfectants. Only a single ectopic expression construct produced stable parasites, and it consisted of the *P. falciparum* Maf1 coding sequence fused to a 'DD24' N-terminal FKBP12 destabi-

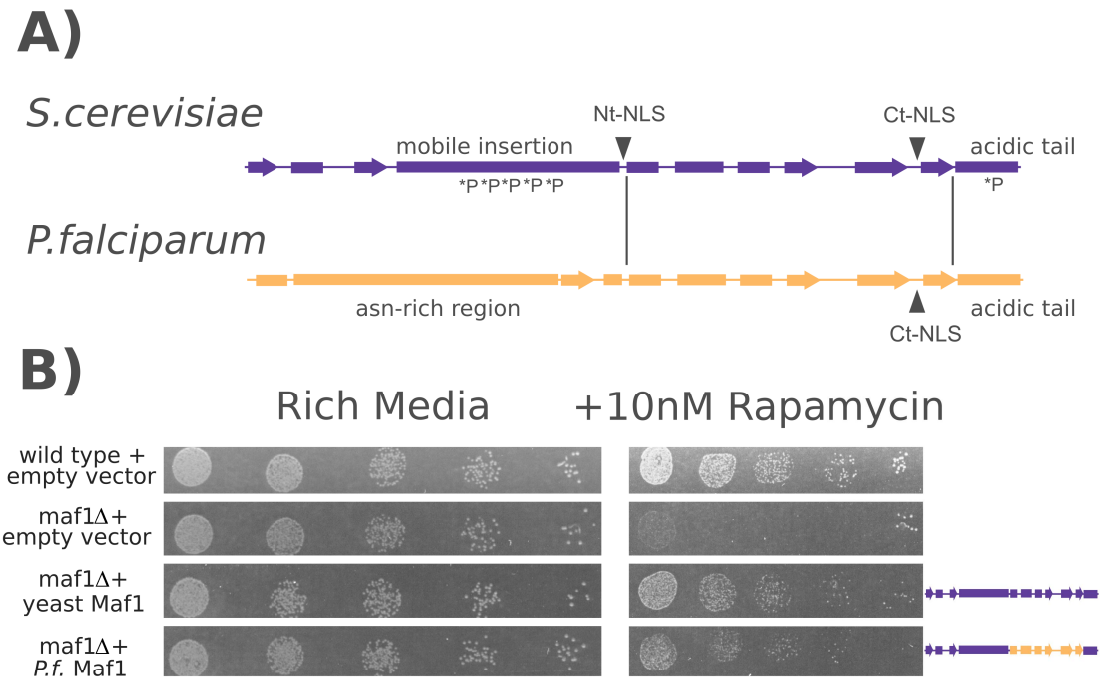

Figure 3.3: **Functional complementation of Maf1-knockout yeast cells with a chimeric *P. falciparum* Maf1. A)** Schematics showing the key structural features of the yeast and *P. falciparum* Maf1 orthologs (Nt = *N-terminus*, Ct = *C-terminus*, NLS = *nuclear localization signal*. Vertical lines indicate the homologous region exchanged to generate the chimera for complementation. A "*P" indicates a known site of phosphorylation in the yeast protein. **B)** Five-fold serial dilutions from 5000 to 8 yeast cells transformed with the indicated complementation vectors were plated on normal rich media, or rich media supplemented with 10nM rapamycin, which is lethal to Maf1 knockout cells.

lization domain (de Azevedo et al., 2012) expressed from the weak mRPL2 promoter. The resulting line expressed the Maf1 transgene well below endogenous levels and was unresponsive to protein stabilization with the ligand *Shield*, limiting its utility in any further analyses (Figure 3.4). These failed efforts suggests Maf1 may be toxic to cells if expressed at the wrong time and/or level.

In their efforts to generate a *piggyBac* mutant collection, Balu *et al.* generated a Maf1 transposon-insertion mutant in an NF54 clone background (Balu et al., 2009). In this clone, identified as PB-11, Balu *et al.* reported the *piggyBac* transposon to be inserted at the TTAA sequence ending at position +8 of the open reading frame, which should disrupt the coding sequence to generate a genetic knockout (Figure 3.5).

We obtained this mutant and discovered that the insertion site had been incorrectly assigned. Instead of the +8 position of the ORF, the insertion is at a TTAA sequence 53bp upstream of the start codon. Whole-genome sequencing of the PB-11 line (Illumina HiSeq paired-end sequencing, 73x coverage), demonstrated extensive read-coverage for the -53 insertion position, and no support for a +8 insertion site (Figure 3.6). To rule out the possibility of additional, unknown *piggyBac* insertions in the genome, we aligned one file of the paired-reads to the transposon sequence and the mate file to the genome (and vice versa) to see where each transposon-aligning paired-read mapped (Balu et al., 2013). Paired-ends were found to only to align to the Maf1 locus or to regions of the genome used as regulatory sequences within the transposon itself (such as the Calmodulin promoter or the HrpII 3'UTR). Additionally, we analyzed the PB-11 genome for SNPs and INDELs within all annotated open reading frames in the genome, but found none of significance when compared to the parental line or a sister *piggyBac* insertion mutant sequenced previously (Balu et al., 2013).

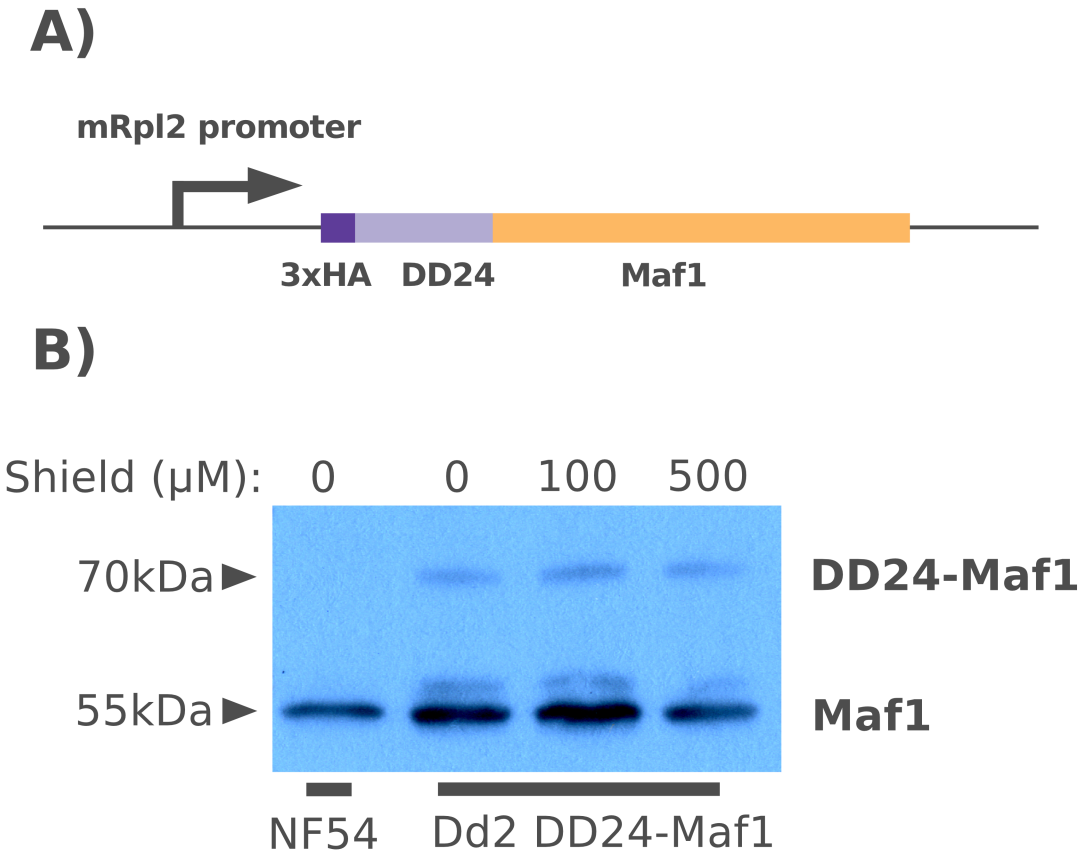

Figure 3.4: **Ectopic expression of *Pf*Maf1 is only attainable using a construct designed to attenuate protein expression**. **A)** A schematic of the transgene used for transfection. A 3xHA tag followed by a DD24 destabilization domain was fused to the N-terminus of the Maf1 coding sequence and driven by the weak *mitochondrial Ribosomal Protein 2 (mRPL2) promoter. **B)** A western blot of schizonts of untransfected NF54 parasites, or Dd2^{attB} stably transfected with the DD24-Maf1 expression plasmid probed with anti-*Pb*Maf1 antisera. The 3xHA and DD24 tag are expected to add 15kDa to the *Pf*Maf1 molecular weight. Increasing concentrations of the *Shield* ligand are expected to increase stability and abundance of DD24-Maf1, but appear to have no effect.

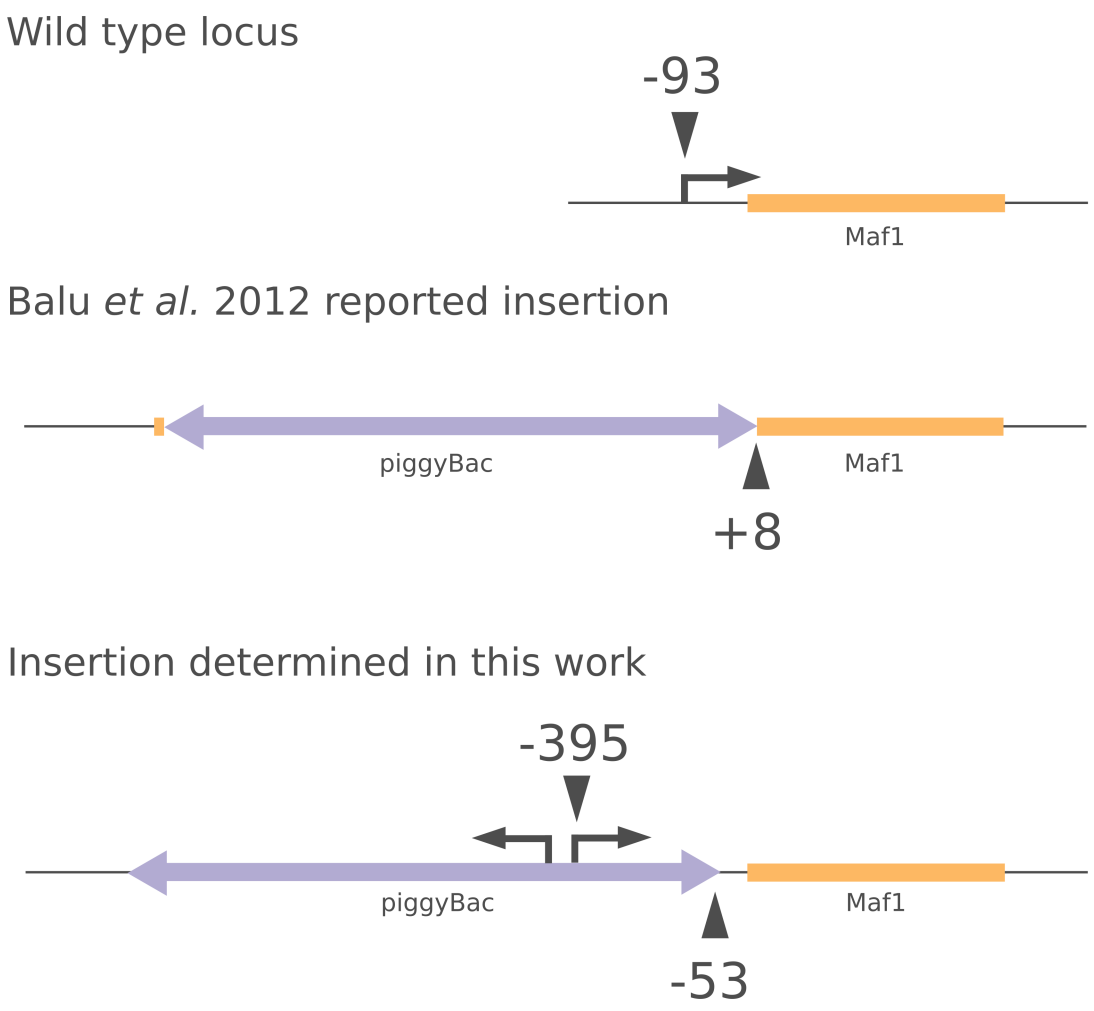

Figure 3.5: **Schematic of the Maf1 genomic locus and *piggyBac* insertion in wild type and mutant parasites.** Numbers below the chromosomal line indicate the reported and verified transposon insertion positions relative to the Maf1 start codon in the PB-11 *piggyBac* insertion mutant. Right-angled arrows and numbers above the chromosome line indicate the 5'-RACE determined transcription start sites in wild type (-93nt) and PB-11 mutant (-395nt) cells. The Maf1 transcript in the PB-11 mutant arises from within the *piggyBac* transposon and is likely due to bidirectional promoter activity of the Calmodulin promoter fragment used for drug selection in the transposon.

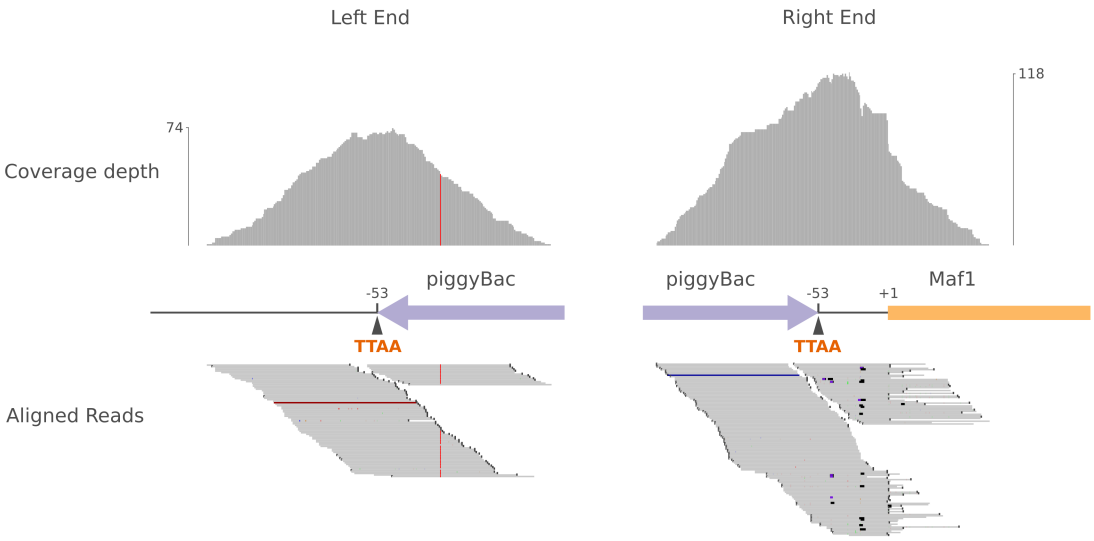

Figure 3.6: **Upstream insertion of the *piggyBac* transposon is supported by whole genome sequencing**. **Top** Coverage depth plots indicating the total numer of reads mapping to each base pair around the two termini of the *piggyBac* insertion at the -53 TTAA site upstream of the Maf1 start codon. The maximum read coverage for each end of the transposon is indicated by the axis on the left and right. **Bottom** Alignment of reads to the termini of the transposon surrounding the -53 insertion site. Each read is 70bp in length. Colored spots indicate base mismatches within a given read and the genomic sequence.

The PB-11 mutant displays an altered Maf1 expression profile

The -53 insertion in the PB-11 line does not ablate expression of Maf1. The Maf1 transcript is detectable in PB-11 throughout the asexual life cycle, but never matches wild type expression pattern (Figure 3.7 and Figure 3.8). Later in the cell cycle, when wild type Maf1 mRNA abundance dramatically increases, expression of mutant Maf1 is only moderate.

The insertion of a ~3kb transposon 53bp upstream of a start codon would normally be expected to disrupt the activity of the native promoter sequence. Therefore, we performed 5'RACE on Maf1 mRNA from both wild type and the PB-11 mutant parasites. In wild type cells, we mapped the transcription start site to 93bp upstream of the Maf1 start codon, meaning in PB-11 cells, *piggyBac* is inserted into the 5'UTR (Figure 3.5). In PB-11 cells, the Maf1 transcription start site mapped 395bp upstream of the start codon, producing a chimeric 5'UTR consisting of 346bp of the right arm of the *piggyBac* transposon (Figure 3.5). When constructing the transposon (pXL-BacII-DHFR), Balu *et al.* used the full intergenic region between the start codons of Calmodulin (PF3D7_1434200) and its opposite gene (PF3D7_1434300) to drive expression of the hDHFR selectable marker (Balu et al., 2005). It appears this region has enough enhancer or promoter activity to drive transcription of the chimeric Maf1 mRNA in PB-11 in the opposite direction of the hDHFR gene. This promoter has been previously reported to be bidirectional when used in plasmids (Epp et al., 2008).

Anti-sera raised against full-length *Plasmodium berghei* Maf1 detected production of Maf1 protein in both wild type and mutant cells. Maf1 is a low abundance protein, and is largely undetectable during the first 24 h of the life cycle (Figure 3.9A). By 27.5 h post-invasion, Maf1 is detectable in wild type parasites, but is not yet detectable in PB-11 parasites (Figure 3.9B). It is detectable, however, in the later hours

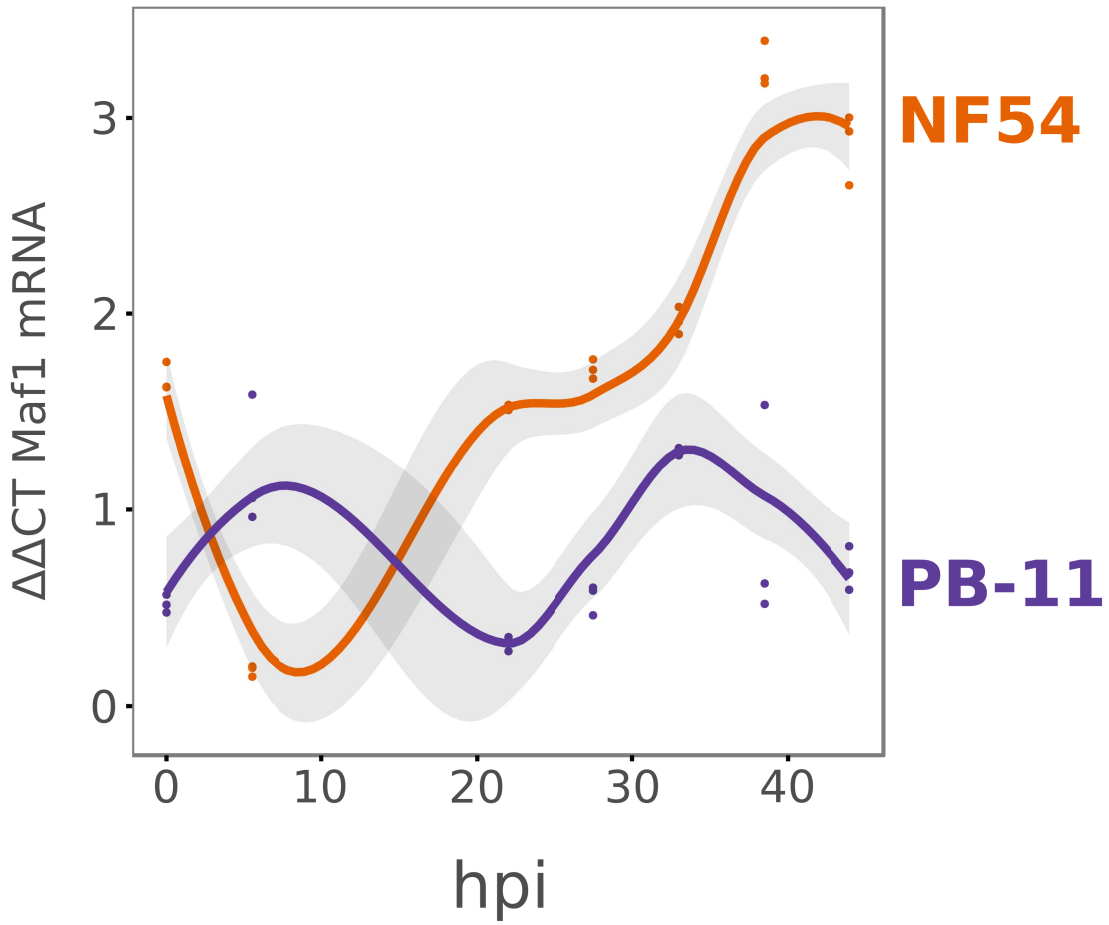

Figure 3.7: **The PB-11 mutant displays a distinct Maf1 mRNA expression profile relative to wild type parasites.** A time course of Maf1 mRNA expression using qRT-PCR was performed at seven time points across the intraerythrocytic cycle in synchronous wild type (NF54) and mutant (PB-11) parasites. Maf1 expression was quantified relative to the seryl-tRNA ligase transcript (PF3D7_0717700). Points represent individual biological replicates and curves represent LOESS smoothed models fit to the data, with the 95% confidence interval indicated by shading. hpi = *hour post-invasion*

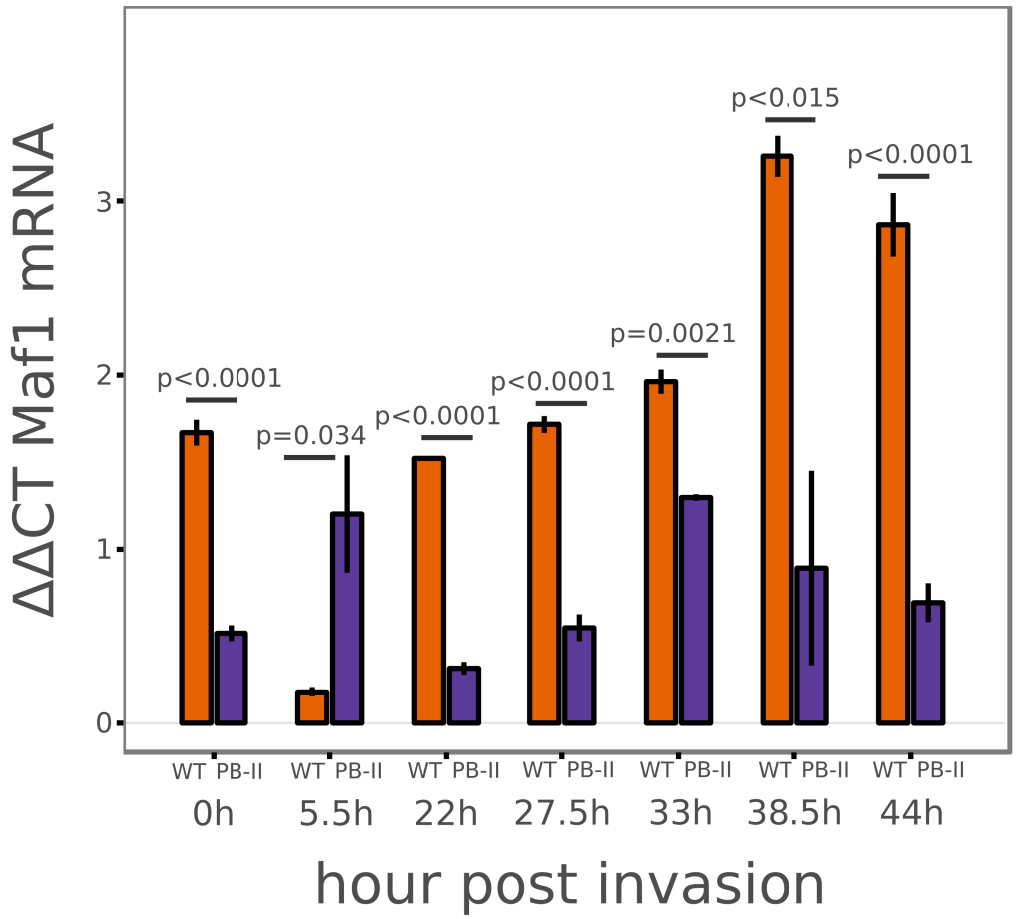

Figure 3.8: **Comparison of Maf1 mRNA expression at individual time points across the intraerythrocytic cycle**. The same data as in Figure 3.7 represented as mean relative expression barplots. P-values represent t-tests for differences in expression between wild type (WT) and mutant (PB-11) parasites at each time point. Error bars represent standard deviation.

of the cell cycle at near wild type levels despite the much lower mRNA expression. A recent global ribosome profiling study of the *Plasmodium falciparum* asexual cycle found Maf1 to be translated at very low efficiency from rings through schizonts (Caro et al., 2014). Perhaps the chimeric 5'UTR generated by the *piggyBac* insertion removes the cis-acting factors in the native 5'UTR responsible for the observed low translational efficiency, allowing for protein production from low mRNA levels, albeit with a notable temporal delay in expression. This endogenous translational control may explain why we were only able to obtain stable transfected lines when expressing Maf1 from a construct designed to reduce protein production levels (Figure 3.4).

The *piggyBac* transposon is well known for its ability to excise cleanly from its insertion site when remobilized (Woodard and Wilson, 2015). We attempted to use this property to restore the wild type Maf1 locus in the PB-11 mutant line by excising *piggyBac*. While we were able to obtain parasites stably expressing the *piggyBac* transposase, no excision of the insertion was detected. Similarly, we attempted to restore the native locus by "crossing-out" the *piggyBac* insertion via CRISPR-Cas9 mediated homologous recombination. We attempted several different strategies with different guide RNAs, however, all failed to restore the wild type locus.

The PB-11 Maf1 mutant fails to recover from a dormancy-like state

TORC1 is best understood as the central hub from which the pro-growth signaling cascades are relayed in response to changes in intracellular levels of amino acids. In yeast, human cells, and *Drosophila* grown in normal conditions, TORC1 is active, and Maf1 is inhibited (Roberts et al., 2006)(Shor et al., 2010)(Marshall et al., 2012). When these organisms are starved of amino acids (or TORC1 is inhibited by rapamycin), Maf1 is activated and shuts down Pol III dependent-transcription of tRNAs to con-

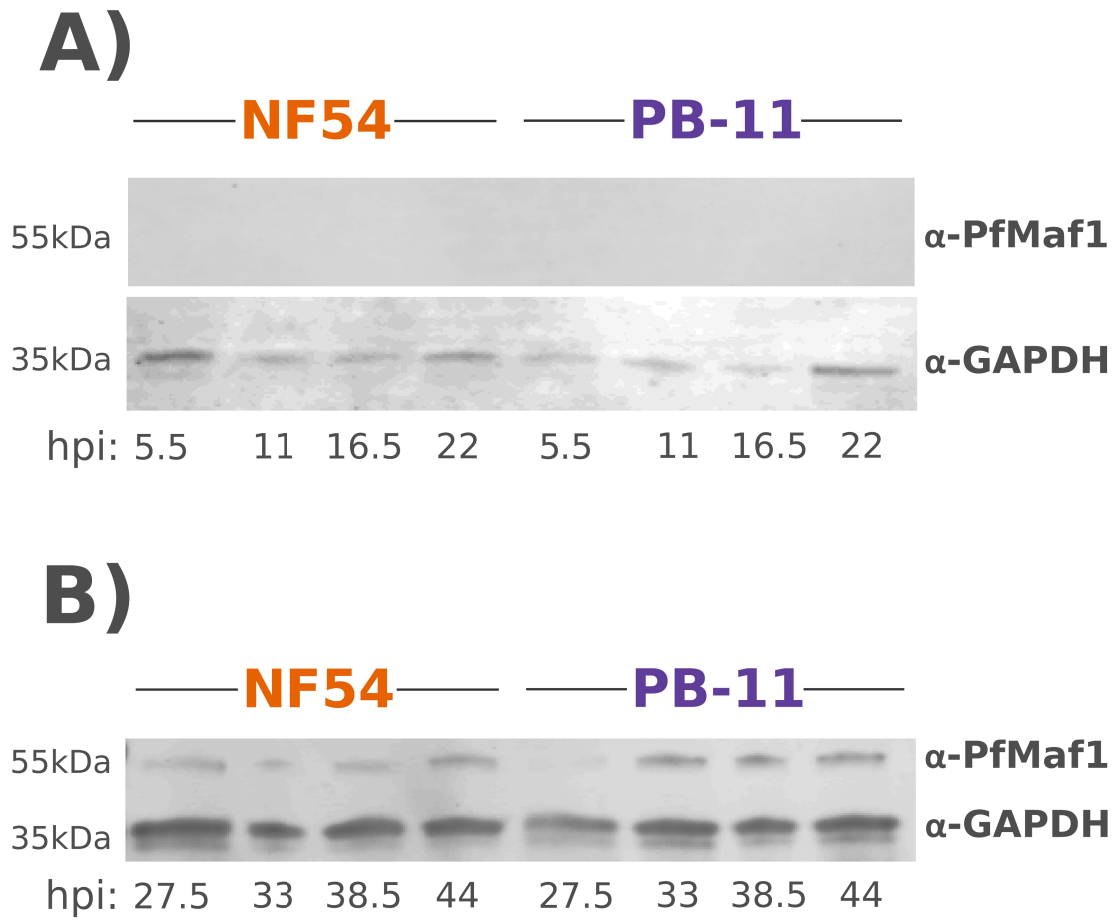

Figure 3.9: **The PB-11 insertion mutant displays delayed Maf1 protein expression. A)** Western blot of Maf1 expression in synchronous wild type (NF54) and mutant (PB-11) parasites at 5.5h intervals across the first 22h of the intraerythrocytic cyle. No Maf1 protein expression was detectable in either parasite line even after prolonged exposure. **B)** Western blot of Maf1 protein expression at 5.5h intervals from 27.5h through 44h of the cell cycle. hpi = $textithourpost - invasion$

serve resources and globally dampen translation. If this safety mechanism is prevented by deletion or silencing of Maf1, death or severe growth defects result upon amino acid starvation.

Over the course of the asexual cell cycle, *Plasmodium falciparum* resides within its host erythrocyte and imports and digests hemoglobin as its primary source of amino acids. Human hemoglobin lacks isoleucine, and since the parasite does not have the capacity to synthesize it itself, it must import isoleucine from the extracellular environment (ie: serum *in vivo* or culture medium *in vitro*). A study of the nutritional requirements for *P. falciparum* found isoleucine to be the only amino acid needed in the culture medium to sustain growth (Liu et al., 2006).

In an important study, Babbit *et al.* analyzed the parasite's response to isoleucine deprivation (Babbitt et al., 2012). Unlike nutrients such as glucose, which leads to rapid death when removed, Babbit *et al.* found that parasites appeared to retard growth and enter a dormancy-like state of low metabolic activity upon isoleucine removal. Upon readdition of isoleucine, parasite growth resumed seemingly unaffected. Parasites could remain in the absence of isoleucine for upwards of several days and only sustain a minor loss in viability. This is reminiscent of stationary phase dormancy observed in yeast, a process for which Maf1 is necessary to maintain viability during prolonged starvation (Powers et al., 2006)(Cai and Wei, 2015).

Babbit *et al.* were unable to identify any genetic factors responsible for this phenotype. Neither deletion of the *P. falciparum* homolog of the GCN2 uncharged tRNA sensor kinase, nor the expression of a non-phosphorylatable form of its target, IF2α, had an effect on surival after isoleucine starvation (Babbitt et al., 2012). Given the role Maf1 plays in the amino acid starvation response in other organisms, we investigated how the PB-11 Maf1 mutant responded to isoleucine withdrawal.

Tightly synchronized young ring-stage wild type and PB-11 mutant parasites were cultured for 72 hours in either normal culture medium, or medium lacking isoleucine. As previously reported, parasites in the isoleucine deficient medium stayed at roughly their starting parasitemia while those in normal medium grew through ~1.5 cell cycles. No detectable difference was observed between wild type and PB-11 parasites over this period (Figure 3.10).

We next tested whether the parasites remained viable over the duration of starvation. Young ring-stage parasites of both wild type and PB-11 incubated in medium lacking isoleucine for 24 hours recovered robustly when returned to normal culture medium for a 72-hour recovery period (Figure 3.10). However, when the starvation period was increased to 48 hours, the PB-11 Maf1 mutant line displayed a notable decrease in recovery, whereas wild type parasites displayed growth levels similar to parasites cultured for 72 hours in normal medium. With a 72-hour starvation, PB-11 mutants displayed no recovery at all, while wild type parasites recovered robustly.

Despite not being a full gene-disruption, the alteration of Maf1 expression in the PB-11 mutant line appears to prevent the parasites from recovering from prolonged amino acid starvation. To investigate further, we used flow cytometry to track the parasitemia of wild type and PB-11 cultures every 24 hours over nine days (216 h) of starvation in isoleucine deficient medium (Figure 3.11). Over the full course of the nine days, the PB-11 parasitemia decreased at a much faster rate ($t_{1/10}$ WT = 301 h, $t_{1/10}$ PB-11 = 196 h)(Figure 3.12). Over the first 72 h, however, the death rates of the two lines were nearly identical ($t_{1/10}$ WT = 390 h, $t_{1/10}$ PB-11 = 369 h)(Figure 3.12). As a verification, aliquots of each replicate sample were transferred to normal medium for three days of recovery at the 72 h, 144 h, and 216 h points of starvation (Figure 3.13). PB-11 displayed no regrowth at any time point, whereas wild type parasites remained viable and recovered after nine days.

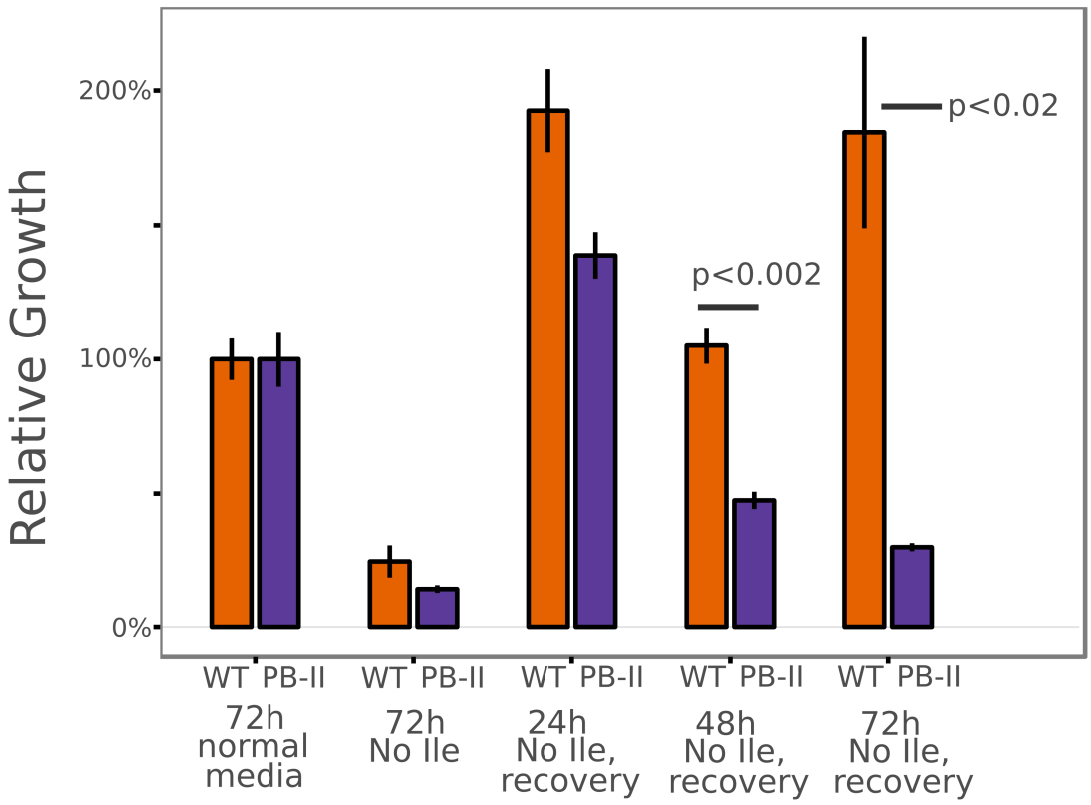

Figure 3.10: **Maf1 mutant parasites cannot recover from a prolonged dormancy-like state induced by isoleucine-starvation**. Synchronous young ring-stage parasites (approx. 4 h post-invasion) were washed repeatedly and transferred to medium lacking isoleucine for the indicated times. Recovery denotes transfer back to normal culture medium (containing isoleucine) for 72 h of growth. Parasitemia was quantified by flow cytometry. Growth was measured relative to the final parasitemia of a control culture incubated in normal culture medium for 72 h. P-values are the result of t-tests of three biological replicates.

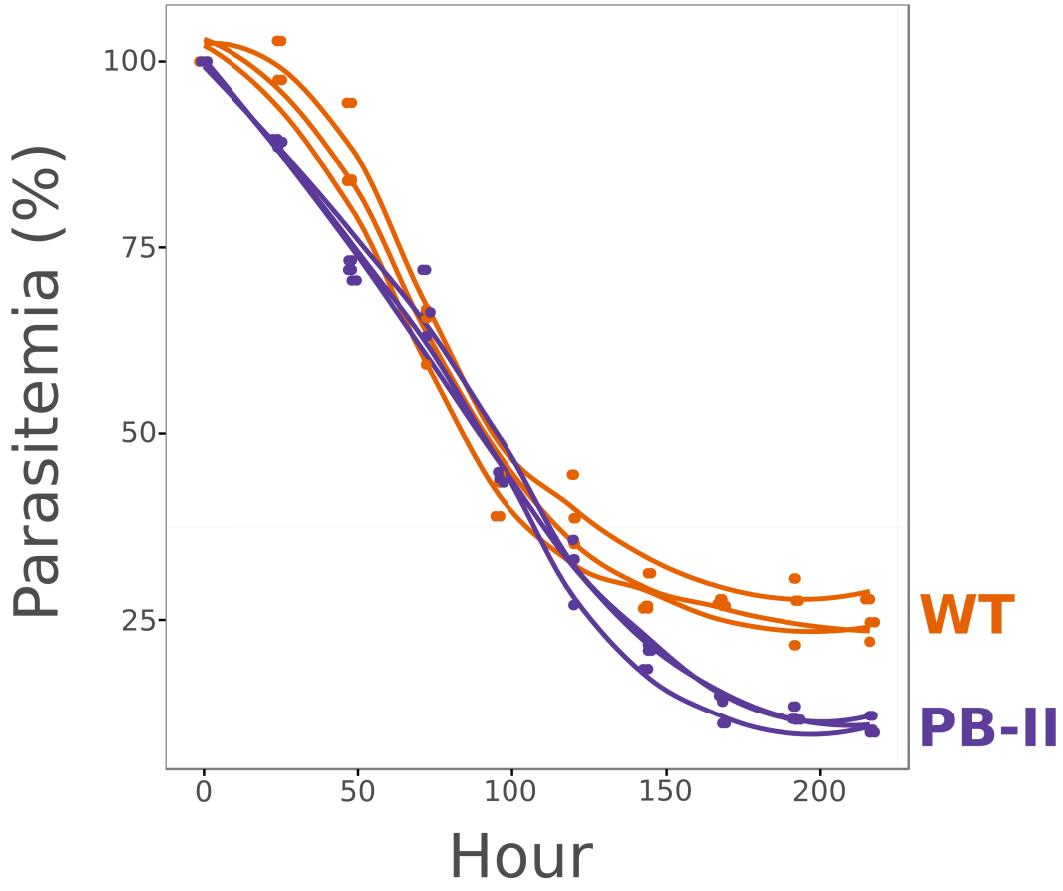

Figure 3.11: **Parasitemia of Maf1 mutant parasites decreases more rapidly during prolonged isoleucine starvation.** Synchronous young ring-stage parasites of NF54 (WT) and Maf1 insertion mutant (PB-11) parasites were washed repeatedly and transferred to medium lacking isoleucine. Samples of each parasite line were taken at 8h intervals over the course of a nine day (216h) period, and parasitemia was determined by flow cytometry. Lines represent LOESS curves fit to the data for each of three biological replicates.

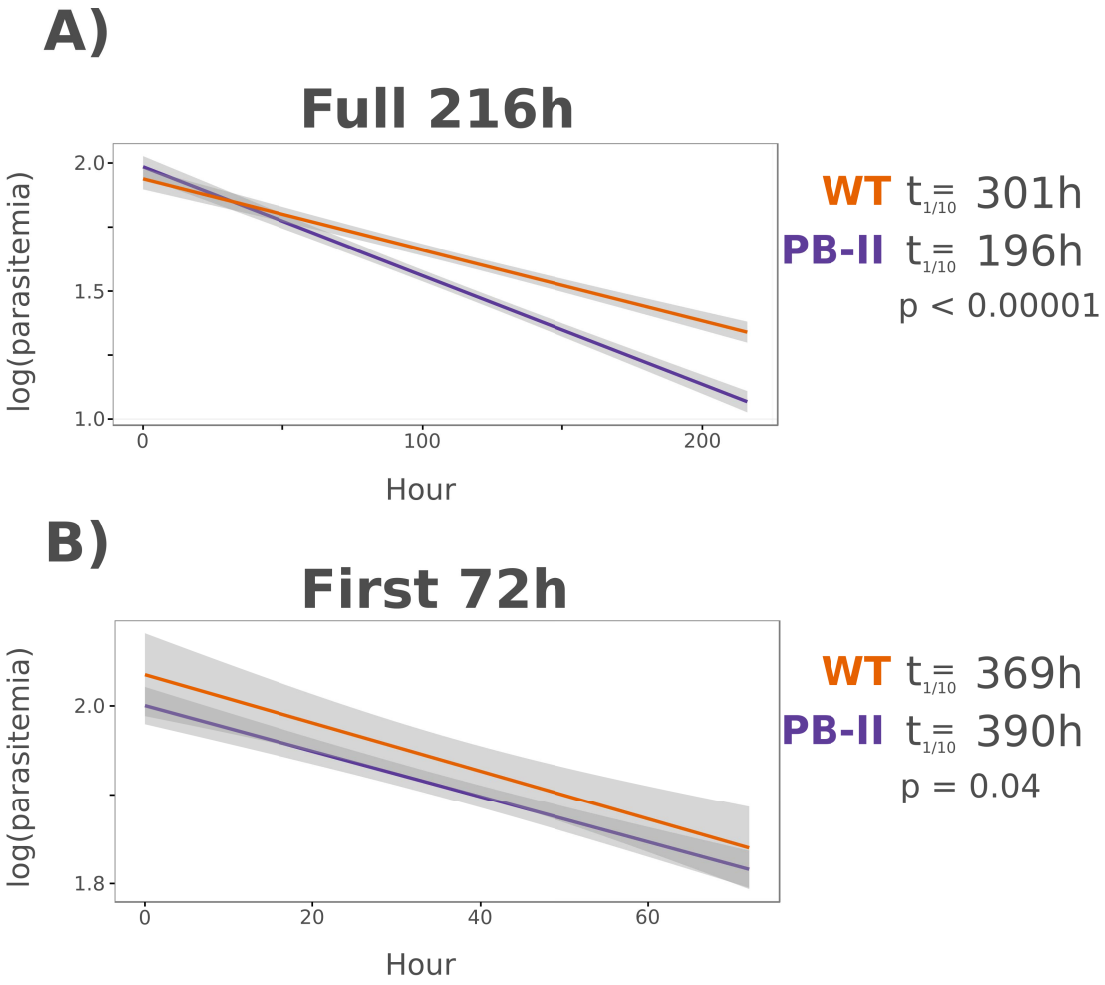

Figure 3.12: **Maf1 mutant parasites display little difference in death rate over the first 72 h of starvation. A)** A regression model fit to the 216 h isoleucine starvation data to determine the rate of death of NF54 (WT) and Maf1 mutant (PB-11) parasites. **B)** A regression model fit to the data from just the first 72 h of isoleucine starvation. $t_{1/10}$ = time required to reach 1/10th the starting parasitemia.

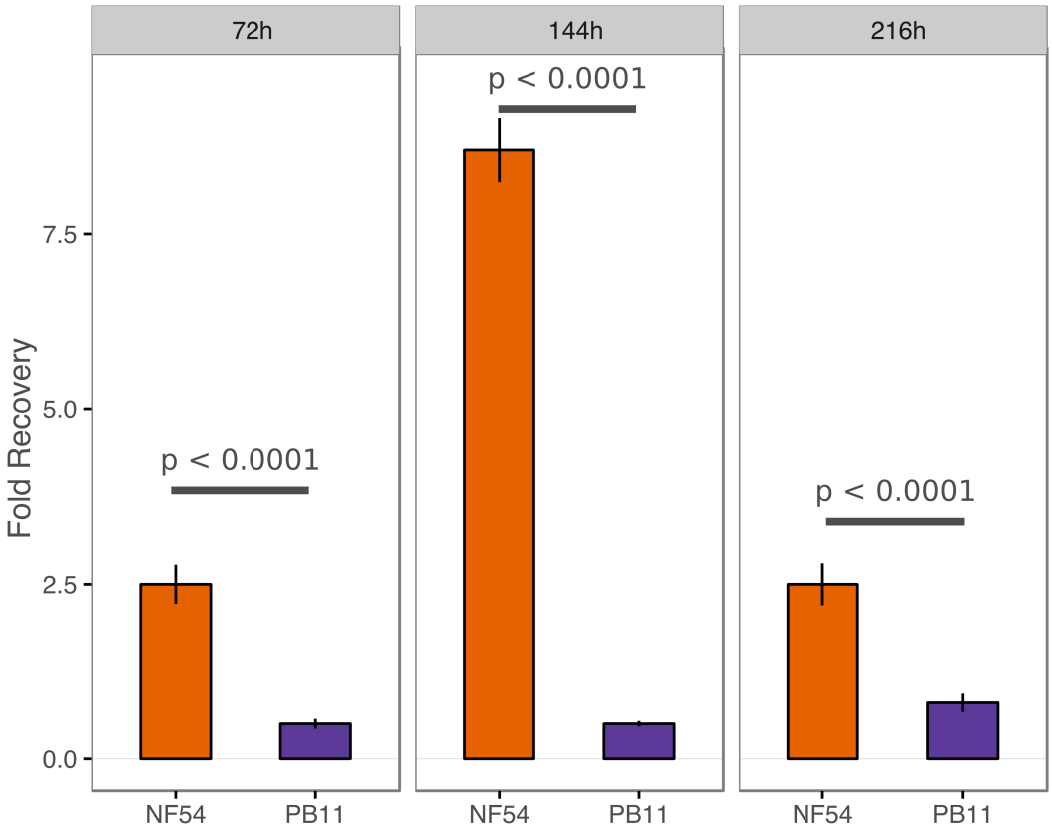

Figure 3.13: **Wild type parasites remain capable of recovery over the full duration of 216 h of starvation**. Supplement for Figure 3.11 and 3.12. Samples of wild type (NF54) and Maf1 mutant (PB-11) parasites taken after 72 h, 144 h, and 216 h of isoleucine starvation were transferred to normal culture medium for 72 h of recovery. The final parasitemia was quantified by flow cytometry, and is expressed as fold-growth relative to the parasitemia at the time of transfer.

Our previous analysis of the *Plasmodium falciparum* response to isoleucine starvation revealed that parasites do not arrest growth upon isoleucine withdrawal, but instead dramatically slow the cell cycle (*Chapter 2*). Parasites deposited into isoleucine deficient medium as young rings take roughly twice as long to complete the cell cycle (~90 h) as compared to culture in normal medium (~45 h). If PB-11 Maf1 mutant cells can fully recover from a 24 h isoleucine starvation but not at all from 72 h starvation, this suggests a specific point in the cell cycle is crossed between those two time points at which the ability to recover is irreversibly compromised, presumably due to altered Maf1 expression.

To map this point, we initiated a culture of early-ring PB-11 parasites in isoleucine deficient medium for a 144-hour incubation (Figure 3.14). Every 8 h, an aliquot of the culture was removed and resuspended in normal medium for a 72 h recovery period. A logistic regression was performed on the relative proportion of parasites recovering at each time point. The results show a transition in the ability to recover as the duration of the starvation period increases. According to the regression fit to the data, the point of 50% recovery occurs at 43.1 h of starvation. Given that the cell-cycle advances at approximately half the normal pace during starvation, this corresponds to sometime after 22 h post-invasion, the time point at which differences in Maf1 mRNA (Figure 3.6), and just prior to difference in Maf1 protein expression (Figure 3.9), are most pronounced.

PB-11 displays growth and recovery defects when exposed to multiple growth-retarding stressors

In yeast, Maf1 arrests Pol III transcription upon a broad array of biotic and abiotic stressors in addition to starvation (Upadhya et al., 2002). Since TORC1, and by

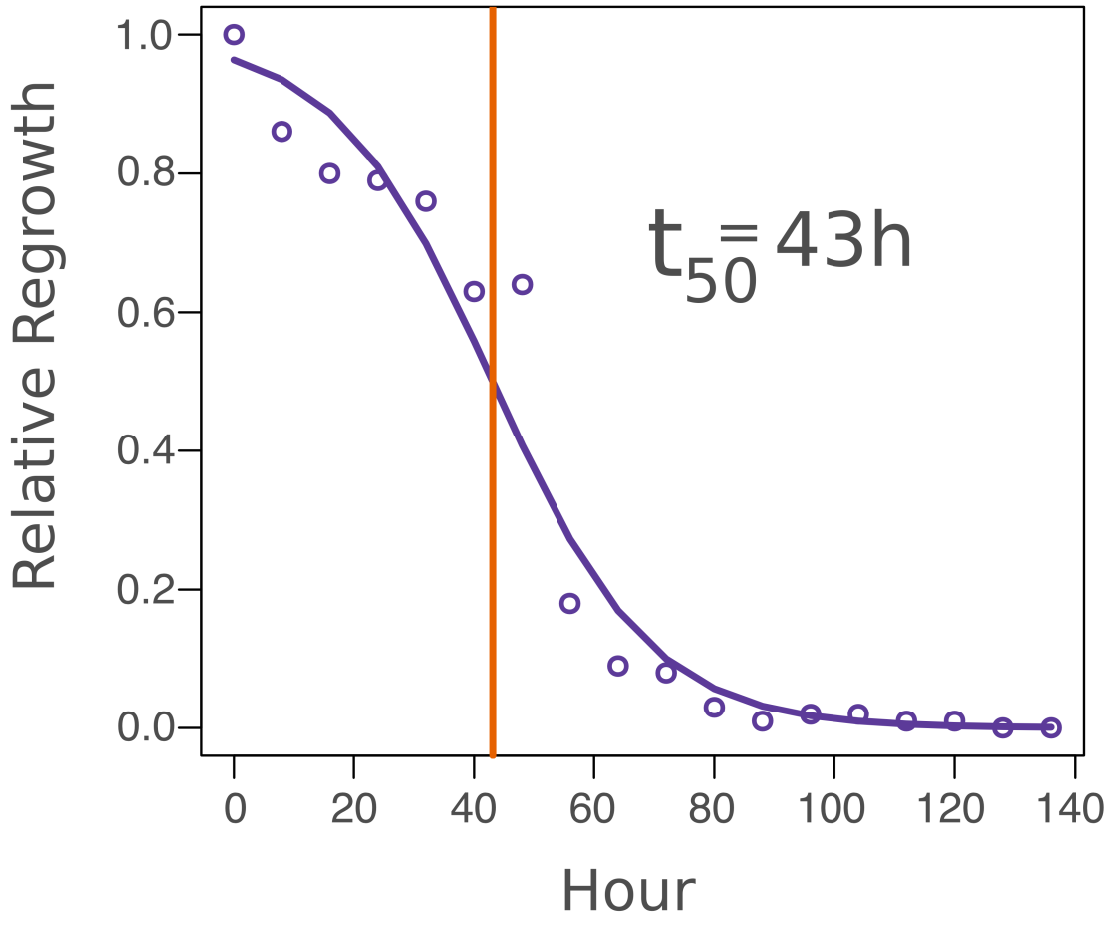

Figure 3.14: **Maf1 mutant parasites lose the ability to recover after 43 h of isoleucine starvation.** Synchronous young rings-stage PB-11 parasites were washed and transferred to medium lacking isoleucine. Every three hours, samples of the culture were transferred to normal medium for 72h of recovery. The final parasitemia after recovery was quantified by flow cytometry. A logistic regression fit to the data shows that each hour of starvation decreases the parasitemia to 93% of the parasitemia of the previous hour (β_o=-0.076, $p < 2.00x10^{-16}$). The logistic model fit to the data predicts 43 h of starvation as the point at which 50% of the PB-11 parasites can recover, and 50% cannot (t_{50}).

extension Maf1, typically regulates progression and arrest of the cell cycle, we investigated whether other stressors that stall or retard the cell cycle similar to isoleucine starvation also cause growth or recovery defects for the PB-11 Maf1 mutant.

The antibiotic Fosmidomycin inhibits isoprenoid biosynthesis in the *Plasmodium* apicoplast. Howe *et al.* previously demonstrated that treatment of parasites with 5 μM Fosmidomycin causes parasites to seemingly arrest in mid schizogeny (Howe et al., 2013). Subsequent treament of cultures with the downstream isoprenoid geranylgeraniol liberates the parasites from arrest. We arrested wild type and PB-11 mutant parasites with 5 μM Fosmidomycin for 72 h then treated them with 5 μM geranylgeraniol for a 72-hour regrowth period, and compared relative recovery to controls treated with both Fosmidomycin and geranylgeraniol simultaneously for 72 h (Figure 3.15). The PB-11 Maf1 mutants displayed a pronounced decrease in recovery relative to the wild type.

Ring-stage *Plasmodium falciparum* is capable of surviving prolonged exposure to temperatures well below 37 °C. In fact, the culture of *P. falciparum* at ambient room temperature has been proposed as a means for routine culture synchronization (Haynes and Moch, 2002). Presumably, the low temperature slows the cell cycle in a manner that may also require proper Maf1 expression for survival. We incubated wild type and PB-11 Maf1 mutant parasites at 18 °C for 72 h and then returned the cultures to 37 °C for 72 h of recovery and compared the relative growth to controls that remained at 37 °C for 72 h (Figure 3.15). Once again, the Maf1 mutant parasite line displayed notably decreased recovery from low temperature stress relative to wild type.

The growth rate of wild type and Maf1 mutant parasites is not notably different when cultured in normal medium (Figure 3.16). However, when cultured in growth

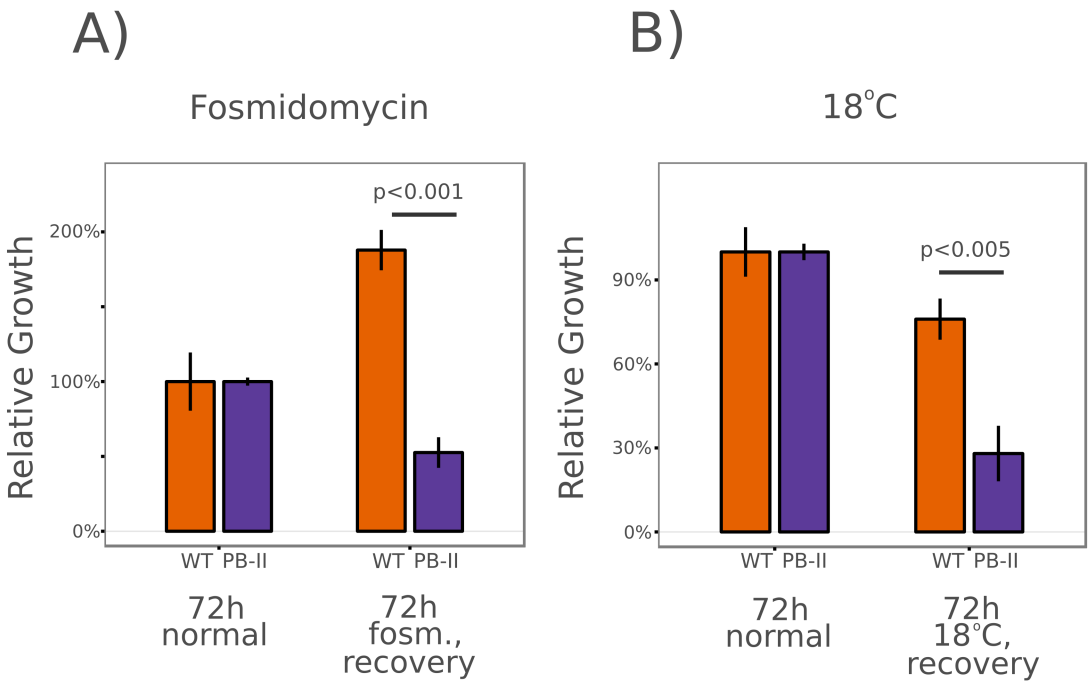

Figure 3.15: **PB-11 Maf1 mutant parasites display defects in recovery from Fosmidomycin and low temperature treatment. A)** Young ring-stage NF54 (WT) and Maf1 mutant (PB-11) parasites were incubated in the presence of 5 μM fosmidomycin (fosm.) for 72 h, and then "recovered" by incubation for a further 72 h in the presence of 5 μM fosmidomycin and 5 μM geranylgeraniol. Growth was measured relative to parasites incubated for 72h in normal medium treated with vehicle (water). **B)** Young ring-stage parasites were incubated at 18^{o}C for 72h, and recovered by a 72 h growth at 37^{o}C. Growth was measured relative to parasites incubated for 72 h at 37 ^{o}C.

limiting concentrations of isoleucine (8 μM, approximately 2% of the normal RPMI 1640 concentration) the doubling time of the PB-11 Maf1 mutant is markedly longer. A similar phenomenon occurs when the parasites are cultured in normal medium at the stress-inducing temperature of 39 ^{o}C (Figure 3.16). Interestingly, the growth rate of both wild type and PB-11 parasites is slowed by culture in medium containing 20% normal RPMI 1640 glucose concentration (ie: 0.4 g/L), but appears to affect both parasite clones equally (Figure 3.16). This suggests that Maf1 is not part of a universal stress response but instead is a component of a specific pathway that responds to certain growth inhibiting and retarding stressors but not others.

tRNA expression in the PB-11 Maf1 mutant is misregulation upon amino acid starvation

Maf1 is the only known regulator of RNA Pol III transcription. When conditions are unfavorable, Maf1 is activated and binds to the Pol III holoenzyme shutting down transcription of tRNAs, the 5s rRNA, and small number of other structural RNAs. This action is presumed to save cellular resources in times of stress and nutrient limitation, and may also globally reduce translational output by limiting the available tRNA pool. Presumably, Maf1 performs a similar function in *Plasmodium falciparum*.

The long half-life of mature tRNAs makes it difficult to quantify changes in their steady-state expression levels. Typically, pre-tRNAs, immature pre-cursors containing 5' and 3' transcriptional leader sequences and introns, are quantified instead, as these species are rapidly processed allowing the assessment of Pol III transcriptional activity. At present, no pre-tRNAs sequences have been annotated in the *Plasmodium falciparum* genome. Nearly every eukaryote tyrosine tRNA gene contains an intron immediately 3' of the anti-codon, the processing of which is believed to be necessary

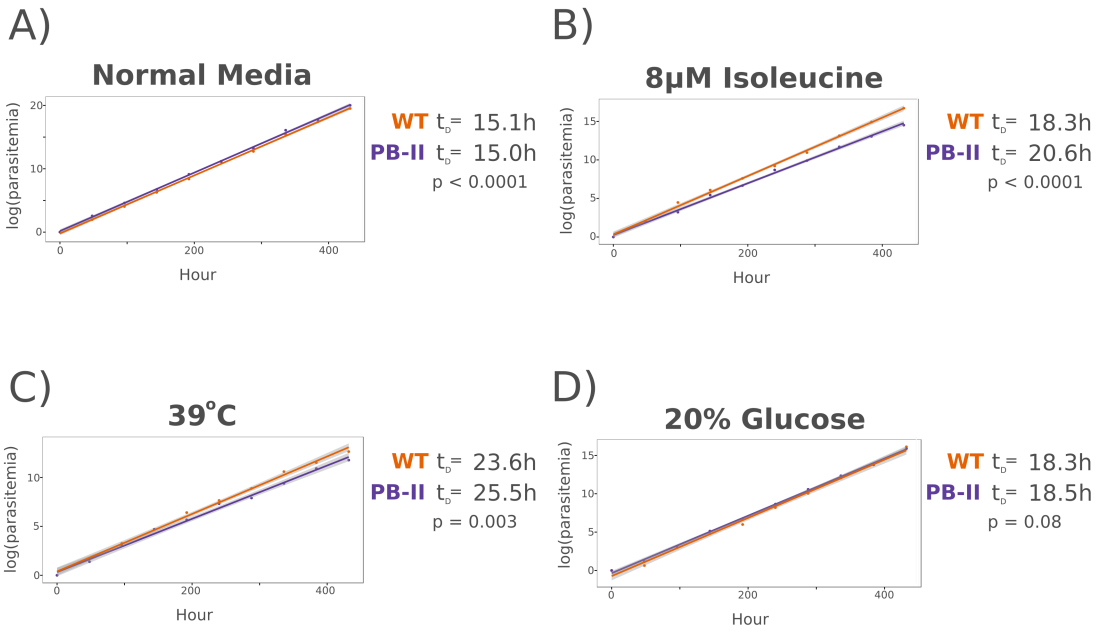

Figure 3.16: **PB-11 Maf1 parasites display a decreased rate of growth in low isoleucine and at elevated temperatures.** Growth curves were measured for NF54 (WT) or Maf1 mutant (PB-11) parasites cultured in **A)** normal culture medium at 37 °C, **B)** 8 μM isoleucine (approximately 2% the concentration of normal medium), **C)** normal culture medium at 39 °C, and **D)** 20% (0.4 g/L) of the glucose level of normal medium (2.0 g/L). P-values represent a test of parasite line (*i.e*: wild type vs PB-11) as a factor in the regression analysis. t_D = doubling time.

for the addition of the pseudouridine modification found in the anticodon of all mature eukaryote $tRNA^{Tyr}$ (Choffat et al., 1988). We reverse transcribed and cloned the mature *Plasmodium falciparum* $tRNA^{Tyr}$ and found an 11-nucleotide sequence adjacent to the anticodon was spliced out in the mature tRNA molecule (Figure 3.17). Using this short intron as a target sequence, we modified a stem-loop RT-qPCR protocol optimized for microRNAs (Chen et al., 2005)(Varkonyi-Gasic et al., 2007) to quantify expression of the pre-$tRNA^{Tyr}$ while using the similarly sized mature 5.8s rRNA (Pol I transcript) as reference.

In normal medium conditions, the PB-11 Maf1 mutant parasites display higher steady-state expression of pre-$tRNA^{Tyr}$ (Figure 3.17), suggesting Maf1 may play a role in regulating tRNA expression in normal growth as well as under conditions of stress. After 24 h of isoleucine deprivation, the difference in pre-$tRNA^{Tyr}$ levels is even more pronounced (Figure 3.17), supporting the notion that failure of the Maf1-dependent regulation of tRNA expression contributes to this mutant's inability to recover from amino acid starvation and other forms of stress.

It has been suggested that the increase in intracellular tRNAs levels caused by genetic suppression of Maf1 can cause a global increase translation due to the increased levels of the initiator $tRNA_i^{Met}$ (Rideout et al., 2012). Regulating translation under times of stress is a fundamental component to most celluar stress responses because it allows cells to conserve cellular resources, decrease the buildup of aggregates and unfolded proteins, and selectively translate specific subsets of mRNAs (Holcik and Sonenberg, 2005). If this process is counteracted by excessive translational initiation, the cells ability to survive stress may be seriously compromised.

To quantify global translation activity, we used a puromycilation assay (Schmidt et al., 2009). Briefly, the translation inhibitor puromycin incorporates into nascent

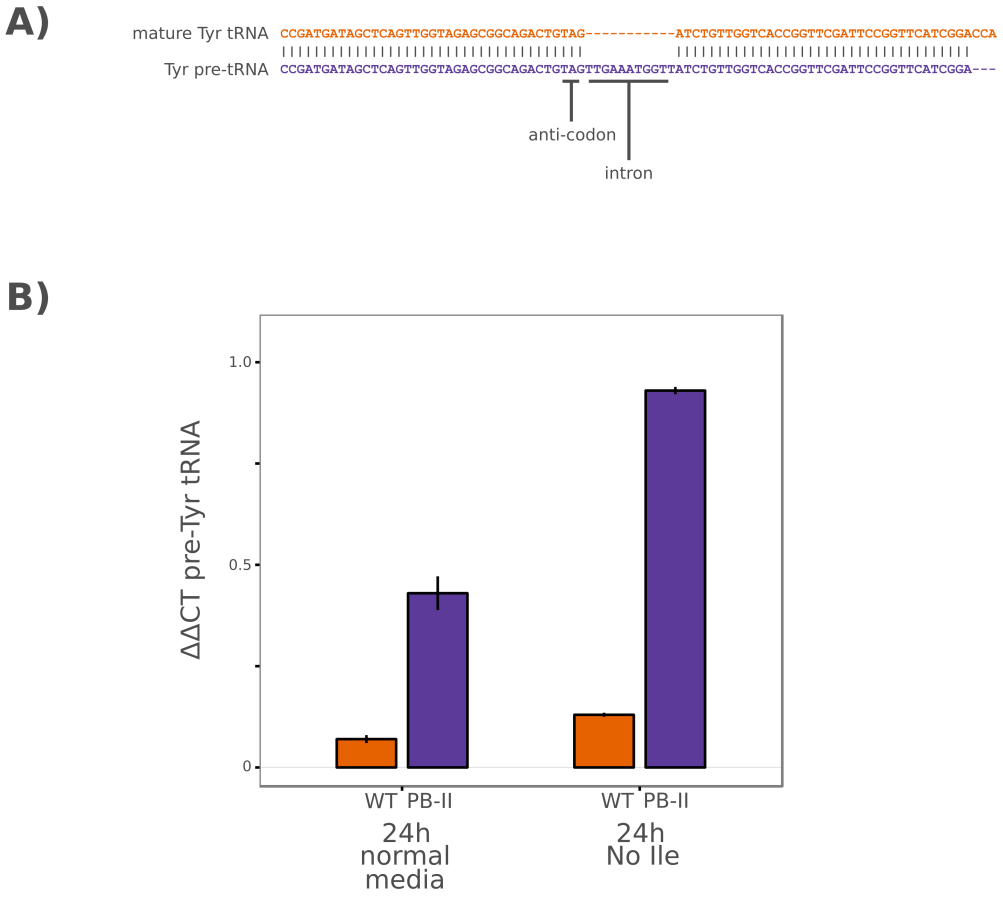

Figure 3.17: **Maf1 mutant parasites display elevated expression of pre-tRNAs under normal and isoleucine-starvation conditions**. **A)** An alignment of the genomic pre-tRNA^{Tyr} sequence and the mature tRNA^{Tyr} reveals an 11-nucleotide intron adjacent the anticodon. **B)** Stem-loop RT-qPCR profiling of pre-tRNA expression in NF54 (WT) and Maf1 mutant (PB-11) parasites. Synchronous young ring-stage parasites were incubated in normal medium or medium lacking isoleucine for 24 h prior to RNA isolation. Pre-tRNA^{Tyr} expression was quantified relative to 5.8S rRNA levels.

peptide chains on actively translating ribosomes. A monoclonal antibody specific for puromycin can then be used to quantify levels of puromycin incorporation as a surrogate for global translational output. We pulsed parasite cultures for 1h with puromycin prior to harvesting protein, then quantified puromycin incorporation by ELISA using anti-*Pf*GAPDH as an internal control.

When cells were cultured in normal medium, the PB-11 Maf1 mutant displayed moderately higher levels of puromycin incorporation relative to wild type cells (Figure 3.18). However, after 24 h of isoleucine starvation, the PB-11 mutant displayed a dramatic increase in puromycin incorporation relative to the wild type control. This inability to shutdown translation under amino acid starvation may further contribute to the mutant line's inability to survive prolonged starvation.

An artemisinin-resistant K13 variant confers increased survival and greater control of pre-tRNA expression upon isoleucine starvation

Artemisin and its derivatives induce growth-retardation in ring-stage parasites (Klonis et al., 2011), and artemisin-resistant isolates appear capable of recovering from this drug-induced growth inhibition while sensitive isolates cannot (Dogovski et al., 2015). A recent study reported that increased activity of *Pf*PI3K and *Pf*PKB, two other putative remnants of the TORC1 pathway in *Plasmodium*, as the mechanistic basis for survival in resistant parasites (Mbengue et al., 2015). We investigated whether this ability to overcome growth-retardation translated to prolonged amino acid starvation, and whether drug-resistant parasites displayed differential regulation of Pol III transcription as a potential point of connection between these other TORC1 pathway remnants and Maf1.

Using an artemisinin-resistant field isolate obtained from Battambang, Cambo-

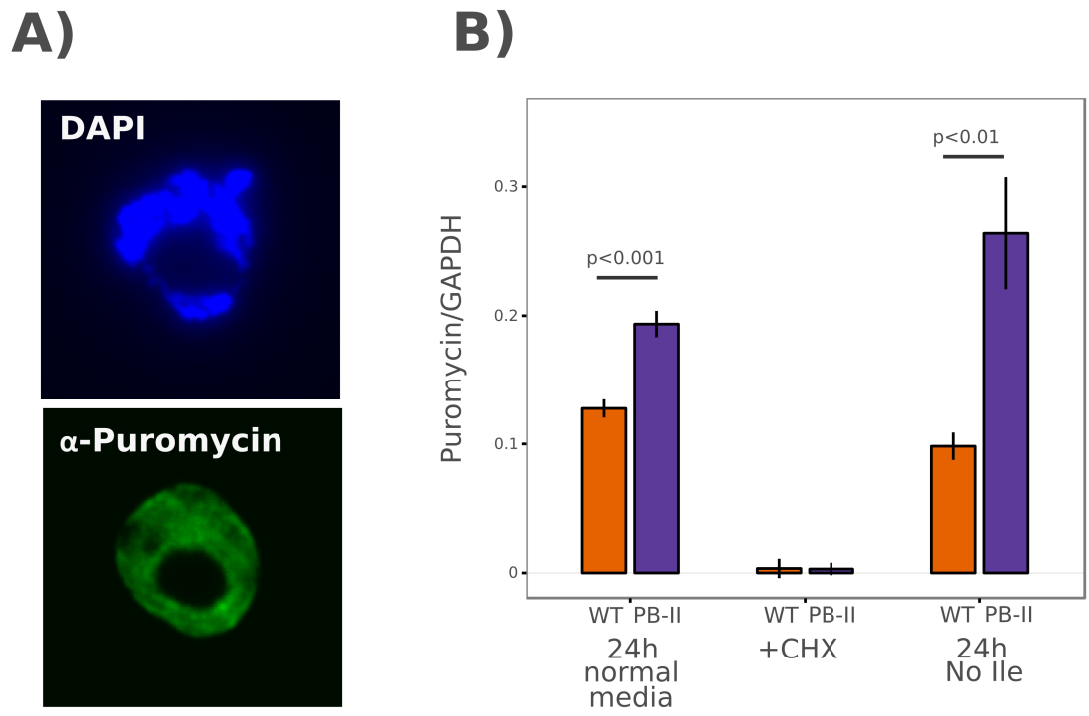

Figure 3.18: **The PB-11 Maf1 mutant displays increased global translation upon isoleucine starvation. A)** An IFA of a schizont labeled with puromycin for 1 h prior to fixation then probed with an anti-Puromycin monoclonal antibody to illustrate the efficiency of puromycin labeling. **B)** ELISA of puromycin incorporation relative to *Pf*GAPDH levels in wild type and mutant parasites under the indicated treatments. Synchronous young ring-stage parasites were incubated in normal medium or medium lacking isoleucine for 24 h prior to the 1-hour puromycin pulse and subsequent harvesting. Translational arrest by Cyclohexamide (CHX) treatment was used as a negative control.

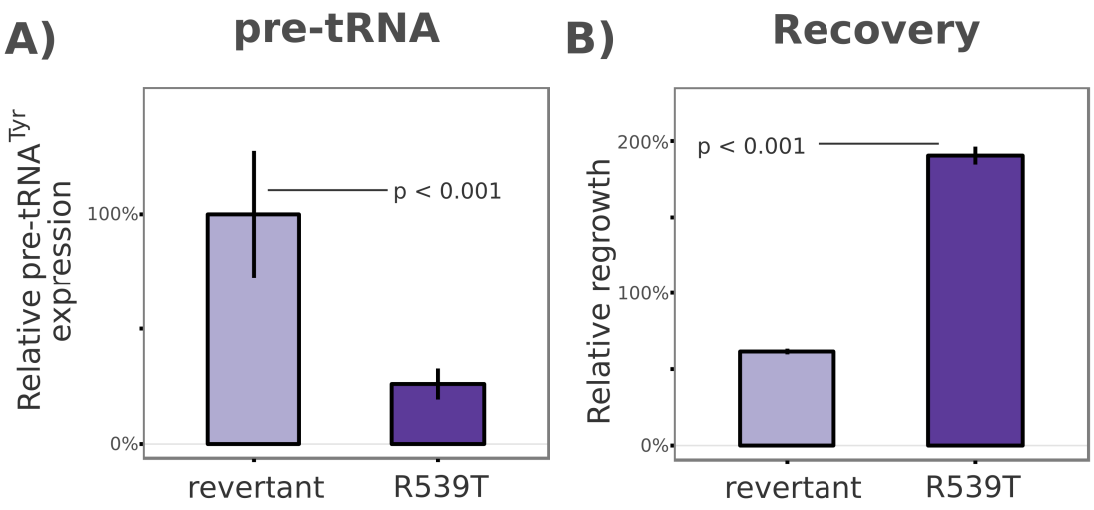

Figure 3.19: **An artemisinin-resistant mutant displays increased pre-tRNA regulation and survival upon isoleucine starvation. A)** qPCR quantification of pre-tRNA^{Tyr} expression after 24 h of isoleucine starvation in an artemisinin-resistant field isolate (”R539T”) and a syngenic clone converted to the artemisinin-sensitive K13 allele (”revertant”). Data are represented as a percent of the ”wild type” revertant expression level. **B)** Sensitive (”revertant”) and artemisinin-resistant (R539T) parasites were starved of isoleucine for 72 h then transferred to normal medium for 72 h of recovery. Growth was quantified by flow cytometry and data are expressed as a percentage of the starting parasitemia of each line. P-values reflect t-tests after three biological replicates.

dia (K13 allele: R539T), and a syngenic line in which the K13 was reverted back to the sensitive allele (Straimer et al., 2015), we cultured the parasites in the absence of isoleucine and evaluated their ability to regulate pre-tRNA expression and recover from starvation (Figure 3.19). After 24 h of isoleucine starvation, the R539T resistant isolate displayed 27% the expression level of pre-tRNA^{Tyr} observed in the syngenic revertant line. Consistent with our observation in the PB-11 Maf1 mutant, the ability to suppress pre-tRNA expression corresponded with an increase in survival. After 72 h of isoleucine starvation, and a subsequent 72 h of recovery, the R539T resistant isolate displayed a relative recovery nearly 3-fold greater than its revertant counterpart (Figure 3.19).

It should be noted that the revertant, which carries the same K13 allele as the NF54 "wild type" clone used elsewhere in this study, suffered considerable loss of viability over the 72 h of starvation, displaying a final parastemia after recovery of only 61% of the starting parasitemia (Figure 3.19). Evidently, the genetic background of this parasite isolate renders it more vulnerable than typical lab strains (NF54, 3D7) to isoleucine starvation under the conditions employed here.

Discussion

The TORC1 pathway is a highly conserved signalling pathway that allows eukaryotes to modulate cellular growth in response to changes in the environement. Most recognizable components of this pathway have been lost in the *Plasmodium* genus. In this study, we have shown that the *Plasmoidum falciparum* ortholog of Maf1, one of the few remaining pathway components, contributes to surival and recovery of parasites treated to various forms of growth-inhibiting stress; a phenotype that corresponds

well with those reported in other organisms.

To study this gene, we made use of a transposon-insertion mutant produced as part of an effort to generate a genome-wide mutant collection. While this mutant was not a genetic knockout as previously reported, insertion of the *piggyBac* element into the Maf1 5'UTR produced profound changes in both mRNA and protein expression. Our observation of the mutant's inability to regulate pre-tRNA expression and protein synthesis, a phenotypes previously described for yeast, human, and *Drosophila* Maf1 mutants (Roberts et al., 2006)(Shor et al., 2010)(Marshall et al., 2012), supports the conclusion that the mutant's altered Maf1 expression profile is responsible for its inability recover from isoleucine starvation and other forms of stress. We were unable to generate a knockout parasite line using standard methods, suggesting basal Maf1 expression may be essential for *in vitro* asexual growth. The reason for why *Pf* Maf1 would be necessary for growth under normal conditions is not clear, as Maf1 knockouts are viable in both yeast and mice (Pluta et al., 2001)(Bonhoure et al., 2015). One possible explanation may stem from the observation that the PB-11 Maf1 mutant displayed elevated levels of global translation relative to the wild type control even under normal growth conditions. *Plasmodium* schizonts are reported to globally suppress translation at the late stages of the intraerythrocytic cycle (Zhang et al., 2012). It is possible that some degree of Maf1 suppression of tRNA and the 5S rRNA transcription is needed for the maintaining this suppression.

In yeast and human cells, Maf1's association with RNA Polymerase III is regulated through phosphorylation. Under favorable conditions, Maf1 is phosphorylated and unable to bind to the polymerase complex. Under stress, phosphorylation is inhibited, and Maf1 binds to Pol III to block formation of the initiation complex (Vannini et al., 2010). In certain human and yeast cell lines, Maf1 is localized in the cytoplasm and translocates to the nucleus and nucleolus upon dephosphorylation

during stress (Roberts et al., 2006)(Shor et al., 2010). In others, it is constitutively nuclear, but still requires dephosphorylation to associate with Pol III (Wei et al., 2009)(Kantidakis et al., 2010). We attempted to localize *Plasmodium* Maf1 by fluorescent microscopy, but were unable to detect it with our current set of reagents.

Our efforts to assess *Pf* Maf1's phosphorylation state have also been unsuccessful. Of the many phosphoproteomic studies performed on blood stage *Plasmodium falciparum*, only two have reported phosphopeptides mapping to Maf1 protein sequence (Lasonder et al., 2012)(Lasonder et al., 2015). The reported phosphopeptides were different in each study (pS86 and pS109) and, in each case, were only supported by a single spectrum. Both are contained within the asparagine rich region within the protein sequence, and are not conserved across other *Plasmodium* species. While not the most attractive candidates, these phospho-sites may merit further study, as they are located within the "mobile insertion" region of the protein, which is one of the major sites of phosphorylation in yeast and human cells. A phosphoproteomic study of *Toxoplasma gondii* found evidence for extensive phosphorylation of its Maf1 ortholog (Xia et al., 2008) (Note that the *T. gondii* ortholog of the protein described in our study is TGME49_248110, and not the recently described (Pernas et al., 2014) *Mitochondria Associated Facotor 1* (MAF1). The later protein bears no sequence or functional relation to the former, and only shares its name due to an unfortunate coincidence in naming). Of the thirteen phosphorylation sites reported in *T. gondii*, most are only supported by a few spectra and are not conserved in the *P.falciparum* sequence. However, one site in the acidic tail, a key regulatory region of the human and yeast orthologs, has extensive spectral support and aligns well with the *P. falciparum* S374. This residue may be the best candidate for future studies of *Pf* Maf1 regulation.

In human cells, association of Maf1 with the Pol III complex appears to be regulated by the mTOR kinase itself (Shor et al., 2010)(Kantidakis et al., 2010). In yeast,

this function is performed by the S6K homolog Sch9 upon TOR activation (Lee et al., 2009)(Huber et al., 2009), though a single study has suggested the yeast TOR homolog may also phosphorylate Maf1 (Wei et al., 2009). Since the *Plasmodium* genus lacks a TOR homolog, the Sch9/S6K homolog, erroneously known as *Pf*PKB, is a strong candidate for the *Pf*Maf1 regulatory kinase. In yeast, other kinases in addition to Sch9 have also been implicated in Maf1 regulation. PKA has been shown to phosphorylate Maf1 *in vivo*, though it appears to regulate localization and not association with the Pol III complex (Moir et al., 2006)(Lee et al., 2009). The CK2 kinase has also been implicated in Maf1 regulation in yeast (Graczyk et al., 2011), though its importance is not clear (Willis et al., 2011). *P. falciparum* encodes orthologs of both these kinases (PKA catalytic subunit: PF3D7_0934800, CK2 catalytic subunit: PF3D7_1108400), and they should be considered potential regulators of *Pf*Maf1 as well. It remains possible that Maf1 is not phosphoregulated in *P.falciparum*, and instead, its activity is regulated through transcriptional and translational control. This could explain why *Pf*Maf1 displays an expression bias toward the late stages of cell cycle, and why our attempts to over-express an ectopic copy failed unless expression was attenuated using a weak promoter and a destabilization domain. We observed increased pre-tRNA expression in the PB-11 mutant relative to wild type cells in normal culture medium, suggesting *Pf*Maf1 performs some level of basal pre-tRNA inhibition under normal conditions.

We observed defects in the PB-11 mutant's ability to recover from not only prolonged amino acid starvation, but also several other forms of stress that slowed growth. We selected fosmidomycin treatment as one such stress for its previously described ability to trap parasites in schizogeny for several days with little effect on parasite viability (Howe et al., 2013). The Maf1 mutant displayed decreased recovery relative to wild type cells upon release from fosmidomycin block. This phenotype may be due to a secondary effect of the mutant's inability to regulate tRNA synthe-

sis. Fosmidomycin inhibits the non-mevalonate isoprenoid biosynthesis pathway in the apicoplast. One of the direct products of this pathway is dimethylallyl pyrophosphate (DMAPP), which serves as a substrate for the isopentenylation modification of certain tRNAs in eukaryotes, a process likely to be conserved in *Plasmodium spp.* (Guggisberg et al., 2014). In yeast, there is evidence for a Maf1-dependent reciprocal relationship between tRNA synthesis and the isoprenoid biosynthesis pathway (Kaminska et al., 2002), and in fact, overexpression of yeast Maf1 to suppress tRNA transcription has been used to increase isoprenoid yield for potential commercial purposes (Liu et al., 2013). The decreased recovery of the PB-11 Maf1 mutant may in part be a result of depletion of the residual isoprenoid pool due to the mutant's elevated pre-tRNA production.

Babbitt *et al.*'s description of the dormancy-like slow-growth response of *Plasmodium falciparum* upon isoleucine starvation was the first thorough documentation of the parasite's ability to modulate its growth rate in response to environmental changes (Babbitt et al., 2012). However, after being unable to implicate any specific molecular pathways in the response (ie: GCN2/*Pf*IK2 - IF2α), and after observing a dose-dependence between isoleucine concentration and growth rate, they concluded that the parasite does not actively regulate its growth, and that isoleucine is likely the rate-limiting factor in progression of the cell cycle. We feel this conclusion may be premature. Similar conclusions were drawn in other organisms, such as yeast, until it was demonstrated that chemical or genetic inhibition of TOR induced the same transition into stationary phase as nutrient starvation, and that partial inhibition of TOR slowed the cell cycle in a similar manner as nutrient limitation (Barbet et al., 1996)(Powers et al., 2006)(Loewith and Hall, 2011). It is well established that different *P. falciparum* isolates display a wide variation in the length of the cell cycle and average number of merozoites produced in each cycle (Reilly et al., 2007)(Reilly Ayala et al., 2010), indicating that genetic factors contribute to parasite growth. We

previously demonstrated that the single point mutation that confers artemisinin resistance can change the growth rate of a parasite line even when isoleucine is limiting (Chaper 1). The fact that these parasites exhibit increased recovery from both starvation and artemisin-induced growth retardation implicates an underlying pathway that regulates growth. We believe our description of *Pf* Maf1's role in maintaining viability upon growth retardation further supports the existence of such a pathway. The remaining components of the pathway, however, have yet to be identified.

In other eukaryotes, the TORC1 complex itself is not the sensor for amino acids, but the hub through which the signal is transduced. The most upstream components that bind and detect amino acids such as leucine (Wolfson et al., 2016) and arginine (Chantranupong et al., 2016) in human cells, are not conserved in yeast and other distal branching lineages. It is possible that *Plasmodium* has retained its upstream sensors and the downstream effectors (eg: *Pf* PKB and *Pf* Maf1) while losing the intermediate signaling steps, such as TORC1. Studies in mammalian cells have found evidence that the class III PI3K *Hs*Vps34 increases PI(3)P production in the presence of amino acids upstream of mTOR, leading to increased phosphorylation of S6K (Nobukuni et al., 2005)(Byfield et al., 2005). This is reminiscent of the observation that *Pf* PI3K inhibition by artemisinin inhibits *Pf* PKB activity in *P. falciparum* (Mbengue et al., 2015). However, given that *Pf* PI3K is associated with both hemoglobin import for digestion and the reclamation of amino acids through autophagy, we would like to entertain the possibility that artemisinin inhibition of PI3K induces intracellular starvation of (all) amino acids, triggering the same growth retardation response as removal of isoleucine from the extracellular medium. This would explain why proteasome inhibitors show synergistic effects with artemisinin (Dogovski et al., 2015), as they block the cell's last remaining means of reclaiming amino acids.

Homologs of other eukaryote pathways that regulate growth, in addition to

TORC1, are conserved in the *P. falciparum* genome. It is possible that Maf1 or the responses to isoleucine or artemisinin are affected by these pathways. *Plasmodium* has a clear homolog of Protein Kinase A (PKA) (PF3D7_0934800), and also has a kinase that resembles AMPK/Snf1 (PF3D7_0934800). Neither has been implicated in the regulation of parasite growth rate to date. In other organisms, both pathways play roles in the direct or indirect detection of glucose levels (Conrad et al., 2014). The fact that both wild type cells and the PB-11 Maf1 mutant equally retard growth in decreased glucose suggests that the mechanism the parasite uses to detect and respond to glucose is unlikely to be also responsible for Maf1 regulation.

The Unfolded Protein Response (UPR) that detects the accumulation of unfolded proteins in the endoplasmic reticulum is another pathway capable of regulating cellular growth in mammalian cells. *P. falciparum* has a greatly reduced UPR pathway, and notably lacks the highly conserved transcription factors (IRE1, ATF6) that define the yeast and human response to unfolded proteins (Gosline et al., 2011)(Harbut et al., 2012). Consequently, *Plasmodium* has been found to be particularly sensitive to ER stress-inducing agents such as DTT (Chaubey et al., 2014). A recent, massive transcriptomics effort found that artemisinin-resistant parasites appear to have higher steady state levels of chaperone complexes normally associated with the UPR in other organisms, and suggested the higher expression of these factors may be protective against artemisinin (Mok et al., 2015). However, at present, artemisinin resistant parasites have not been shown to be more resistant to ER stress than wild type parasites, and artemisinin-derivatives have not been shown to induce ER stress. In mammalian cells, the UPR is capable of slowing and arresting cell growth by phosphorylation of eIF2α by the ER-unfolded protein sensor and kinase PERK (Brewer and Diehl, 2000)(Hamanaka et al., 2005). The *P. falciparum* genome does encode a kinase (*Pf* PK4, PF3D7_0628200) with modest similarity to mammalian PERK (Gosline et al., 2011), and *P.falciparum* eIF2α is phosphorylated upon DTT treatment (Chaubey et al., 2014),

though PK4 has not been implicated in this phosphorylation. The link between an enhanced-UPR and the ability of artemisinin-resistant parasites to survive and recover from artemisinin-induced growth retardation is intriguing. However, at this stage there is too little evidence to definitively make this connection. ER stress has not been shown to slow or arrest the cell cycle in *P. falciparum* (it does not in yeast)(Henry et al., 2010), and blocking phosphorylation of eIF2α upon isoleucine starvation has no impact on growth retardation or survival, suggesting a different pathway regulates slow growth at least under conditions of isoleucine starvation. Maf1 has not been demonstrated to be regulated under ER stress or be part of the UPR in other organisms.

Unlike TOR, Maf1 has never been shown to arrest or retard growth on its own. It is instead needed to maintain viability during the period of stress or nutrient limitation, much as we observed in *P. falciparum*. It will be interesting to see whether the PB-11 Maf1 mutant also displays defects in recovery from artemisinin-induced growth-retardation. The genetic background of the PB-11 mutant is NF54, which is acutely sensitive to artemisinin. The current standard for evaluating artemisinin resistance, the Ring Survival Assay (Witkowski et al., 2013), is not optimized for detecting sensitivity well below that of resistant clinical isolates. Instead, 0-3-hour ring LD50 assay (Dogovski et al., 2015) will need to be adapted for this mutant. Nonetheless, it is intriguing that the single point mutation in the K13 gene that confers artemisin survival also displays increased survival upon prolonged amino acid starvation, and greater suppression of tRNA expression. If growth is actively regulated in *Plasmodium* by a residual TORC1 pathway as we hypothesize, then the K13 mutation, and the subsequent elevation in *Pf*PI3K levels (Mbengue et al., 2015), may allow the parasite to more effectively shut down growth when faced with undesirable circumstances, or more effectively resume growth again after a growth-retarding insult.

Methods

Yeast Complementation

A full length *Plasmodium falciparum* Maf1 coding sequence was synthesized with codon usage optimized for *S. cerevisiae* expression (Genscript). Using Gibson Assembly (NEB, #E2611S), the core region of *Pf* Maf1 (amino acids 237-346) was fused between the *S. cerevisiae* N-terminus (amino acids 1-233) and C-terminal "acidic tail" (amino acids 338-395). The resulting chimeric open reading frame was cloned into the *Bam*HI and *Xho*I sites of the yeast expression vector p416-Met25-3xHA. The full length yeast Maf1 open reading frame (YDR005C) was similarly cloned into the same vector. The Maf1Δ knockout line (BY4741 MATa library, ΔYDR005C) was transformed using the LiAc/ssDNA/PEG method (Gietz and Woods, 2002). Survival assays were carried out on synthetic minimal dextrose medium lacking uracil (for plasmid selection) and methionine (to de-repress the Met25 promoter for transgene expression) with or without 10nM rapamycin (Cell Signaling Technologies, #9904).

Parasite Culture and Media

Parasites were cultured using standard methods (Jensen and Trager, 1977) in flasks gassed with a mixture of 90% N_2, 5% CO_2, 5% O_2 (Airgas, #Z03NI9022000033). Normal culture medium consisted of RPMI 1640 with L-glutamine and 25 mM HEPES (Corning, #10-041-CV), with 5.0g/L Albumax II Lipid-Rich BSA (ThermoFisher Scientific, #11021029), 3.7mM Hypoxanthine, and 50μg/mL gentamicin. The Isoleucine deficient medium consisted of 10.3g/L RPMI 1640 Ile-Dropout medium (US Biologicals, #R9014), supplemented with 2.0g/L NaHCO3, 6.0g/L

HEPES, 5.0g/L Albumax II, 3.7mM Hypoxanthine, and 50μg/mL gentamicin. The 8μM Isoleucine medium was the same as the Isoleucine medium, except was supplemented with 8μM L-Isoleucine. The 20% Glucose media consisted of 8.4g/L of No Glucose RPMI 1640 (Sigma-Aldrich, #R1383), with 2.0g/L NaHCO3, 6.0g/L HEPES, 5.0g/L Albumax II, 3.7mM Hypoxanthine, 50μg/mL gentamicin, and 0.4g/L glucose. Fosmidomycin was obtained from Sigma-Aldrich (#F8682-5MG), and Geranylgeraniol was obtained from Santa Cruz Biotechnology (sc-200858).

Flow Cytometry

For each sample to be analyzed, 1mL of parasite culture was pelleted and resuspended in 1mL of PBS containing 4%w/v paraformaldehyde. Samples were rocked at 4°C for 20-30h of fixation. Samples were then pelleted and resuspended in PBS containing 0.1% v/v Triton-X 100 and rocked at room temperature for 1h for permeabilization. This process was then repeated three additional times with PBS (without Triton-X 100) to remove as much hemoglobin as possible. Samples were then diluted approximately 100-fold into normal culture medium containing 1x SYBR Green I (ThermoFisher Scientific, #S7563) and analyzed on a FACSCalibur (BD Biosciences) flow cytometer. The resulting data was further analyzed using FLOWJO 10.0.7 analysis software.

Transfection

The DD24-Maf1 construct was synthesized (Genscript) with N-terminal 3xHA tag followed by a DD24 destabilization domain and a yeast codon optimized Maf1 open reading frame (the same synthesized construct used for yeast complementation). This

open reading frame was cloned into the *Xho*I and *Xma*I sites of the vector pLN-mRPL2pr to generate pLN-mRPL2pr-DD24-Maf1. This vector was used to transfect $Dd2^{attB}$ parasites (Nkrumah et al., 2006) by the pre-loading method (Deitsch et al., 2001) using a modified Bxb1 integrase transfection method (Spalding et al., 2010). Stably transfected cells were maintained with 2.5μg/mL Blasticidin S. The *Shield* ligand was obtained from Aobious (#1848).

Genome Sequencing and Analysis

High quality, high molecular weight genomic DNA was prepared from 400mL of 2% hematocrit, ~10% parasitemia PB-11 culture enriched in late stage parasites. Parasites were liberated from erythrocytes by saponin treatment and washed twice with PBS to remove excess hemoglobin. The resulting parasite pellet was used as starting material for genomic DNA isolation using the Blood and Cell Culture Mini Kit (Qiagen, #13323). Genomic DNA was sent to Axeq Technologies (Seoul, South Korea) care of MacrogenUSA (Maryland, USA) for library preparation and sequencing. An amplification-free library (Kozarewa et al., 2009) was sequenced by paired-end sequencing to 73x coverage using an Illumina HiSeq2000.

Sequencing Analysis

The analysis of the sequencing data largely followed the protocol described by Balu *et al.* (Balu et al., 2013), which previously sequenced the NF54 clone that was used as the parental line in the transposon screen which produced the PB-11 mutant (Balu et al., 2009). Two sets of paired end reads for the parental NF54 clone, produced by two different sequencing platforms, were obtained from the European Nucleotide Archive

(ERS038926 and ERS184445). These reads were used to "update" the PlasmoDB-26 *P. falciparum* 3D7 genome sequence using ICORN as part of the PAGIT software package (Swain et al., 2012). Seven iterations of ICORN generated 561 1bp substitions and 774 small insertions or deletions across the entire reference genome. The PB-11 reads were aligned to this updated reference sequence using bwa (Li and Durbin, 2009) with the default parameters. Approximately 82% of reads aligned to the reference sequence. The resulting sam file was sorted, indexed, and filtered of duplicates using picard-tools v1.119. Reads were re-aligned around indels using The Genome Analysis Toolkit (GATK) (McKenna et al., 2010), and raw variants were called using the GATK HaploTypeCaller with ploidy set to 1. The raw variants were then filtered using vcftools v0.1.13 (Danecek et al., 2011) to only include calls with a quality score greater than 60 and a minimum depth of 10 reads. The program snpEff v3 (Cingolani et al., 2012) was then used to filter only those variants found within open reading frames. This resulted in 32 potential variants within open reading frames. However, upon visual inspection using the Integrated Genomics Viewer v2.3.9 (Robinson et al., 2011), every call was found in either a low complexity (*e.g*: an extended mononucleotide tract) or repetitive region. In each case, there was read support for the reference sequence, leaving us to conclude that these variants are more than likely false-positives. To verify that our pipeline was indeed capable of detecting variants, we re-ran the pipeline using the reads from the C9 *piggyBac* insertion mutant sequenced by Balu *et al.* (ENA ERS038913)(Balu et al., 2013). We were able to easily detect the same two SNPs reported previously.

mRNA Expression qPCR Timecourse

Synchronous cultures were established by sequential sorbitol treatments. For each time point, 50mL of 2% hematocrit culture at approximately 10% par-

asitemia was pelleted and immediatey disrupted with 10mL of TRIzol (ThermoFisher Scientific, #15596018), and used for subsequent phenol/chloroform extraction and ethanol precipitation, as per the manufacturer's protocol. First strand cDNA synthesis was performed using a mixture of oligo-dT and random hexamers using Superscript III (ThermoFisher Scientific, #18080044) using the standard protocol. For quantitative PCR, the Maf1 transcript was amplified using the forward primer 5'-GATGCCCACGATCGTTTTAT-3' and reverse primer 5'-CGGAGCTAAATATTTGTGTATTGC-3'. The seryl-tRNA ligase transcript, PF3D7_0717700, was used as an internal control, with 5'-AAGTAGCAGGTCATCGTGGTT-3' as a forward primer and 5'-TTCGGCACATTCTTCCATAA-3' as reverse primer. Quantitave PCR was performed using SYBR Green PCR Master Mix (ThermoFisher Scientific, #4309155) on a StepOnePlus (ThermoFisher Scientific) Real-time PCR system.

5'-RACE

RNA was extracted from 50mL of 2% hematocrit, 10% parasitemia mixed stage culture using TRIzol (ThermoFisher Scientific, #15596018). 5'-RACE was performed using the FirstChoice RLM-RACE Kit (ThermoFisher Scientific, #AM1700). The resulting PCR product was cloned using the CloneJET PCR Cloning Kit (ThermoFisher Scientific, #K1231) and sequenced (MacrogenUSA) to determine the 5' transcription start site.

Recombinant protein expression and Antibody production

For recombinant protein production, the *Plasmodium berghei* Maf1 ortholog (PBANKA_0718500) was selected instead of the *P. falciparum* ortholog, as it is much smaller and contains a short repeat in the place of the *P. falciparum* asparagine-rich region. Outside this region, the sequences are nearly identical. The *P. berghei* Maf1 sequence was synthesized with *E. coli* optimized codon usage (DNA2.0) with an N-terminal 6xHis tag in a T7 promoter expression plasmid. Protein expression was conducted in NiCo21(DE3) cells (NEB, #C2529). Expression was performed in 1L cultures induced at an OD_{600} of 3.0 with 0.5mM IPTG in Terrific Broth for 20h at room temperature. Cells were lysed by sonication, and protein was isolated using Ni-NTA agarose (Qiagen, #30210). The recombinant protein was used to produce antiserum from two separate Guinea Pigs by Cocalico Biologicals (Pennsylvania, USA) using the standard protocol. Antiserum was affinity isolated against the recombinant *Pb*Maf1 protein. Western blots were visualized using a LI-COR Odyssey imaging system with 680RD linked anti-mouse (LI-COR, #925-68070) and anti-guinea pig (LI-COR, #925-68077) secondary antibodies. The 1-10b *Pf* GAPDH monoclonal (mouse) (Daubenberger et al., 2003) was used as a loading control.

Growth Curves

Asynchronous parasite cultures were maintained under the conditions described and sampled every 48h to quantify parasitemia by flow cytometry. Cultures were then diluted between 2 and 10-fold to maintain a parasitemia between 0.5-1.0% parasitemia and the dilution factor was recorded. The growth at each time point was measured as the parasitemia multiplied by the dilution factor of the previous dilution. The final dataset was normalized such that the initial parasitemia for each line started at 1.0 to

account for differences in the starting parasitemias of the different parasite lines. A two-factor regression of ln(adjusted parasitemia) ~ hour + genotype was fit for each condition to test the effect of parasite genotype on growth rate with time as a covariate. Doubling time (t_D) was calculated for each line from single factor regressions against time alone, using $t_D = \log(2)/\beta_o$, where β_o is the coefficient from the single factor regression.

tRNA^{Tyr} intron verification and stem-loop PCR

For tRNA analysis, RNA was isolated using miRvana miRNA Isolation Kit (ThermoFisher Scientific, #AM1560) to specifically enrich small RNAs. Due to the inherent high-stability of tRNA secondary structure, a modified reverse-transcription protocol was employed. Total small RNA was mixed with 5μM of the RT-primer 5'-ttacttgtacagctcgtccatgccgagaTCCGATGAACCGGAATCG-3' which anneals to the 3' end of the tRNA^{Tyr} (PF3D7_0702800) sequence but contains a RACE-like 5' extension of an unrelated primer sequence for subsequent PCR amplification (to avoid amplifying the genomic locus). The small RNA-primer mixture was heated to 98°C for 5min, then cooled slowly to 4°C. Reverse transcription was then performed using Superscript III (ThermoFisher Scientific, #18080044) by the manufacturers protocol, with the exception that it was performed at the elevated temperature of 65°C for 1h to minimize the effects of tRNA secondary structure. The cDNA was then amplified using Phusion High-Fidelity Polymerase (NEB, #M0530L), using the forward primer 5'-CCGATGATAGCTCAGTTGGTAGA-3', which anneals to the 5' end of the tRNA^{Tyr} sequence, and the reverse primer 5'-CTTGTACAGCTCGTCCATGCC-3', which anneals to the RT-primer's 5' extension. The resulting PCR product was cloned using the CloneJET PCR Cloning Kit (ThermoFisher Scientific, #K1231) and sequenced (MacrogenUSA) to verify

the excision of the predicted 11nt intron.

pre-tRNA^{Tyr} stem-loop qPCR

For analysis of of pre-tRNA^{Tyr}, highly synchronous parasites cultures were initiated by percoll-sorbitol treatment to generate 50mL of 2% hematocrit culture between 5% and 10% parasitemia with a maximum parasite age of 4hpi. These cultures were then washed three times in 50mL PBS and resuspended in either normal media or media lacking isoleucine, then incubated for 24h prior to harvesting. Cultures were pelleted and treated with 0.1% Saponin in PBS, and washed twice with 50mL PBS to remove liberated hemoglobin. A small RNA sample was then isolated from parasite pellets using the miRvana miRNA Isolation Kit (ThermoFisher Scientific, #AM1560) according to the manufacturer's protocol. In order to specifically detect the presence of the 11nt intron in the pre-tRNA^{Tyr}, a stem-loop PCR method originally developed for miRNA detection (Chen et al., 2005)(Varkonyi-Gasic et al., 2007) was adapted. In this method, a self-annealing 5' stem-loop extension to the RT-primer both adds length to the final product for downstream qPCR amplification, and may also provide additional stability for the annealing of the short complementary primer sequence due to stacking interactions provided by the stem-loop. For reverse transcription, small RNA samples were combined with a 5μM mixture of the stem-loop RT-primers 5'-GTCGTATCCAGTGCAGGGTCCGAGGTATTCGCACTGGATACGACataaccatttc-3' and GTCGTATCCAGTGCAGGGTCCGAGGTATTCGCACTGGATAC-GACcagcattctga, which anneal to the pre-tRNA^{Tyr} intron and the 3' end of the 5.8s rRNA respectively. The primer-RNA mixture was heated to 98^{o} for 5min then cooled to 4^{o}C. Reverse transcription was carried out at 65^{o}C for 1h to overcome RNA-secondary structure, but otherwise followed the manufacturers protocol for Superscript III (ThermoFisher Scientific, #18080044). Quantitative PCR was

performed using the common reverse primer 5'-CAGTGCAGGGTCCGAGGT-3' which anneals to the shared stem-loop structure, and the gene-specific forward primers 5'-AGTTGGTAGAGCGGCAGACT-3' ($tRNA^{Tyr}$) and 5'-AGCAAAACGCGATAAGCAAT-3' (5.8s rRNA) on a StepOnePlus Real-Time PCR system (ThermoFisher Scientific) using the Power SYBR Green Master Mix (ThermoFisher Scientific, #4367659).

Puromycilation Assay

Cultures were initiated using percoll-sorbitol synchronization to produce 50mL cultures at 2% hematocrit at approximately 10% parasitemia. Cultures were then pelleted and washed three times with 50mL PBS and resuspended in either normal or isoleucine-lacking medium. After 24h, puromycin was added to a final concentration of 1.0μM and parasites were incubated for an additional 1h. Samples were then pelleted and resuspended in 50mL 0.1% Saponin in PBS, and subsequently washed twice with 50mL PBS to remove hemoglobin. Parasite pellets were then lysed using RIPA buffer containing protease inhibitors. For ELISA, 500ng/well of each biological replicate was separately probed with either the anti-puromycin monoclonal antibody 3RH11 (Kerafast, #EQ0001), or monoclonal anti-*Plasmodium falciparum* GAPDH as an internal control. As a negative control, parasites grown in normal media were treated with 10μg/mL cyclohexamide simulataneously with puromycin to arrest protein synthesis and block puromycin incorporation.

Statistical Analysis

All statiscal analyses were performed using R version 3.2.3 (2015-12-10)(R Core Team, 2015). T-tests, linear and logistic regressions, and some figures were generated using R base functions. The *drc* package (Ritz, C. and Streibig, J.C., 2005) was used for determining the 50% survival point of PB-11, and the *ggplot2* package (Wickham, Hadley, 2009) was used for the production of several figures.

Chapter 4

Re-evaluation of mutants defective in the early stages of gametocyte differentiation and identification of the *Start*-like commitment point to sexual differentiation.

Abstract

Unlike a dormancy-like response, the transition of asexual reproducing blood-stage malaria parasites to transmissible sexual forms known as gametocytes represents a true cell cycle exit and differentiation event. Our lab previously conducted a forward genetic screen to identify genes necessary for gametocytogenesis. Analysis of the mutants obtained from the screen showed a temporal hierarchical order, suggesting several mutants may be affected at the earliest stages of commitment to differentiation. Here, we re-evaluate these findings in light of the discovery of an underlying mutation present in the starting population of cells used for the screen, and find that the basis of the mutant phenotypes observed may be more complex than originally appreciated. Furthermore, using a newly available transgenic parasite line in which gametocytogenesis can be induced, we mapped the timing of the *Start*-like checkpoint in the asexual cycle at which commitment to gametocytogenesis occurs to 18 h post-invasion.

Introduction

Previous chapters have investigated whether *Plasmodium falciparum* is capable of entering a programmed state of dormancy when faced with unfavorable environmental conditions. While there is evidence that artemisinin derivatives and amino acid starvation can affect the parasite's growth rate, and that different genes (*e.g*: Maf1, K13) can affect a parasite's ability to recover from growth-retarding forms of stress, we found no evidence of a specialized differentiation pathway into a dormant state. However, there is a well-established differentiation program that *Plasmodium falciparum* uses to exit the cell cycle: the transition of the parasite from the asexual cycle to the sexual differentiation pathway, or as it is commonly referred, gametocytogenesis.

Gametocytes are the only form of the malaria parasite transmissible to the mosquito vector. Once ingested by mosquito, gametocytes rapidly differentiate in the midgut into male and female gametes, fuse to form a zygote, and progress through the mosquito stages of the parasite lifecycle. *P. falciparum* mature gametocytes are morphologically distinct from the asexual forms (Figure 4.1), and the process by which they develop from a ring stage into elongated, transmissible forms over seven to ten days has been well documented. However, the mechanism that triggers exit from the asexual cycle and commitment to the sexual lineage remains poorly understood.

The first important discovery in regards to commitment to gametocytogenesis was the finding that all merozoites from single schizont are committed to the same developmental pathway (Figure 4.1) (Bruce et al., 1990). All merozoites either develop into gametocytes, or continue on with the asexual cycle. Later work revealed that this finding holds true for the sex of gametocytes as well: a single schizont either produces all male or all female gametocytes (Silvestrini et al., 2000)(Smith et al.,

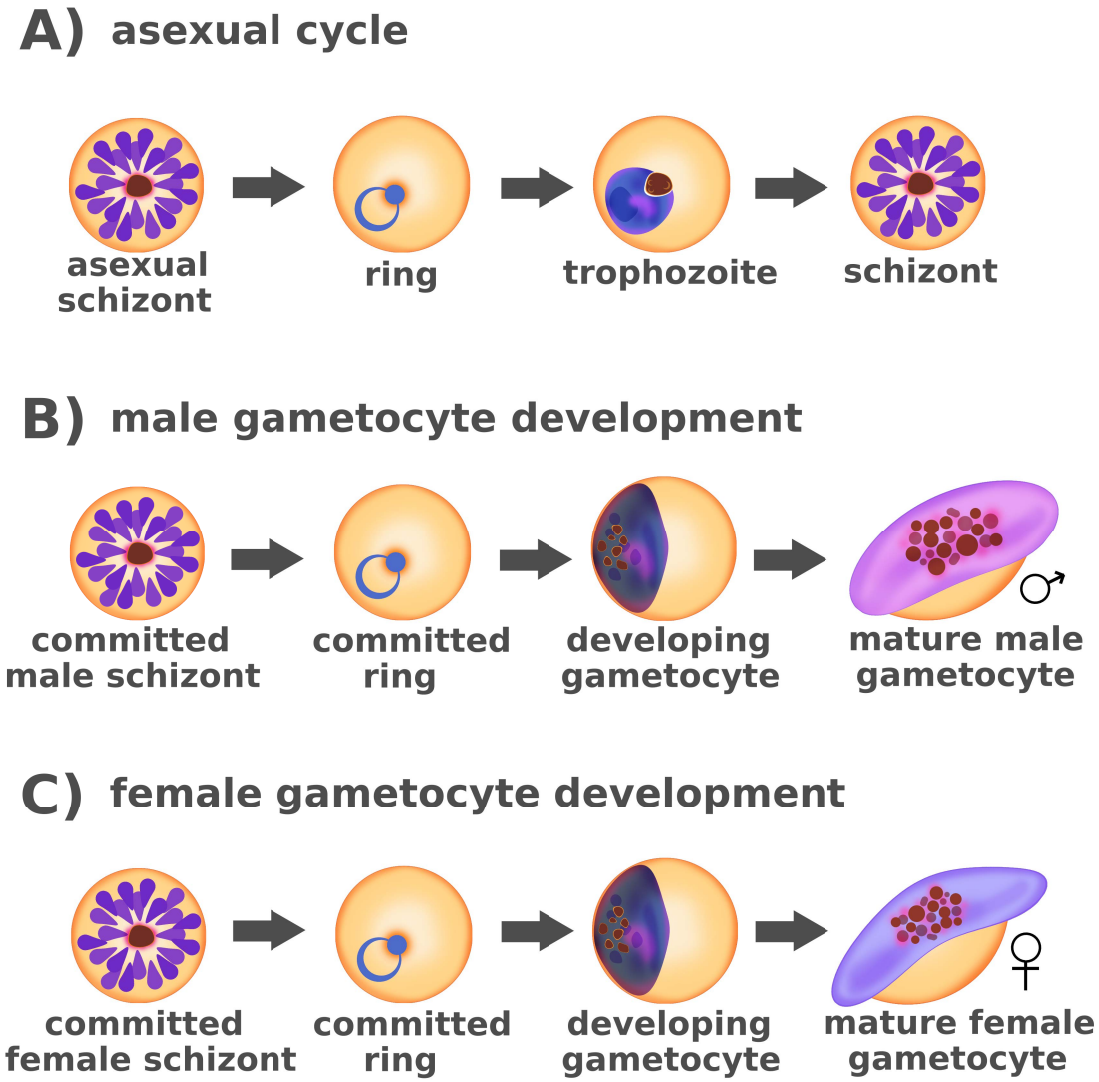

Figure 4.1: **Commitment to gametocytogenesis occurs during the cell cycle prior to gametocyte differentiation.** Early studies of commitment to gametocytogenesis revealed that all the progeny merozoites from a single schizont are destined for the same developmental fate: all cycling asexual parasites **(A)**, all male gametocytes **(B)**, or all female gametocytes **(C)**. The commitment event must occur during the cell cycle prior to the cycle in which morphologically identifiable gametocytes manifest. The timing of the commitment event in the preceding cell cycle is unknown, but is presumed to occur prior to the onset of DNA replication.

2000). Thus, commitment to either the sexual or asexual lineage is already established prior to the end of schizogeny, sometime in the preceeding ~45-hour asexual cycle.

In an effort to understand this commitment process at the molecular level, our lab conducted a forward genetic screen to identify genes involved in the commitment process (Ikadai et al., 2013). Most of this work was completed prior to my joining the lab. Initial results were quite promising, though, as describe below, follow-up work (performed by me) has revealed that the interpretation of some of our findings may be more complex than originally believed. What follows is a description of my contributions to this study and an effort to interpret our findings in the context of our current understanding of gametocytogenesis. Lastly, using a reagent generated by others and methods similar to those used in *Chapter 2*, we have attempted to determine the timing of commitment point to gametocytogenesis in the asexual cycle.

Results

Expression analysis of transposon insertion mutants suggests an epistatic ordering of gametocyte mutants

Hiromi Ikadai and Kathryn Shaw Saliba conducted a forward genetic screen for gametocyte development using insertional-mutagenesis with the *piggyBac* transposon (Ikadai et al., 2013). After a series of transfections, they isolated 189 parasite clones containing transposition events. Of these, 29 clones, representing 16 distinct insertion events, did not produce detectable gametocytes when analyzed. Inverse PCR was used to identify the sites of insertion. Of the 16 distinct insertions, 5 were within annotated open reading frames and the remaining 11 occurred in intergenic regions.

While many of the genes associated with the insertions had annotated functions or identifiable domains, as a whole, the collection of genes did not suggest an obvious shared pathway or mechanism.

The insertion mutants were determined to be gametocyte non-producers based on the absence of observable gametocytes in Giemsa smears. However, Giemsa staining can only be used to distinguish gametocytes from asexual cells starting from the Stage II morphological form of gametocytogenesis through to maturity (Stage V), as these stages are clearly morphologically distinct from the asexual cycle. Stage II gametocytes manifest approximately 48 h into gametocyte development, meaning that the mutants could produce ring stage gametocytes or Stage I gametocytes (which are indistinguishable from asexual trophozoites on Giemsa smears) prior to reaching the point at which the gametocytogenesis program is affected. No known markers exist to identify ring stage gametocytes. However, the expression of several early gametocyte proteins, including *Pf* mdv1 (Furuya et al., 2005), has been assigned to Stage I gametocytes.

K. Shaw Saliba screened the sixteen gametocyte mutant clones for their ability to produce *Pf* mdv1-expressing Stage I gametocytes using an immunofluorescence assay. Seven of the sixteen mutants were found to produce rare, *Pf* mdv1-positive cells. No Stage I cells were detected in the remaining mutant clones. From this finding, we reasoned that the mutations in some of the mutants must affect the transition from Stage I of gametocytogenesis to later stages of maturity. The mutations in the remaining clones must affect either the ring-stage gametocyte, or events in the preceding cell cycle necessary for establishment of committment. Since the timing of the commitment event is unknown, these mutant parasites could potentially arrest development anywhere in a 72h window: from the earliest point of the ring stage of the preceding generation, through the 45-hour cell cycle, or anytime during the 24 h

ring-stage gametocyte prior to development into Stage I.

If we assume that once commitment to the gametocyte lineage is established a distinct transcriptional program is activated to drive differentiation program, then it may be possible to identify differential arrest points of each mutant clone based on differential transcript expression profiles. We attempted this by performing RT-PCR for the expression of a panel of 30 genes on each of the sixteen mutants as well as the 'parental' gametocyte-producing clone. The genes analyzed included all the genes identified as affected by transposon-insertion in our screen, as well as a collection of transcripts previously reported in other studies to be expressed across gametocytogenesis. K. Shaw Saliba performed RT-PCR for each transcript on mixed-stage RNA from each mutant clone, and each clone was scored in a binary fashion, as either expressing the transcript or not.

Several transcripts displayed differential expression across the mutant collection, with some mutants expressing most of the analyzed transcripts, and others only expressing a select few. I performed hierarchical clustering on the expression data to see whether any patterns could be discerned. The results of my analysis are shown in Figure 4.2. The transcript analysis clearly separates the mutants into two major clusters and several sub-clusters. Importantly, one of the clusters consists of all the clones previously found by independent means to produce Stage I gametocytes (plus one additional clone), validating the hierarchical ordering.

We do not know how to interpret the sub-clusters of the non-Stage I producing mutants. Presumably, those that produce more transcripts proceed further into gametocytogenesis program than those that produce fewer transcripts, such as the ring-stage just prior to Stage I development. Those producing the fewest transcripts may be defective in the earliest developmental events after commitment or may be

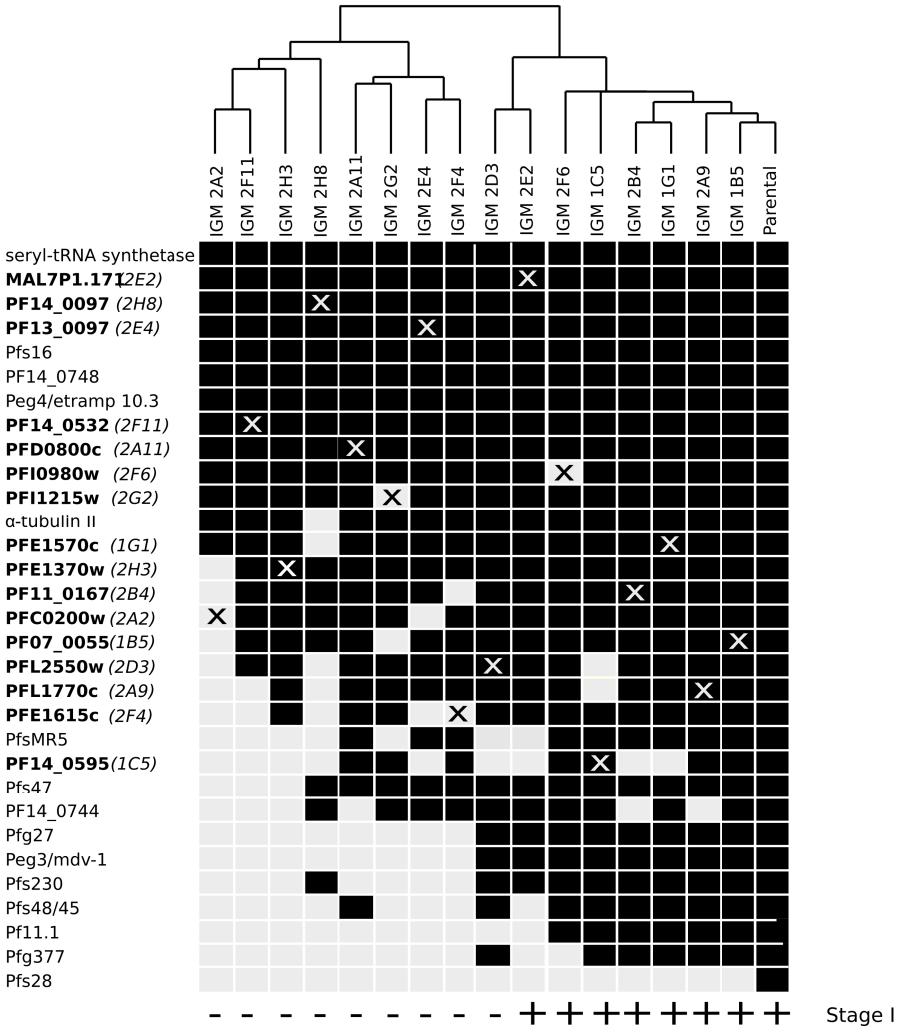

Figure 4.2: **mRNA expression analysis displays a hierarchical clustering of insertion mutants, suggesting an epistatic ordering of genes in the gametocyte development pathway.** Insertional gametocyte mutant (IGM) clone identifiers are listed across the top. Transcripts analyzed are listed to the left. The expression profiles indicate transcripts that were expressed (black boxes) or not expressed (light gray boxes) as measured by semi quantitative RT-PCR. The transcripts listed correspond to the 16 genes identified as putatively affected in the transposon-mutagenesis screen, as well as known early (Pfs16, PF14_0748, Peg4/etramp10.3, Pfg27, PF14_0744, and Pfmdv1/peg3) and late (Pf11.1, Pfg377, Pfs48/45, PfMR5, Pfs47, and Pfs28) gametocyte-specific genes. The X in certain boxes indicates the gene affected by transposon insertion in a given mutant. For certain putatively disrupted genes, transcript abundance was only decreased and not completely inhibited (gray Xs on black boxes). The mutant lines are hierarchically clustered based on the similarity of their expression profiles to each other and the parental line. All mutants able to differentiate into Stage I gametocytes cluster to the right next to the wild type parental line (Ikadai et al., 2013).

deficient in the ability to commit to gametocytogenesis altogether. Resolving these points of arrest will require additional early markers and a better understanding of the earliest stages of commitment and development.

All insertion mutants carry a non-synonymous mutation in AP2-G that likely affects gametocyte development

In 2014, a year after our transposon-insertion screen was published, two complementary studies were published identifying an AP2 domain-containing transcription factor as the key regulator of gametocyte development in both *P. falciparum* (Kafsack et al., 2014) and the model murine parasite *P. berghei* (Sinha et al., 2014). The authors concluded that this transcription factor, named AP2-G (PF3D7_1222600), was likely the earlierst-acting regulator of gametocyte development. Furthermore, the authors reported that several gametocyte-deficient lab strains, that had been used for decades to study gametocytogenesis, all contained inactivating mutations in AP2-G. The authors concluded that spontaneous mutations in AP2-G were likely the cause of the loss of gametocytogenesis frequently observed after prolonged maintenance of parasites in culture, as disruption of AP2-G and elimination of gametocytogenesis conferred a growth advantage over gametocytogenesis-competent wild type parasites.

AP2-G was not one of the genes identified in our forward genetic screen, despite the fact that we obtained insertions in several loci multiple times, suggesting some degree of saturation mutagenesis was attained. To investigate further, we sequenced the coding sequence of AP2-G in our insertion mutants. To our surprise, every single one of the 29 insertion mutants contained the same guanine to thymine transversion at position 6487 of the AP2-G open reading frame. This transversion is in the first position of the codon of amino acid 2163, converting a valine residue to a leucine

residue (Figure 4.3A).

A valine to leucine conversion is considered to be a conservative mutation, as these two amino acids are both hydrophobic and have a similar size and structure. However, given that the mutation was within the AP2 DNA binding domain, the finding was somewhat concerning. We re-examined the gametocytogenesis-competent 3D7 clone used as the 'parental' line for transposon screen to see if it too carried this mutation.

Using mixed-stage genomic DNA from the 3D7 parental line, a region surrounding the G6487T mutation was amplified and cloned into a shuttle vector. Plasmids were isolated from 42 independent *E. coli* colonies and sequenced. Of the 42 colonies, five carried the G6487T transversion while the other 37 displayed the wild type G allele. This suggests that the parental line may be a mixture of both AP2-G allelic variants, with the mutant T allele occurring at frequency of roughly 0.12 (5/42).

To investigate further, the parental 3D7 line was cloned by limiting dilution. A total of 46 clones were obtained and screened for the presence of the G6487T mutation. Of these, 10 clones carried the mutant T allele, corresponding to a frequency of 0.21, which is not statistically different than the 0.12 frequency obtained from PCR owing to the small sample sizes ($p = 0.08$, Poisson test) (Figure 4.3B). Importantly, of the 189 transposon insertion mutants obtained after transfection, 29 did not produce gametocytes, for a frequency of 0.15. The gametocyte-competent insertion-mutants were discarded after screening, so cannot be tested for the presence of the G6487T mutation. However, the fact that all of the gametocyte-deficient mutants obtained in the screen carried the mutation and were obtained at a frequency similar to the frequency of the mutant allele in the parental culture, raises the concern that the gametocyte-deficient mutants may simply have been cloned from the parental

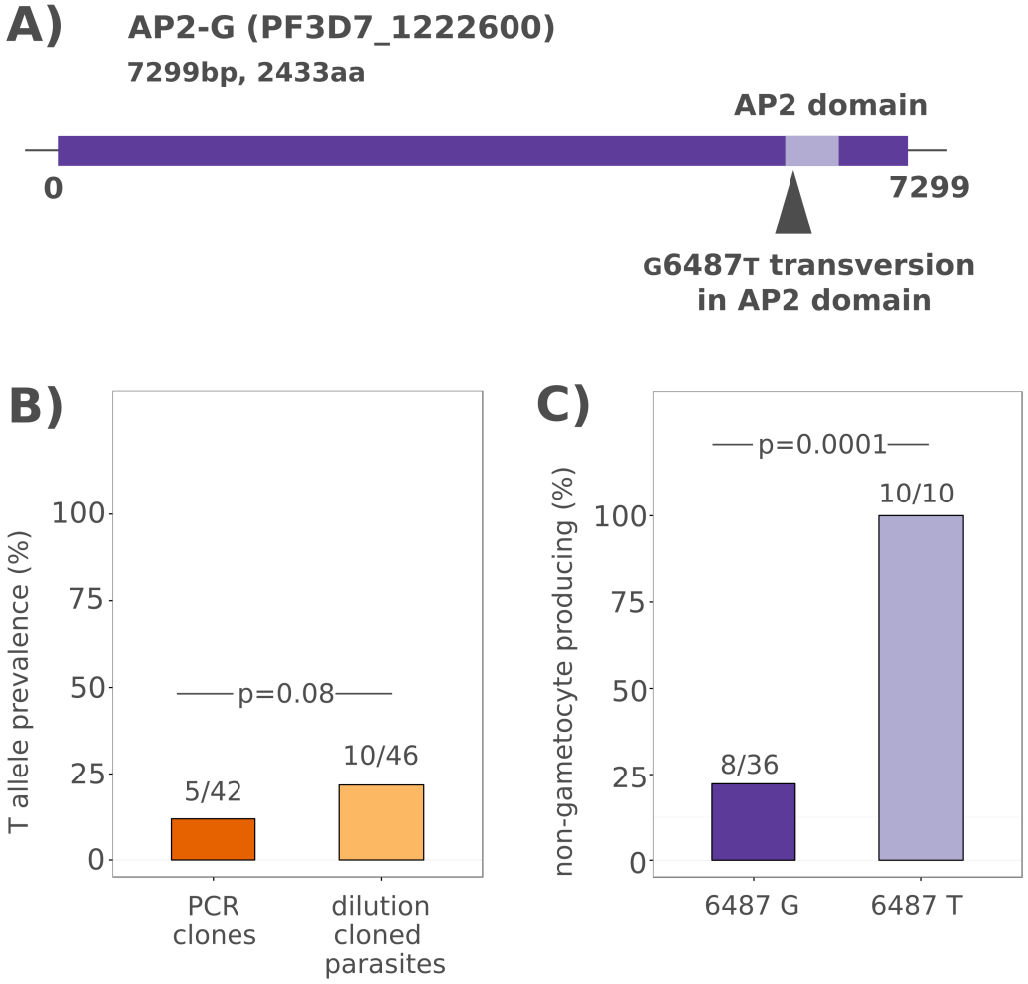

Figure 4.3: **Parasites carrying a non-synonymous mutation in the AP2-domain of AP2-G do not produce mature gametocytes. A)** A schematic representation of the AP2-G gene locus indicating the location of the AP2 DNA binding domain and the position of the G6487T transversion. **B)** Determination of the prevalence of the G6487T transversion in the parental parasite line as estimated by PCR cloning and sequencing of genomic DNA from the parental culture and dilution cloning of individual parasites from the parental line. **C)** The proportion of clones obtained from dilution cloned parasites incapable of producing mature gametocytes carrying either the wild type G allele or mutant T allele at position 6847 of AP2-G. P-values are derived from Poisson tests.

culture and may not have been due to mutation from insertional mutagenesis.

The 46 clones from the parental culture were screened for their ability to produce mature gametocytes. Of the 36 clones carrying a wild type G at position 6487, 8 did not produce mature gametocytes (Figure 4.3C). The remainder of the AP2-G coding sequence was not sequenced in these clones to look for additional mutations. All of the 10 clones carrying the G6487T mutation failed to produce gametocytes after multiple assays. This frequency is statistically above what would be predicted if the gametocytogenesis-deficiency were due to the same "background" level deficiency observed in the 36 clones carrying the wild type allele ($p = 0.0001$, Poisson test).

It is difficult to reconcile these findings with the hierarchical clustering of the mutants described earlier. The insertion mutants appear to arrest at different stages of differentiation, yet all carry the same mutation that appears to block gametocytogenesis. The 46 sub-clones from the parental line were only screened for their ability to produce mature gametocytes, and were not tested for the ability to produce Stage I gametocytes. Perhaps the mutation(s) cause(s) an arrest at Stage I of gametocyte development, but has/have little to no effect on earlier events. If this is the case, the validity of the seven mutants found to produce Stage I gametocytes will need to be re-examined. Regardless, the finding of the G6487T complicates the interpretation of the insertional-mutagenesis screen. Any future work on these mutants will have to take this mutation into consideration.

The PB-11 Maf1 mutant displays no defects in gametocytogenesis

One of the insertion mutants obtained in the screen (2A11) had a *piggyBac* insertion in the intergenic region between two genes on Chromosome 4 (Figure 4.4A). Initial RT-PCR screening of the mutant found that the gene proximal to the insertion site (PF3D7_0416600) was not affected at the transcript level by the insertion, but expression of the transcript of the distal gene (PF3D7_0416500) was completely inhibited, leading us to attribute the gametocytogenesis-deficiency phenotype to the distal gene. Subsequent RT-PCR analysis found that the transcript was not inhibited afterall (Figure 4.2), complicating this interpretation.

The distal gene to which the phenotype was initially attributed encodes the *Plasmodium falciparum* homolog of the RNA Pol III repressor Maf1. The identification of the mutant in this screen is what led to our interest in this gene, ultimately resulting in the studies performed in *Chapter 3*.

As detailed in *Chapter 3*, we obtained an independent transposon insertion mutant (identified as PB-11) produced by the lab of John Adams (Balu et al., 2009) that contained an insertion much closer to the Maf1 open reading frame (Figure 4.4A). Despite insertion of the transposon into the Maf1 5' UTR (*Chapter 3*), the PB-11 mutant still expressed detectable levels of the Maf1 mRNA and protein, albeit with a different expression profile from that observed in wild type parasites.

We investigated whether the PB-11 mutant is capable of producing gametocytes, and indeed, it produced gametocytes at a high rate. Since the PB-11 mutant is not a complete knockout, it remains a possibility that the low levels of Maf1 expression in this line are sufficient to support gametocytogenesis. However, based on these results, the assignment of Maf1 as the causative mutation in the 2A11 clone obtained in our screen should probably be re-evaluated.

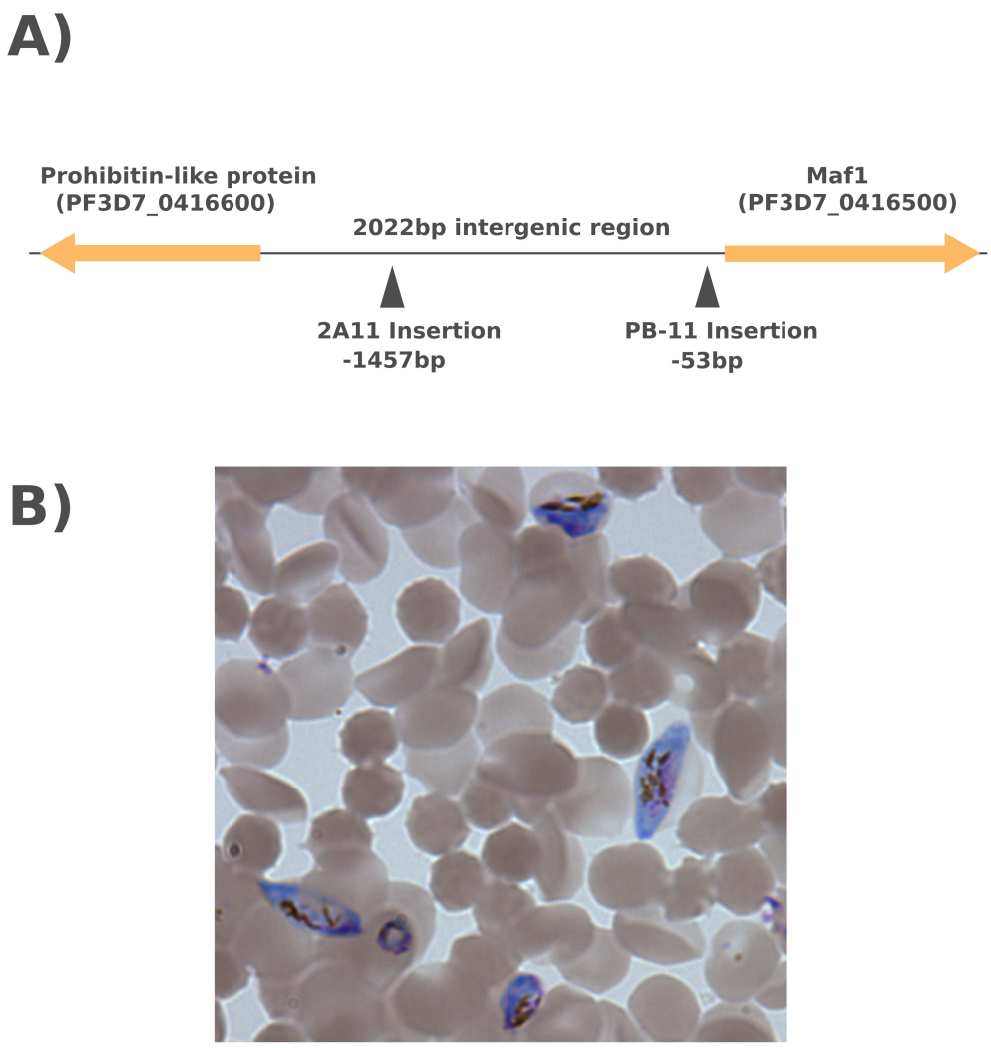

Figure 4.4: **The PB-11 Maf1 mutant parasite produces mature gametocytes. A)** A schematic representation of the Maf1 locus on Chromosome 4 indicating the *piggyBac* transposon insertion sites identified in the 2A11 mutant obtained in our genetic screen, and the PB-11 mutant produced by Balu *et al.* **B)** A blood smear of the PB-11 mutant displaying gameotyctes at various stages of maturation.

HP1-dependent committment to gametocytogenesis occurs in the late ring-stage

The current model for commitment to gametocytogenesis is centered on activation the AP2-G transcription factor (Kafsack et al., 2014) (Sinha et al., 2014). Cells that activate AP2-G transcription in their current generation will undergo gametocyte commitment in the subsequent generation. How this activation occurs is not understood. It may be triggered by a signal or may be stochastic. What is clear, however, is that in its inactive state the AP2-G gene locus is enriched with histone H3K9 trimethylation (Lopez-Rubio et al., 2009) and is bound by the Heterochromatin Protein 1 (HP1)(Flueck et al., 2009), two hallmarks of transcriptionally-inactive chromatin.

Two recent studies have followed-up on the role of chromatin modification in the silencing of AP2-G expression in the control of gametocytogenesis commitment. One study found that destabilization of the Class II histone deacetylase *Pf* HdaII in synchronous parasites in culture causes a dramatic increase in gametocyte development in the subsequent generation (Coleman et al., 2014). Class II histone deacetylase enzymes remove transcription-activating histone acetylation marks to allow for the deposition of the transcription-silencing HP1 protein and histone H3K9 trimethylation. Similarly, a second study found that controlled destabilization of the gene-silencing HP1 protein itself also causes an increase in the number of developing gametocytes in the following generation (Brancucci et al., 2014). In the case of HP1 destabilization, however, upwards of 50% of parasites committed to gametocyte development. HP1 destabilization is the single most effective inducer of gametocytogenesis reported to date.

HP1 destabilization causes an increase in AP2-G transcript expression in the first asexual generation, and this high level of expression is maintained in the subse-

quent gametocyte development generation (Brancucci et al., 2014). While indirect, it effectively allows for the controlled induction of commitment to gametocytogenesis. As discussed above, it is known that commitment occurs in the generation prior to gametocyte development, but it is not known when in the previous cycle this commitment occurs.

In the haploid stages of the yeast *S. cerevisiae*, treatment with pheromones causes cells to undergo differentiation into the mating-competent forms. However, treatment with the pheromone must occur prior to a certain point in the cell cycle, known as *Start*, for differentiation to occur (Hartwell et al., 1974). Once *Start* is passed, cells become refractory to pheromone treatment and complete cell division and form daughter cells before becoming sensitive to the mating pheromone once again. We reasoned that there may be an analogous point in the *P. falciparum* cell cycle before which AP2-G expression must be activated for gametocytogenesis commitment to occur.

To investigate this, we obtained the HP1 conditional mutant parasite line produced by Brancucci *et al.*. In this parasite line, the HP1 protein has been modified with a ligand-regulatable degron. In the absence of the stabilizing ligand, known as *Shield*, the HP1 protein is rapidly degraded. Cells maintained in continuous culture in the presence of the *Shield* ligand are indistinguishable from wild type cells. To determine whether there is a time-dependent effect of HP1-destabilization (and thereby AP2-G activation) on commitment to gametocytogenesis, a culture was initiated with highly synchronous young rings (~3 h post invasion) in the presence of *Shield*. Every three hours over the course of the 45 h cell cycle, an aliquot of culture was removed, washed repeatedly, and re-cultured in media lacking *Shield* to cause HP1 destabilization. After 50 h, when all parasites would be expected to have completed the cell cycle and reinvaded new erythrocytes, heparin was added to each subculture. Hep-

arin blocks erythrocyte invasion by merozoites (Boyle et al., 2010), and should select for cells induced to commit to gametocytogenesis during the time course (gametocytes do not produce merozoites), and eliminate asexual cells from the culture. After another four days of incubation, after which any induced gametocytes would have developed well beyond Stage I of gametocytogenesis, cells were fixed and stained with an anti-*Pf*Peg4 antibody and analyzed by flow cytometry. Peg4 is expressed in gametocytes from Stage I through V and is not expressed in asexual cells (Silvestrini et al., 2005).

The results of the analysis are shown in Figure 4.5B. A logistic regression model fit to the data shows the likelihood commitment to gametocytogenesis decreases as the hour post invasion of *Shield* removal increases ($p < 2.00x10^{-16}$). These results suggest, just as the *Start* checkpoint in yeast, that there is a point in the asexual cycle after which cells become insensitive to AP2-G induction. Based on the model, this point occurs at approximately 18 hpi, the point at which 50% of parasites commit to gametocytogenesis and 50% do not. As in yeast, this point occurs well before the onset of DNA replication in the parasite's cell cycle (~30 hpi, see *Chapter 2*). In fact, this point coincides roughly with the transition from the ring stage of parasite development to the trophozoite stage.

This finding has potentially important ramifications for our understanding of the commitment process. If AP2-G induction and commitment must occur prior to 18 hpi, then it follows that there must be both trophozoite and schizont stages of the parasite that are irreversibly committed to the gametocyte lineage (Figure 4.6). Similarly, these data suggest the event that triggers commitment (if one exists) must occur during the ring stage, as later stages of the parasite would be expected to be refractory to such a trigger. It would be interesting to re-evaluate the pre-Stage I arresting mutants from our transposon-insertion screen with this model in mind.

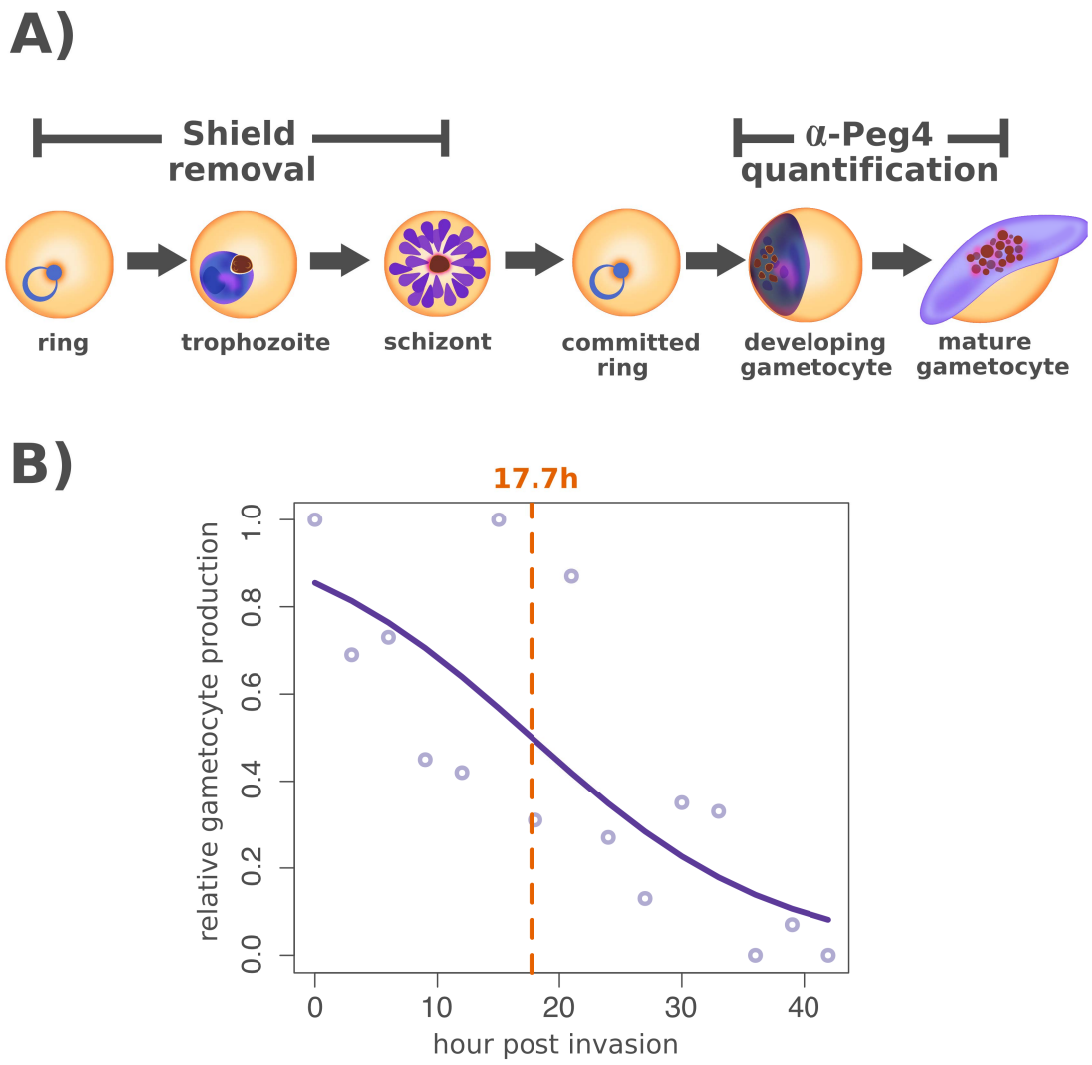

Figure 4.5: **Asexual *P. falciparum* commits to gametocytogenesis in the subsequent cycle if HP1 is destabilized prior to 18hpi. A)** The *Shield* stabilizing ligand was removed from a highly synchronous culture at three-hour intervals across the 45 h asexual cycle. After an additional 96h, when any cells induced to develop into gametocyte would have reached beyond Stage I of gametocytogenesis, cells were fixed and stained with the an anti-Peg4 antibody to quantify Stage I through V gametocytes by flow cytometry. **B)** A logistic regression model fit to the data shows that the likelihood of gametocytogenesis induction decreases as time post invasion increases ($p < 2.00 \times 10^{-16}$). The model predicts that when *Shield* is removed at 17.7 h post invasion, only 50% of parasites commit to the gametocyte lineage, indicative of a *Start*-like sexual differentiation checkpoint in the asexual cell cycle.

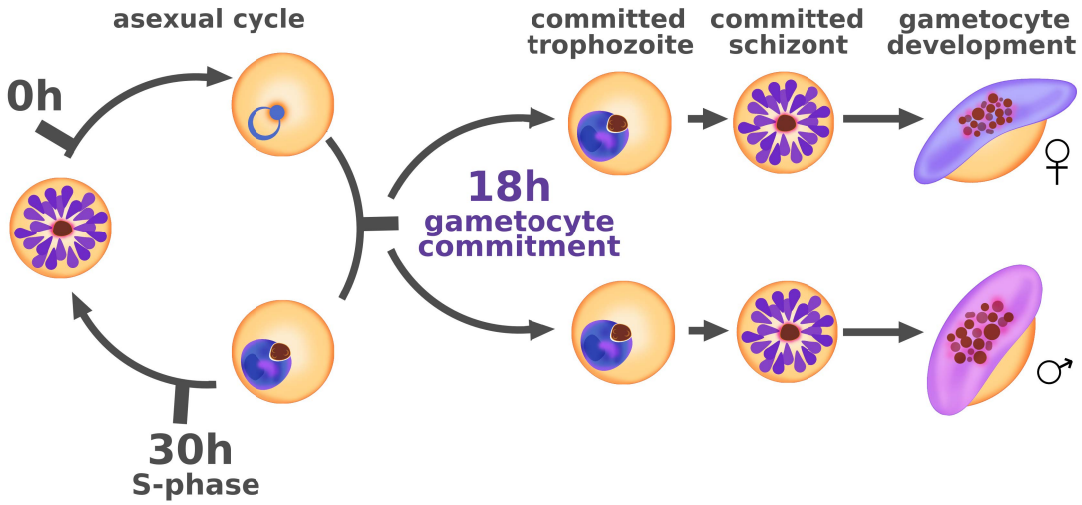

Figure 4.6: **The *Plasmodium falciparum* cell cycle displays a sexual differentiation checkpoint at 18hpi.** Early studies on *P. falciparum* gametocytogenesis suggested all progeny merozoites from a single schizont commit to the same developmental fate as all asexual parasites, all male gametocytes, or all female gametocytes. It was not known when prior to schizont rupture the commitment to each cell lineage was established. Our data suggests there is an HP1/AP2-G dependent *Start*-like commitment point at approximately 18 h post invasion. This implies that there exists both trophozoites and schizonts irreversibly committed to either the sexual or asexual lineage. It is not known if commitment to the male and female lineages occurs at this same point in time.

Conclusions

Many lab strains *P. falciparum* do not produce gametocytes at all, and those that do often produce them at very low levels. Our screen for genetic factors affecting gametocytogenesis was an attempt to decipher this complicated process. The mutants obtained from this screen appeared to arrest development, at least at the transcript level, at a range of different stages. Mutants of this nature could be an invaluable tool for further understanding what occurs in the cryptic early stages of gametocytogenesis.

However, it appears that all of our mutants carry a mutation that may have a direct effect on gametocytogenesis. We have yet to formally demonstrate that this mutation directly inhibits gametocytogenesis (by, for example, reverting it back to the wild type allele and restoring gametocytes), but the finding that all parasites carrying the mutation are incapable in producing gametocytes suggests this may be the case. Understanding the effects of this mutation will be key to interpreting the value of the mutants from our genetic screen.

Using techniques similar to those employed in *Chapter 2*, we have determined that *P. falciparum* displays a *Start*-like checkpoint at which commitment to gametocytogenesis occurs. This reshapes our understanding of the black box that is commitment to gametocytogenesis. Using this *Start*-like checkpoint as point of reference will be helpful for studies of the committed trophozoite and schizont stages as well as studies of mechanisms that naturally drive commitment to gametocytogenesis.

Methods

Parasite Culture and Media

Parasites were cultured using standard methods (Jensen and Trager, 1977) in flasks gassed with a mixture of 90% N_2, 5% CO_2, 5% O_2 (Airgas, #Z03NI9022000033). Normal culture medium consisted of RPMI 1640 with L-glutamine and 25 mM HEPES (Corning, #10-041-CV), with 5.0g/L Albumax II Lipid-Rich BSA (ThermoFisher Scientific, #11021029), 3.7mM Hypoxanthine, and 50μg/mL gentamicin. The *Shield* ligand was obtained from Aobious (#1848).

Clustering

The binary RT-PCR expression data from K. Shaw Saliba (Ikadai et al., 2013) was used to construct a dissimilarity matrix by Euclidean distance and subsequently hierarchically clustered by Ward's method.

PCR cloning and sequencing of the G6487T transversion

Genomic DNA from the parental 3D7-Pfs28::GFP parasite line was amplified using Phusion High-Fidelity Polymerase (NEB, #M0530L), using the forward primer 5'-GGAGATATGAATTACAAAAGGCAAT-3' and reverse primer 5'-TAGCCATTCTCAATGCACCA-3' which amplify a 302bp region from 6338 to 6610 of the AP2-G (PF3D7_1222600) open reading frame. The resulting PCR product was cloned using the CloneJET PCR Cloning Kit (ThermoFisher Scientific,

#K1231). Plasmids were isolated from individual *E. coli* colonies and sequenced (MacrogenUSA) using the forward primer.

Limiting dilution cloning

The number of parasites per mL of culture was determined for the parental 3D7-Pfs28::GFP parasite line by blood smear and hemocytometer. The culture was then serially diluted in 10-fold increments down to 10 parasites/mL. A total of 60μL of this dilution was deposited into 80 wells of five 96-well plates, such that each well is expected to receive 0.60 parasites. The wells were then supplemented with 140μL of a mixture of standard culture medium and erythrocytes such that each well contained a final volume of 200μL of 1% hematocrit culture. Every three days, 100μL of media was removed and replaced with fresh media containing 0.5% v/v fresh erythrocytes. After twenty days, 100μL from each plate was used for a SYBR GREEN I plate reader assay (Smilkstein et al., 2004) to determine positive wells. All wells that scored positive were subsequently verified by Giemsa smears. A total of 46 parasite clones were obtained. The AP2-G locus was sequenced as described above.

Gametocyte production for PB-11

An asynchronous culture of PB-11 parasites was initiated in standard culture medium at 4% hematocrit at a starting parasitemia of 0.5%. The culture was maintained with daily media changes but no dilution or subculturing for 14 days. Early stage gameocytes became detectable by day 8. Mature stages were enriched at later time points.

Statistical Analysis

All statiscal analyses were performed using R version 3.2.3 (2015-12-10)(R Core Team, 2015). T-tests, linear and logistic regressions, and some figures were generated using R base functions. The *drc* package (Ritz, C. and Streibig, J.C., 2005) was used for determining the 50% survival point of PB-11, and the *ggplot2* package (Wickham, Hadley, 2009) was used for the production of several figures.

Chapter 5

Perspectives

Dormancy, or Robust Growth & Resilience?

Initial observations led several authors to put forth a model of dormancy to explain *Plasmodium falciparum*'s ability to survive artemisinin treatment (Teuscher et al., 2010)(Witkowski et al., 2010)(Codd et al., 2011)(Cheng et al., 2012). Instead of a point mutation decreasing the affinity of the drug to its target enzyme, or an overactive efflux pump decreasing the intracellular drug concentration, the model proposed that resistant parasites arrest the cell cycle and enter a state of low metabolic activity, surviving silently in the blood stream until conditions become more favorable. If true, the ability of the parasite to enter dormancy could have serious implications for the future of malaria control. In theory, a dormancy response could provide cross-resistance to any number of other drugs, both those in current use and those in development, and dormant infections would severely complicate epidemiological tracking of infected individuals. Like is the case for dormant *P. vivax* hypnozoites, patients believed to be cleared of parasites could suffer relapsing infections months to years later. If dormant parasites were insusceptible to drug treatment, *P. falciparum* elimination from endemic areas would be nearly impossible.

However, more recent studies have steered our understanding of artemisinin resistance away from dormancy and relapse. If anything, the results suggest quite the opposite. Artemisinin appears to have an intracellular target, the *Pf* PI3K lipid-kinase, and resistance is conferred through elevation in the target protein's expression (Mbengue et al., 2015). Resistance does not appear to be conferred through the entrance into a dormant state, but an increased ability to recover from the growth-inhibiting effects of the drug itself (Klonis et al., 2011)(Dogovski et al., 2015). Resistance is due to an enhanced ability to recrudesce, not programmed dormancy and relapse.

We attempted to study the parasite's reported ability to enter dormancy when starved of the amino acid isoleucine. While many of our findings supported the observations of the previous study (Babbitt et al., 2012), we found no evidence of dormancy. Starved parasites respond to isoleucine starvation by entering a state of slow growth. Yet, surprisingly, there appears to be more parallels between our findings and the current understanding of artemisinin resistance than the original dormancy model suggested. Inhibition of of *Pf*PI3K, the purported artemisinin target, induces slow growth much like that observed with isoleucine starvation, and artemisinin-resistant parasites grow more robustly under normal conditions and survive prolonged amino acid starvation much better than their drug-sensitive counterparts. Our study suggests that more robust growth and resilience to growth inhibition seem to be key to the parasite's ability to survive both artemisinin treatment and isoleucine starvation.

Over the past decade, there has been an increased focus on the role of enhanced growth signaling in the progression of human cancers. Many tumors acquire mutations that elevate signaling through the TORC1 pathway (Guertin and Sabatini, 2005)(Cargnello et al., 2015). Over-activity of this pathway is believed to cause tumors to grow more robustly, acquire more nutrients, and suppress apoptosis. Inhibitors of TORC1 signaling have shown promising results in anti-tumor therapy. We found that one of the few residual components of TORC1 signaling in *P. falciparum*, *Pf*Maf1, is critical for the parasite's ability to recover from prolonged starvation. The two genes implicated in artemisinin resistance, *Pf*PI3K and *Pf*PKB, are also residual components of the TORC1 pathway (Mbengue et al., 2015). Perhaps, as in cancer chemotherapy, the development of therapeutics that inhibit these conserved growth and recovery pathways could hold promise for the future of malaria treatment.

Bibliography

Abraham, R.T., and Wiederrecht, G.J. (1996). Immunopharmacology of rapamycin. Annu. Rev. Immunol. *14*, 483–510.

Adjalley, S.H., Johnston, G.L., Li, T., Eastman, R.T., Ekland, E.H., Eappen, A.G., Richman, A., Sim, B.K.L., Lee, M.C.S., Hoffman, S.L., et al. (2011). Quantitative assessment of Plasmodium falciparum sexual development reveals potent transmission-blocking activity by methylene blue. Proc. Natl. Acad. Sci. U.S.A. *108*, E1214–1223.

Ariey, F., Witkowski, B., Amaratunga, C., Beghain, J., Langlois, A.-C., Khim, N., Kim, S., Duru, V., Bouchier, C., Ma, L., et al. (2014). A molecular marker of artemisinin-resistant Plasmodium falciparum malaria. Nature *505*, 50–55.

Ashley, E.A., and White, N.J. (2014). The duration of Plasmodium falciparum infections. Malar. J. *13*, 500.

Ashley, E., Dhorda, M., Fairhurst, R., Amaratunga, C., Lim, P., Suon, S., Sreng, S., Anderson, J., Mao, S., Sam, B., et al. (2014). Spread of Artemisinin Resistance in Plasmodium falciparum Malaria. N Engl J Med *371*, 411–423.

Babbitt, S.E., Altenhofen, L., Cobbold, S.A., Istvan, E.S., Fennell, C., Doerig, C., Llinás, M., and Goldberg, D.E. (2012). Plasmodium falciparum responds to amino acid starvation by entering into a hibernatory state. Proc. Natl. Acad. Sci. U.S.A. *109*, E3278–3287.

Backer, J.M. (2008). The regulation and function of Class III PI3Ks: Novel roles for Vps34. Biochem. J. *410*, 1–17.

Baertl, J.M., Placko, R.P., and Graham, G.G. (1974). Serum proteins and plasma free

amino acids in severe malnutrition. Am. J. Clin. Nutr. *27*, 733–742.

Balabaskaran Nina, P., Morrisey, J.M., Ganesan, S.M., Ke, H., Pershing, A.M., Mather, M.W., and Vaidya, A.B. (2011). ATP synthase complex of Plasmodium falciparum: Dimeric assembly in mitochondrial membranes and resistance to genetic disruption. J. Biol. Chem. *286*, 41312–41322.

Balu, B., Shoue, D.A., Fraser, M.J., and Adams, J.H. (2005). High-efficiency transformation of Plasmodium falciparum by the lepidopteran transposable element piggyBac. Proc. Natl. Acad. Sci. U.S.A. *102*, 16391–16396.

Balu, B., Chauhan, C., Maher, S.P., Shoue, D.A., Kissinger, J.C., Fraser, M.J., and Adams, J.H. (2009). piggyBac is an effective tool for functional analysis of the Plasmodium falciparum genome. BMC Microbiol. *9*, 83.

Balu, B., Campbell, C., Sedillo, J., Maher, S., Singh, N., Thomas, P., Zhang, M., Pance, A., Otto, T.D., Rayner, J.C., et al. (2013). Atypical mitogen-activated protein kinase phosphatase implicated in regulating transition from pre-S-Phase asexual intraerythrocytic development of Plasmodium falciparum. Eukaryotic Cell *12*, 1171–1178.

Baragaña, B., Hallyburton, I., Lee, M.C.S., Norcross, N.R., Grimaldi, R., Otto, T.D., Proto, W.R., Blagborough, A.M., Meister, S., Wirjanata, G., et al. (2015). A novel multiple-stage antimalarial agent that inhibits protein synthesis. Nature *522*, 315–320.

Barbet, N.C., Schneider, U., Helliwell, S.B., Stansfield, I., Tuite, M.F., and Hall, M.N. (1996). TOR controls translation initiation and early G1 progression in yeast. Mol.

Biol. Cell *7*, 25–42.

Beck, J.R., Muralidharan, V., Oksman, A., and Goldberg, D.E. (2014). PTEX component HSP101 mediates export of diverse malaria effectors into host erythrocytes. Nature *511*, 592–595.

Besson, P., Robert, J.F., Reviron, J., Richard-Lenoble, D., and Gentilini, M. (1976). 2 cases of transfusional malaria. Attempted prevention combining an indirect immunofluorescence test with clinical selection critera. Rev. Fr. Transfus. Immunohematol. *19*, 369–373.

Bonhoure, N., Byrnes, A., Moir, R.D., Hodroj, W., Preitner, F., Praz, V., Marcelin, G., Chua, S.C., Martinez-Lopez, N., Singh, R., et al. (2015). Loss of the RNA polymerase III repressor MAF1 confers obesity resistance. Genes Dev. *29*, 934–947.

Boyle, M.J., Richards, J.S., Gilson, P.R., Chai, W., and Beeson, J.G. (2010). Interactions with heparin-like molecules during erythrocyte invasion by Plasmodium falciparum merozoites. Blood *115*, 4559–4568.

Bozdech, Z., Llinás, M., Pulliam, B.L., Wong, E.D., Zhu, J., and DeRisi, J.L. (2003). The transcriptome of the intraerythrocytic developmental cycle of Plasmodium falciparum. PLoS Biol. *1*, E5.

Brancucci, N.M.B., Bertschi, N.L., Zhu, L., Niederwieser, I., Chin, W.H., Wampfler, R., Freymond, C., Rottmann, M., Felger, I., Bozdech, Z., et al. (2014). Heterochromatin protein 1 secures survival and transmission of malaria parasites. Cell Host Microbe *16*, 165–176.

Brauer, M.J., Huttenhower, C., Airoldi, E.M., Rosenstein, R., Matese, J.C., Gresham, D., Boer, V.M., Troyanskaya, O.G., and Botstein, D. (2008). Coordination of growth

rate, cell cycle, stress response, and metabolic activity in yeast. Mol. Biol. Cell *19*, 352–367.

Brewer, J.W., and Diehl, J.A. (2000). PERK mediates cell-cycle exit during the mammalian unfolded protein response. Proc. Natl. Acad. Sci. U.S.A. *97*, 12625–12630.

Bruce, M.C., Alano, P., Duthie, S., and Carter, R. (1990). Commitment of the malaria parasite Plasmodium falciparum to sexual and asexual development. Parasitology *100 Pt 2*, 191–200.

Byfield, M.P., Murray, J.T., and Backer, J.M. (2005). hVps34 is a nutrient-regulated lipid kinase required for activation of p70 S6 kinase. J. Biol. Chem. *280*, 33076–33082.

Cai, Y., and Wei, Y.-H. (2015). Distinct regulation of Maf1 for lifespan extension by Protein kinase A and Sch9. Aging (Albany NY) *7*, 133–143.

Cargnello, M., Tcherkezian, J., and Roux, P.P. (2015). The expanding role of mTOR in cancer cell growth and proliferation. Mutagenesis *30*, 169–176.

Caro, F., Ahyong, V., Betegon, M., and DeRisi, J.L. (2014). Genome-wide regulatory dynamics of translation in the Plasmodium falciparum asexual blood stages. Elife *3*.

Chantranupong, L., Scaria, S.M., Saxton, R.A., Gygi, M.P., Shen, K., Wyant, G.A., Wang, T., Harper, J.W., Gygi, S.P., and Sabatini, D.M. (2016). The CASTOR Proteins Are Arginine Sensors for the mTORC1 Pathway. Cell *165*, 153–164.

Chaubey, S., Grover, M., and Tatu, U. (2014). Endoplasmic reticulum stress triggers gametocytogenesis in the malaria parasite. J. Biol. Chem. *289*, 16662–16674.

Chen, C., Ridzon, D.A., Broomer, A.J., Zhou, Z., Lee, D.H., Nguyen, J.T., Barbisin,

M., Xu, N.L., Mahuvakar, V.R., Andersen, M.R., et al. (2005). Real-time quantification of microRNAs by stem-loop RT-PCR. Nucleic Acids Res. *33*, e179.

Cheng, Q., Kyle, D.E., and Gatton, M.L. (2012). Artemisinin resistance in Plasmodium falciparum: A process linked to dormancy? Int J Parasitol Drugs Drug Resist *2*, 249–255.

Choffat, Y., Suter, B., Behra, R., and Kubli, E. (1988). Pseudouridine modification in the tRNA(Tyr) anticodon is dependent on the presence, but independent of the size and sequence, of the intron in eucaryotic tRNA(Tyr) genes. Mol. Cell. Biol. *8*, 3332–3337.

Ciesla, M., Towpik, J., Graczyk, D., Oficjalska-Pham, D., Harismendy, O., Suleau, A., Balicki, K., Conesa, C., Lefebvre, O., and Boguta, M. (2007). Maf1 is involved in coupling carbon metabolism to RNA polymerase III transcription. Mol. Cell. Biol. *27*, 7693–7702.

Cingolani, P., Platts, A., Wang, L.L., Coon, M., Nguyen, T., Wang, L., Land, S.J., Lu, X., and Ruden, D.M. (2012). A program for annotating and predicting the effects of single nucleotide polymorphisms, SnpEff: SNPs in the genome of Drosophila melanogaster strain w1118; iso-2; iso-3. Fly (Austin) *6*, 80–92.

Codd, A., Teuscher, F., Kyle, D.E., Cheng, Q., and Gatton, M.L. (2011). Artemisinin-induced parasite dormancy: A plausible mechanism for treatment failure. Malar. J. *10*, 56.

Coleman, B.I., Skillman, K.M., Jiang, R.H.Y., Childs, L.M., Altenhofen, L.M., Ganter, M., Leung, Y., Goldowitz, I., Kafsack, B.F.C., Marti, M., et al. (2014). A Plasmodium falciparum histone deacetylase regulates antigenic variation and gametocyte conver-

sion. Cell Host Microbe *16*, 177–186.

Conrad, M., Schothorst, J., Kankipati, H.N., Van Zeebroeck, G., Rubio-Texeira, M., and Thevelein, J.M. (2014). Nutrient sensing and signaling in the yeast Saccharomyces cerevisiae. FEMS Microbiol Rev *38*, 254–299.

Daignan-Fornier, B., and Sagot, I. (2011). Proliferation/quiescence: The controversial "aller-retour". Cell Div *6*, 10.

Danecek, P., Auton, A., Abecasis, G., Albers, C.A., Banks, E., DePristo, M.A., Handsaker, R.E., Lunter, G., Marth, G.T., Sherry, S.T., et al. (2011). The variant call format and VCFtools. Bioinformatics *27*, 2156–2158.

Daubenberger, C.A., Tisdale, E.J., Curcic, M., Diaz, D., Silvie, O., Mazier, D., Eling, W., Bohrmann, B., Matile, H., and Pluschke, G. (2003). The N'-terminal domain of glyceraldehyde-3-phosphate dehydrogenase of the apicomplexan Plasmodium falciparum mediates GTPase Rab2-dependent recruitment to membranes. Biol. Chem. *384*, 1227–1237.

de Azevedo, M.F., Gilson, P.R., Gabriel, H.B., Simões, R.F., Angrisano, F., Baum, J., Crabb, B.S., and Wunderlich, G. (2012). Systematic analysis of FKBP inducible degradation domain tagging strategies for the human malaria parasite Plasmodium falciparum. PLoS ONE *7*, e40981.

Deitsch, K., Driskill, C., and Wellems, T. (2001). Transformation of malaria parasites by the spontaneous uptake and expression of DNA from human erythrocytes. Nucleic Acids Res. *29*, 850–853.

Desai, S.A. (2012). Ion and nutrient uptake by malaria parasite-infected erythrocytes.

Cell. Microbiol. *14*, 1003–1009.

Dogovski, C., Xie, S.C., Burgio, G., Bridgford, J., Mok, S., McCaw, J.M., Chotivanich, K., Kenny, S., Gnädig, N., Straimer, J., et al. (2015). Targeting the cell stress response of Plasmodium falciparum to overcome artemisinin resistance. PLoS Biol. *13*, e1002132.

Dondorp, A.M., Nosten, F., Yi, P., Das, D., Phyo, A.P., Tarning, J., Lwin, K.M., Ariey, F., Hanpithakpong, W., Lee, S.J., et al. (2009). Artemisinin resistance in Plasmodium falciparum malaria. N. Engl. J. Med. *361*, 455–467.

Epp, C., Raskolnikov, D., and Deitsch, K.W. (2008). A regulatable transgene expression system for cultured Plasmodium falciparum parasites. Malar. J. *7*, 86.

Flueck, C., Bartfai, R., Volz, J., Niederwieser, I., Salcedo-Amaya, A.M., Alako, B.T.F., Ehlgen, F., Ralph, S.A., Cowman, A.F., Bozdech, Z., et al. (2009). Plasmodium falciparum heterochromatin protein 1 marks genomic loci linked to phenotypic variation of exported virulence factors. PLoS Pathog. *5*, e1000569.

Furuya, T., Mu, J., Hayton, K., Liu, A., Duan, J., Nkrumah, L., Joy, D.A., Fidock, D.A., Fujioka, H., Vaidya, A.B., et al. (2005). Disruption of a Plasmodium falciparum gene linked to male sexual development causes early arrest in gametocytogenesis. Proc. Natl. Acad. Sci. U.S.A. *102*, 16813–16818.

Ghorbal, M., Gorman, M., Macpherson, C.R., Martins, R.M., Scherf, A., and Lopez-Rubio, J.-J. (2014). Genome editing in the human malaria parasite Plasmodium falciparum using the CRISPR-Cas9 system. Nat. Biotechnol. *32*, 819–821.

Gietz, R.D., and Woods, R.A. (2002). Transformation of yeast by lithium acetate/single-stranded carrier DNA/polyethylene glycol method. Meth. En-

zymol. *350*, 87–96.

Gosline, S.J.C., Nascimento, M., McCall, L.-I., Zilberstein, D., Thomas, D.Y., Matlashewski, G., and Hallett, M. (2011). Intracellular eukaryotic parasites have a distinct unfolded protein response. PLoS ONE *6*, e19118.

Graczyk, D., Debski, J., Muszy□ ska, G., Bretner, M., Lefebvre, O., and Boguta, M. (2011). Casein kinase II-mediated phosphorylation of general repressor Maf1 triggers RNA polymerase III activation. Proc. Natl. Acad. Sci. U.S.A. *108*, 4926–4931.

Guertin, D.A., and Sabatini, D.M. (2005). An expanding role for mTOR in cancer. Trends Mol Med *11*, 353–361.

Guggisberg, A.M., Amthor, R.E., and Odom, A.R. (2014). Isoprenoid Biosynthesis in Plasmodium falciparum. Eukaryotic Cell *13*, 1348–1359.

Gulati, P., Gaspers, L.D., Dann, S.G., Joaquin, M., Nobukuni, T., Natt, F., Kozma, S.C., Thomas, A.P., and Thomas, G. (2008). Amino acids activate mTOR complex 1 via Ca2+/CaM signaling to hVps34. Cell Metab. *7*, 456–465.

Hamanaka, R.B., Bennett, B.S., Cullinan, S.B., and Diehl, J.A. (2005). PERK and GCN2 contribute to eIF2alpha phosphorylation and cell cycle arrest after activation of the unfolded protein response pathway. Mol. Biol. Cell *16*, 5493–5501.

Harbut, M.B., Patel, B.A., Yeung, B.K.S., McNamara, C.W., Bright, A.T., Ballard, J., Supek, F., Golde, T.E., Winzeler, E.A., Diagana, T.T., et al. (2012). Targeting the ERAD pathway via inhibition of signal peptide peptidase for antiparasitic therapeutic design. Proc. Natl. Acad. Sci. U.S.A. *109*, 21486–21491.

Hartwell, L.H. (1974). Saccharomyces cerevisiae cell cycle. Bacteriol Rev *38*, 164–

198.

Hartwell, L.H., Culotti, J., Pringle, J.R., and Reid, B.J. (1974). Genetic control of the cell division cycle in yeast. Science *183*, 46–51.

Haynes, J.D., and Moch, J.K. (2002). Automated synchronization of Plasmodium falciparum parasites by culture in a temperature-cycling incubator. Methods Mol. Med. *72*, 489–497.

Henry, K.A., Blank, H.M., Hoose, S.A., and Polymenis, M. (2010). The unfolded protein response is not necessary for the G1/S transition, but it is required for chromosome maintenance in Saccharomyces cerevisiae. PLoS ONE *5*, e12732.

Herman, J.D., Pepper, L.R., Cortese, J.F., Estiu, G., Galinsky, K., Zuzarte-Luis, V., Derbyshire, E.R., Ribacke, U., Lukens, A.K., Santos, S.A., et al. (2015). The cytoplasmic prolyl-tRNA synthetase of the malaria parasite is a dual-stage target of febrifugine and its analogs. Sci Transl Med *7*, 288ra77.

Hoepfner, D., McNamara, C.W., Lim, C.S., Studer, C., Riedl, R., Aust, T., McCormack, S.L., Plouffe, D.M., Meister, S., Schuierer, S., et al. (2012). Selective and specific inhibition of the plasmodium falciparum lysyl-tRNA synthetase by the fungal secondary metabolite cladosporin. Cell Host Microbe *11*, 654–663.

Holcik, M., and Sonenberg, N. (2005). Translational control in stress and apoptosis. Nat. Rev. Mol. Cell Biol. *6*, 318–327.

Hoppe, H.C., van Schalkwyk, D.A., Wiehart, U.I.M., Meredith, S.A., Egan, J., and Weber, B.W. (2004). Antimalarial quinolines and artemisinin inhibit endocytosis in Plasmodium falciparum. Antimicrob. Agents Chemother. *48*, 2370–2378.

Hoshen, M.B., Na-Bangchang, K., Stein, W.D., and Ginsburg, H. (2000). Mathe-

matical modelling of the chemotherapy of Plasmodium falciparum malaria with artesunate: Postulation of 'dormancy', a partial cytostatic effect of the drug, and its implication for treatment regimens. Parasitology *121 (Pt 3)*, 237–246.

Howe, R., Kelly, M., Jimah, J., Hodge, D., and Odom, A.R. (2013). Isoprenoid biosynthesis inhibition disrupts Rab5 localization and food vacuolar integrity in Plasmodium falciparum. Eukaryotic Cell *12*, 215–223.

Huber, A., Bodenmiller, B., Uotila, A., Stahl, M., Wanka, S., Gerrits, B., Aebersold, R., and Loewith, R. (2009). Characterization of the rapamycin-sensitive phosphoproteome reveals that Sch9 is a central coordinator of protein synthesis. Genes Dev. *23*, 1929–1943.

Ikadai, H., Shaw Saliba, K., Kanzok, S.M., McLean, K.J., Tanaka, T.Q., Cao, J., Williamson, K.C., and Jacobs-Lorena, M. (2013). Transposon mutagenesis identifies genes essential for Plasmodium falciparum gametocytogenesis. Proc. Natl. Acad. Sci. U.S.A. *110*, E1676–1684.

Jensen, J.B., and Trager, W. (1977). Plasmodium falciparum in culture: Use of outdated erthrocytes and description of the candle jar method. J. Parasitol. *63*, 883–886.

Kafsack, B.F.C., Rovira-Graells, N., Clark, T.G., Bancells, C., Crowley, V.M., Campino, S.G., Williams, A.E., Drought, L.G., Kwiatkowski, D.P., Baker, D.A., et al. (2014). A transcriptional switch underlies commitment to sexual development in malaria parasites. Nature *507*, 248–252.

Kaminska, J., Grabinska, K., Kwapisz, M., Sikora, J., Smagowicz, W.J., Palamarczyk, G., Zoladek, T., and Boguta, M. (2002). The isoprenoid biosynthetic pathway in Saccharomyces cerevisiae is affected in a maf1-1 mutant with altered tRNA synthesis.

FEMS Yeast Res. *2*, 31–37.

Kantidakis, T., Ramsbottom, B.A., Birch, J.L., Dowding, S.N., and White, R.J. (2010). mTOR associates with TFIIIC, is found at tRNA and 5S rRNA genes, and targets their repressor Maf1. Proc. Natl. Acad. Sci. U.S.A. *107*, 11823–11828.

Klonis, N., Crespo-Ortiz, M.P., Bottova, I., Abu-Bakar, N., Kenny, S., Rosenthal, P.J., and Tilley, L. (2011). Artemisinin activity against Plasmodium falciparum requires hemoglobin uptake and digestion. Proc. Natl. Acad. Sci. U.S.A. *108*, 11405–11410.

Klonis, N., Xie, S.C., McCaw, J.M., Crespo-Ortiz, M.P., Zaloumis, S.G., Simpson, J.A., and Tilley, L. (2013). Altered temporal response of malaria parasites determines differential sensitivity to artemisinin. Proc. Natl. Acad. Sci. U.S.A. *110*, 5157–5162.

Kozarewa, I., Ning, Z., Quail, M.A., Sanders, M.J., Berriman, M., and Turner, D.J. (2009). Amplification-free Illumina sequencing-library preparation facilitates improved mapping and assembly of (G+C)-biased genomes. Nat. Methods *6*, 291–295.

Krotoski, W.A. (1985). Discovery of the hypnozoite and a new theory of malarial relapse. Trans. R. Soc. Trop. Med. Hyg. *79*, 1–11.

Krotoski, W.A., Collins, W.E., Bray, R.S., Garnham, P.C., Cogswell, F.B., Gwadz, R.W., Killick-Kendrick, R., Wolf, R., Sinden, R., Koontz, L.C., et al. (1982). Demonstration of hypnozoites in sporozoite-transmitted Plasmodium vivax infection. Am. J. Trop. Med. Hyg. *31*, 1291–1293.

Kyle DE, Webster HK (1996). Postantibiotic effect of quinine and dihydroartemisinin derivatives on Plasmodium falciparum in vitro: Implications for a mechanism of recrudescence (Nagasaki, Japan: abstract).

Lambros, C., and Vanderberg, J.P. (1979). Synchronization of Plasmodium falci-

parum erythrocytic stages in culture. J. Parasitol. *65*, 418–420.

Laporte, D., Lebaudy, A., Sahin, A., Pinson, B., Ceschin, J., Daignan-Fornier, B., and Sagot, I. (2011). Metabolic status rather than cell cycle signals control quiescence entry and exit. J. Cell Biol. *192*, 949–957.

Lasonder, E., Green, J.L., Camarda, G., Talabani, H., Holder, A.A., Langsley, G., and Alano, P. (2012). The Plasmodium falciparum schizont phosphoproteome reveals extensive phosphatidylinositol and cAMP-protein kinase A signaling. J. Proteome Res. *11*, 5323–5337.

Lasonder, E., Green, J.L., Grainger, M., Langsley, G., and Holder, A.A. (2015). Extensive differential protein phosphorylation as intraerythrocytic Plasmodium falciparum schizonts develop into extracellular invasive merozoites. Proteomics *15*, 2716–2729.

Lee, J., Moir, R.D., and Willis, I.M. (2009). Regulation of RNA polymerase III transcription involves SCH9-dependent and SCH9-independent branches of the target of rapamycin (TOR) pathway. J. Biol. Chem. *284*, 12604–12608.

Lewis, I.A., Wacker, M., Olszewski, K.L., Cobbold, S.A., Baska, K.S., Tan, A., Ferdig, M.T., and Llinás, M. (2014). Metabolic QTL analysis links chloroquine resistance in Plasmodium falciparum to impaired hemoglobin catabolism. PLoS Genet. *10*, e1004085.

Li, H., and Durbin, R. (2009). Fast and accurate short read alignment with Burrows-Wheeler transform. Bioinformatics *25*, 1754–1760.

Lillie, S.H., and Pringle, J.R. (1980). Reserve carbohydrate metabolism in Saccha-

romyces cerevisiae: Responses to nutrient limitation. J. Bacteriol. *143*, 1384–1394.

Liu, J., Istvan, E.S., Gluzman, I.Y., Gross, J., and Goldberg, D.E. (2006). Plasmodium falciparum ensures its amino acid supply with multiple acquisition pathways and redundant proteolytic enzyme systems. Proc. Natl. Acad. Sci. U.S.A. *103*, 8840–8845.

Liu, J., Zhang, W., Du, G., Chen, J., and Zhou, J. (2013). Overproduction of geraniol by enhanced precursor supply in Saccharomyces cerevisiae. J. Biotechnol. *168*, 446–451.

Loewith, R., and Hall, M.N. (2011). Target of Rapamycin (TOR) in Nutrient Signaling and Growth Control. Genetics *189*, 1177–1201.

Lopez-Rubio, J.-J., Mancio-Silva, L., and Scherf, A. (2009). Genome-wide analysis of heterochromatin associates clonally variant gene regulation with perinuclear repressive centers in malaria parasites. Cell Host Microbe *5*, 179–190.

Marshall, L., Rideout, E.J., and Grewal, S.S. (2012). Nutrient/TOR-dependent regulation of RNA polymerase III controls tissue and organismal growth in Drosophila. EMBO J. *31*, 1916–1930.

Martin, R.E., and Kirk, K. (2007). Transport of the essential nutrient isoleucine in human erythrocytes infected with the malaria parasite Plasmodium falciparum. Blood *109*, 2217–2224.

Mbengue, A., Bhattacharjee, S., Pandharkar, T., Liu, H., Estiu, G., Stahelin, R.V., Rizk, S.S., Njimoh, D.L., Ryan, Y., Chotivanich, K., et al. (2015). A molecular mechanism of artemisinin resistance in Plasmodium falciparum malaria. Nature *520*, 683–687.

McKenna, A., Hanna, M., Banks, E., Sivachenko, A., Cibulskis, K., Kernytsky, A.,

Garimella, K., Altshuler, D., Gabriel, S., Daly, M., et al. (2010). The Genome Analysis Toolkit: A MapReduce framework for analyzing next-generation DNA sequencing data. Genome Res. *20*, 1297–1303.

Moir, R.D., Lee, J., Haeusler, R.A., Desai, N., Engelke, D.R., and Willis, I.M. (2006). Protein kinase A regulates RNA polymerase III transcription through the nuclear localization of Maf1. Proc. Natl. Acad. Sci. U.S.A. *103*, 15044–15049.

Mok, S., Ashley, E.A., Ferreira, P.E., Zhu, L., Lin, Z., Yeo, T., Chotivanich, K., Imwong, M., Pukrittayakamee, S., Dhorda, M., et al. (2015). Drug resistance. Population transcriptomics of human malaria parasites reveals the mechanism of artemisinin resistance. Science *347*, 431–435.

Muhamad, P., Phompradit, P., Sornjai, W., Maensathian, T., Chaijaroenkul, W., Rueangweerayut, R., and Na-Bangchang, K. (2011). Polymorphisms of Molecular Markers of Antimalarial Drug Resistance and Relationship with Artesunate-Mefloquine Combination Therapy in Patients with Uncomplicated Plasmodium falciparum Malaria in Thailand. Am J Trop Med Hyg *85*, 568–572.

Munson, M.J., Allen, G.F., Toth, R., Campbell, D.G., Lucocq, J.M., and Ganley, I.G. (2015). mTOR activates the VPS34-UVRAG complex to regulate autolysosomal tubulation and cell survival. EMBO J. *34*, 2272–2290.

Nkrumah, L.J., Muhle, R.A., Moura, P.A., Ghosh, P., Hatfull, G.F., Jacobs, W.R., and Fidock, D.A. (2006). Efficient site-specific integration in Plasmodium falciparum chromosomes mediated by mycobacteriophage Bxb1 integrase. Nat. Methods *3*, 615–621.

Nobukuni, T., Joaquin, M., Roccio, M., Dann, S.G., Kim, S.Y., Gulati, P., Byfield, M.P., Backer, J.M., Natt, F., Bos, J.L., et al. (2005). Amino acids mediate mTOR/raptor

signaling through activation of class 3 phosphatidylinositol 3OH-kinase. Proc. Natl. Acad. Sci. U.S.A. *102*, 14238–14243.

Pardee, A.B. (1974). A restriction point for control of normal animal cell proliferation. Proc. Natl. Acad. Sci. U.S.A. *71*, 1286–1290.

Pernas, L., Adomako-Ankomah, Y., Shastri, A.J., Ewald, S.E., Treeck, M., Boyle, J.P., and Boothroyd, J.C. (2014). Toxoplasma effector MAF1 mediates recruitment of host mitochondria and impacts the host response. PLoS Biol. *12*, e1001845.

Pluta, K., Lefebvre, O., Martin, N.C., Smagowicz, W.J., Stanford, D.R., Ellis, S.R., Hopper, A.K., Sentenac, A., and Boguta, M. (2001). Maf1p, a negative effector of RNA polymerase III in Saccharomyces cerevisiae. Mol. Cell. Biol. *21*, 5031–5040.

Popolo, L., Vanoni, M., and Alberghina, L. (1982). Control of the yeast cell cycle by protein synthesis. Exp. Cell Res. *142*, 69–78.

Powers, R.W., Kaeberlein, M., Caldwell, S.D., Kennedy, B.K., and Fields, S. (2006). Extension of chronological life span in yeast by decreased TOR pathway signaling. Genes Dev. *20*, 174–184.

R Core Team (2015). R: A Language and Environment for Statistical Computing (Vienna, Austria: R Foundation for Statistical Computing).

Reilly, H.B., Wang, H., Steuter, J.A., Marx, A.M., and Ferdig, M.T. (2007). Quantitative dissection of clone-specific growth rates in cultured malaria parasites. Int. J. Parasitol. *37*, 1599–1607.

Reilly Ayala, H.B., Wacker, M.A., Siwo, G., and Ferdig, M.T. (2010). Quantitative trait loci mapping reveals candidate pathways regulating cell cycle duration in Plasmodium

falciparum. BMC Genomics *11*, 577.

Rideout, E.J., Marshall, L., and Grewal, S.S. (2012). Drosophila RNA polymerase III repressor Maf1 controls body size and developmental timing by modulating tRNAiMet synthesis and systemic insulin signaling. Proc. Natl. Acad. Sci. U.S.A. *109*, 1139–1144.

Ritz, C., and Streibig, J.C. (2005). Bioassay Analysis using R. Journal of Statistical Software *12*.

Roberts, D.N., Wilson, B., Huff, J.T., Stewart, A.J., and Cairns, B.R. (2006). Dephosphorylation and genome-wide association of Maf1 with Pol III-transcribed genes during repression. Mol. Cell *22*, 633–644.

Robinson, J.T., Thorvaldsdóttir, H., Winckler, W., Guttman, M., Lander, E.S., Getz, G., and Mesirov, J.P. (2011). Integrative genomics viewer. Nat. Biotechnol. *29*, 24–26.

Saldanha, A.J., Brauer, M.J., and Botstein, D. (2004). Nutritional homeostasis in batch and steady-state culture of yeast. Mol. Biol. Cell *15*, 4089–4104.

Saqcena, M., Menon, D., Patel, D., Mukhopadhyay, S., Chow, V., and Foster, D.A. (2013). Amino acids and mTOR mediate distinct metabolic checkpoints in mammalian G1 cell cycle. PLoS ONE *8*, e74157.

Schmidt, E.K., Clavarino, G., Ceppi, M., and Pierre, P. (2009). SUnSET, a nonradioactive method to monitor protein synthesis. Nat. Methods *6*, 275–277.

Serfontein, J., Nisbet, R.E.R., Howe, C.J., and de Vries, P.J. (2010). Evolution of the

TSC1/TSC2-TOR signaling pathway. Sci Signal *3*, ra49.

Shanks, G.D. (2015). Historical review: Does stress provoke Plasmodium falciparum recrudescence? Trans. R. Soc. Trop. Med. Hyg. *109*, 360–365.

Shanks, G.D., and White, N.J. (2013). The activation of vivax malaria hypnozoites by infectious diseases. Lancet Infect Dis *13*, 900–906.

Shor, B., Wu, J., Shakey, Q., Toral-Barza, L., Shi, C., Follettie, M., and Yu, K. (2010). Requirement of the mTOR kinase for the regulation of Maf1 phosphorylation and control of RNA polymerase III-dependent transcription in cancer cells. J. Biol. Chem. *285*, 15380–15392.

Shute, P.G. (1946). Latency and long-term relapses in benign tertian malaria. Trans. R. Soc. Trop. Med. Hyg. *40*, 189–200.

Sidhu, A.B.S., Verdier-Pinard, D., and Fidock, D.A. (2002). Chloroquine resistance in Plasmodium falciparum malaria parasites conferred by pfcrt mutations. Science *298*, 210–213.

Silvestrini, F., Alano, P., and Williams, J.L. (2000). Commitment to the production of male and female gametocytes in the human malaria parasite Plasmodium falciparum. Parasitology *121 Pt 5*, 465–471.

Silvestrini, F., Bozdech, Z., Lanfrancotti, A., Di Giulio, E., Bultrini, E., Picci, L., Derisi, J.L., Pizzi, E., and Alano, P. (2005). Genome-wide identification of genes upregulated at the onset of gametocytogenesis in Plasmodium falciparum. Mol. Biochem. Parasitol. *143*, 100–110.

Sinha, A., Hughes, K.R., Modrzynska, K.K., Otto, T.D., Pfander, C., Dickens, N.J., Religa, A.A., Bushell, E., Graham, A.L., Cameron, R., et al. (2014). A cascade of

DNA-binding proteins for sexual commitment and development in Plasmodium. Nature *507*, 253–257.

Smilkstein, M., Sriwilaijaroen, N., Kelly, J.X., Wilairat, P., and Riscoe, M. (2004). Simple and inexpensive fluorescence-based technique for high-throughput antimalarial drug screening. Antimicrob. Agents Chemother. *48*, 1803–1806.

Smith, T.G., Lourenço, P., Carter, R., Walliker, D., and Ranford-Cartwright, L.C. (2000). Commitment to sexual differentiation in the human malaria parasite, Plasmodium falciparum. Parasitology *121 (Pt 2)*, 127–133.

Spalding, M.D., Allary, M., Gallagher, J.R., and Prigge, S.T. (2010). Validation of a modified method for Bxb1 mycobacteriophage integrase-mediated recombination in Plasmodium falciparum by localization of the H-protein of the glycine cleavage complex to the mitochondrion. Mol. Biochem. Parasitol. *172*, 156–160.

Straimer, J., Gnädig, N.F., Witkowski, B., Amaratunga, C., Duru, V., Ramadani, A.P., Dacheux, M., Khim, N., Zhang, L., Lam, S., et al. (2015). Drug resistance. K13-propeller mutations confer artemisinin resistance in Plasmodium falciparum clinical isolates. Science *347*, 428–431.

Swain, M.T., Tsai, I.J., Assefa, S.A., Newbold, C., Berriman, M., and Otto, T.D. (2012). A post-assembly genome-improvement toolkit (PAGIT) to obtain annotated genomes from contigs. Nat Protoc *7*, 1260–1284.

Talman, A.M., Blagborough, A.M., and Sinden, R.E. (2010). A Plasmodium falciparum strain expressing GFP throughout the parasite's life-cycle. PLoS ONE *5*, e9156.

Tavares, M.R., Pavan, I.C.B., Amaral, C.L., Meneguello, L., Luchessi, A.D., and

Simabuco, F.M. (2015). The S6K protein family in health and disease. Life Sci. *131*, 1–10.

Teuscher, F., Gatton, M.L., Chen, N., Peters, J., Kyle, D.E., and Cheng, Q. (2010). Artemisinin-induced dormancy in plasmodium falciparum: Duration, recovery rates, and implications in treatment failure. J. Infect. Dis. *202*, 1362–1368.

Upadhya, R., Lee, J., and Willis, I.M. (2002). Maf1 is an essential mediator of diverse signals that repress RNA polymerase III transcription. Mol. Cell *10*, 1489–1494.

Urban, J., Soulard, A., Huber, A., Lippman, S., Mukhopadhyay, D., Deloche, O., Wanke, V., Anrather, D., Ammerer, G., Riezman, H., et al. (2007). Sch9 is a major target of TORC1 in Saccharomyces cerevisiae. Mol. Cell *26*, 663–674.

Vaid, A., and Sharma, P. (2006). PfPKB, a protein kinase B-like enzyme from Plasmodium falciparum: II. Identification of calcium/calmodulin as its upstream activator and dissection of a novel signaling pathway. J. Biol. Chem. *281*, 27126–27133.

Vaid, A., Ranjan, R., Smythe, W.A., Hoppe, H.C., and Sharma, P. (2010). PfPI3K, a phosphatidylinositol-3 kinase from Plasmodium falciparum, is exported to the host erythrocyte and is involved in hemoglobin trafficking. Blood *115*, 2500–2507.

van Dam, T.J.P., Zwartkruis, F.J.T., Bos, J.L., and Snel, B. (2011). Evolution of the TOR pathway. J. Mol. Evol. *73*, 209–220.

Vannini, A., Ringel, R., Kusser, A.G., Berninghausen, O., Kassavetis, G.A., and Cramer, P. (2010). Molecular basis of RNA polymerase III transcription repression by Maf1. Cell *143*, 59–70.

Varkonyi-Gasic, E., Wu, R., Wood, M., Walton, E.F., and Hellens, R.P. (2007). Protocol: A highly sensitive RT-PCR method for detection and quantification of microR-

NAs. Plant Methods *3*, 12.

Wei, Y., Tsang, C.K., and Zheng, X.F.S. (2009). Mechanisms of regulation of RNA polymerase III-dependent transcription by TORC1. EMBO J. *28*, 2220–2230.

Wickham, Hadley (2009). Ggplot2: Elegant Graphics for Data Analysis (Springer-Verlag New York).

Willis, I.M., Moir, R.D., and Lee, J. (2011). Does casein kinase II phosphorylation of Maf1 trigger RNA polymerase III activation? Proc. Natl. Acad. Sci. U.S.A. *108*, E300; author reply E301.

Witkowski, B., Lelièvre, J., Barragán, M.J.L., Laurent, V., Su, X.-z., Berry, A., and Benoit-Vical, F. (2010). Increased tolerance to artemisinin in Plasmodium falciparum is mediated by a quiescence mechanism. Antimicrob. Agents Chemother. *54*, 1872–1877.

Witkowski, B., Amaratunga, C., Khim, N., Sreng, S., Chim, P., Kim, S., Lim, P., Mao, S., Sopha, C., Sam, B., et al. (2013). Novel phenotypic assays for the detection of artemisinin-resistant Plasmodium falciparum malaria in Cambodia: In-vitro and ex-vivo drug-response studies. Lancet Infect Dis *13*, 1043–1049.

Wolfson, R.L., Chantranupong, L., Saxton, R.A., Shen, K., Scaria, S.M., Cantor, J.R., and Sabatini, D.M. (2016). Sestrin2 is a leucine sensor for the mTORC1 pathway. Science *351*, 43–48.

Woodard, L.E., and Wilson, M.H. (2015). piggyBac-ing models and new therapeutic strategies. Trends Biotechnol. *33*, 525–533.

World Health Organization (2015). World Malaria Report (Geneva, Switzerland:

World Health Organization).

Xia, D., Sanderson, S.J., Jones, A.R., Prieto, J.H., Yates, J.R., Bromley, E., Tomley, F.M., Lal, K., Sinden, R.E., Brunk, B.P., et al. (2008). The proteome of Toxoplasma gondii: Integration with the genome provides novel insights into gene expression and annotation. Genome Biol. *9*, R116.

Yan, Y., Flinn, R.J., Wu, H., Schnur, R.S., and Backer, J.M. (2009). hVps15, but not Ca2+/CaM, is required for the activity and regulation of hVps34 in mammalian cells. Biochem. J. *417*, 747–755.

Yoon, M.-S., Du, G., Backer, J.M., Frohman, M.A., and Chen, J. (2011). Class III PI-3-kinase activates phospholipase D in an amino acid-sensing mTORC1 pathway. J. Cell Biol. *195*, 435–447.

Zhang, M., Mishra, S., Sakthivel, R., Rojas, M., Ranjan, R., Sullivan, W.J., Fontoura, B.M.A., Ménard, R., Dever, T.E., and Nussenzweig, V. (2012). PK4, a eukaryotic initiation factor 2-alpha(eIF2-alpha) kinase, is essential for the development of the erythrocytic cycle of Plasmodium. Proc Natl Acad Sci U S A *109*, 3956–3961.

Curriculum Vitae

Kyle Jarrod McLean

Johns Hopkins Bloomberg School of Public Health
Department of Molecular Microbiology and Immunology
615 N Wolfe St
Baltimore, MD 21205

Phone: 443 825-0582

Email 1: kmclean6@jhu.edu

Email 2: kyle.jarrod.mclean@gmail.com

Education

2016 Doctor of Philosophy

Molecular Microbiology and Immunology
Johns Hopkins Bloomberg Scool of Public Health
Advisor: Marcelo Jacobs-Lorena ljacob13@jhu.edu

2007 Bachelor of Science

Forensic Biology Specialist
University of Toronto at Mississauga
cGPA: 3.96

Publications

McLean KJ, Jacobs-Lorena M (2016). Genetic control of malaria mosquitoes. *Trends in Parasitology* 32(3); 174

Ke H, Lewis IA, Morrisey JM, **McLean KJ**, Ganesan SM, Painter HJ, Mather MW, Jacobs- Lorena M, Llinás M, Vaidya AB (2015). Genetic investigation of tricarboxylic acid metabolism during the *Plasmodium falciparum* life cycle. *Cell Reports* 11(1); 164

Wiley JD, Merino EF, Krai PM, **McLean KJ**, Tripathi AK, Vega-Rodríguez J, Jacobs- Lorena M, Klemba M, Cassera MB (2014). Isoprenoid Precursor Biosynthesis is the Essential Metabolic Role of the Apicoplast during Gametocytogenesis in *Plasmodium falciparum*. *Eukaryote Cell* pii; EC.00198

Ikadai H, Shaw Saliba K, Kanzok S, **McLean KJ**, Cao J, Williamson K, Jacobs-Lorena, M (2013). Transposon-mutagenesis identifies genes essential for Plasmodium falciparum gametocytogenesis. *Proceedings of the National Academy of Sciences* 110(18); E1676

Dong Y, Das S, Cirimotich C, Souza-Neto JA, **McLean KJ**, Dimopoulos G (2011). Engineered immunity of *Anopheles* to *Plasmodium* infection. *PLoS Pathogens* 7(12):e1002458

Honors & Awards

2012-2014
Johns Hopkins Malaria Research Institute Pre-Doctoral Fellowship
Two year's tuition and stipend

2008
Dr. J. Harold Drudge Scholarship for Parasitology
One year's tuition and stipend

2007
NSERC PGS D Awardee (declined)
$21, 000 CAD per year to be held within Canada

2005-2007
University of Toronto Scholar (Scholarship)
$1500 CAD, awarded to top 1% of students

2003-2007
Dean's List for Academic Achievement, University of Toronto

2006
Alan F. Coventry Memorial Scholarship for High Achievement in Biology
$2000 CAD, awarded to top second year biology students

2004
University of Toronto Mathematics' Honor Roll

2003
Life Sciences Entrance Scholarship
$1500 CAD, awarded to top 1% of students

Conference Presentations

2013
"A relic of the TOR pathway is required for Plasmodium falciparum survival upon amino acid starvation"
24th Annual Molecular Parasitology Meeting
Marine Biological Laboratory, Woods Hole, MA
Poster Presentation

2011
"Characterization of a transposon-insertion mutant of Plasmodium falciparum incapable of early gametocyte differentiation"
22nd Annual Molecular Parasitology Meeting
Marine Biological Laboratory, Woods Hole, MA
Poster Presentation

2009
"High efficiency gene-targeting and gene-replacement in the malaria parasite, Plasmodium falciparum its vector mosquito, Anopheles gambiae"
5th International Congress of Vector Ecology
Antalya, Turkey
Oral Presentation

Professional Development

2014
Coursera Johns Hopkins Data Science Specialization
A 10 course series covering data acquisition, data manipulation, statistical analysis, machine learning, and presentation

2010
Presenting Data and Information: A One-Day Course Taught by Edward Tufte
Arlington, VA
On the theory and practice of the effective visual display of quantitative information

Computational Skills and Programming

R/Bioconductor

Python/Biopython

Linux/Unix bash scripting

Teaching Experience

2010-2011
Teaching Assistant
Johns Hopkins Bloomberg School of Public Health
Biology of Parasitism (260.635.01)

2009
Teaching Assistant
Johns Hopkins Bloomberg School of Public Health
Graduate Immunology (260.717.01)

Mentoring Activities

2010 Supervisor of PhD student's 11-week laboratory rotation project
Johns Hopkins Bloomberg School of Public Health
Rasgon Laboratory
Ben Blumberg - *"Engineering the Anopheles gambiae densovirus as a mi*RNA *delivery agent"*

2009 Supervisor of a PhD student's 11-week laboratory rotation project
Rasgon Laboratory
Johns Hopkins Bloomberg School of Public Health
Peter Dumoulin - *"Engineering the Anopheles gambiae densovirus as a mi*RNA *delivery agent"*

Related Academic Activities

2008-2012
Member of Department Recruitment Committee
Johns Hopkins Bloomberg School of Public Health
Department of Molecular Microbiology and Immunology

2009-2011
Coordinator of Student Research Forum
Johns Hopkins Bloomberg School of Public Health
Department of Molecular Microbiology and Immunology